Dynamics and Evolution of Random Boolean Networks

Vom Fachbereich Physik
der Technischen Universität Darmstadt
zur Erlangung des Grades
eines Doktors der Naturwissenschaften
(Dr. rer. nat.)
genehmigte

D i s s e r t a t i o n

von
Dipl.-Phys. Tamara Mihaljev
aus Pula, Kroatien

Referentin: Prof. Dr. Barbara Drossel
Korreferent: Prof. Dr. Markus Porto

Tag der Einreichung: 14.10.2008
Tag der mündlichen Prüfung: 10.11.2008

Darmstadt 2008
D17

Mojim roditeljima

Abstract

Random Boolean networks are used as generic models for the dynamics of complex systems of interacting entities, such as social and economic networks, neural networks, and gene or protein interaction networks. The model studied in this thesis was introduced by S. Kauffman as a simple model for gene regulation. The system consists of N nodes, each of which receives inputs from K randomly chosen nodes. The state of a node is a Boolean function of the states of its input nodes. The functions are assigned to the nodes at random, and the states of all nodes in a network are updated in parallel. Asymptotic dynamical states of a network are represented by attractors in state space. Thus, their number and lengths are important features of the networks. The nodes in a network can be classified as frozen, irrelevant, or relevant, according to their dynamics on an attractor. The relevant nodes determine completely the number and the period of attractors. Although the random Boolean network model is simple, it shows a rich dynamical behavior with a phase transition between a frozen and a disordered phase and a very complex dynamics at the critical point between the phases.

In this thesis dynamics and evolution of random Boolean networks are studied. The investigation of the dynamical properties of the model starts with the simplest realization of a random Boolean network, that is, with the network with one input per node. The topology of these networks is analyzed by generating networks through a growth process. Using probabilistic arguments and estimating the lower bounds, it is analytically proven that in this class of networks both, the mean number and the mean length of attractors grow faster than any power law with the size of the network.

Next, the dynamics of critical networks with two inputs per node is studied and these studies are then generalized to networks with a larger number of inputs. Using methods from the theory of stochastic processes, the scaling behavior of the numbers of nonfrozen and relevant nodes is determined analytically. For all critical networks with $K > 1$ the same power-laws are found. The results obtained for the $K = 1$ networks are then used to show that in all critical random Boolean networks the mean number and length of attractors diverge faster than any power law with the network size. For the modeling of gene regulatory networks this means that the attractors are too long and too many to represent cellular differentiation, to which the model was originally applied.

However, real networks are not random but are the result of evolutionary processes. Therefore, the evolution of populations of random Boolean networks under selection for robustness of the dynamics under small perturbations is investigated. The results of this study show that the fitness landscape contains a huge plateau of maximum fitness that spans the entire network space. It is found that the networks evolved on such a landscape are robust to changes in their structure, while being at the same time able to preserve their function under small environmental changes.

Zusammenfassung

Boolesche Zufallsnetzwerke finden ihre Anwendung als generisches Modell für die Dynamik von komplexen Systemen wechselwirkender Einheiten wie zum Beispiel soziale oder ökonomische Netzwerke, neuronale Netzwerke und Gen- oder Proteinwechselwirkungsnetzwerke. Das Modell, das im Rahmen dieser Arbeit untersucht wird, wurde von S. Kauffman als ein einfaches Modell für Genregulation eingeführt. Das System besteht aus N Knoten, von denen jeder Eingänge von K zufällig ausgewählten Knoten erhält. Der Zustand eines Knotens ist eine Boolesche Funktion der Zustände seiner Eingangsknoten. Diese Funktionen werden den Knoten zufällig zugewiesen und die Zustände aller Knoten eines Netzwerkes werden parallel aktualisiert. Asymptotische dynamische Zustände eines Netzwerkes werden durch Attraktoren im Zustandsraum repräsentiert. Ihre Anzahl und Länge sind wichtige Eigenschaften der Netzwerke. Die Knoten eines Netzwerkes können, gemäß ihrer Dynamik auf einem Attraktor, als gefroren, irrelevant oder relevant klassifiziert werden. Die relevanten Knoten bestimmen vollständig die Anzahl und die Periode der Attraktoren. Obwohl Boolesche Zufallsnetzwerke ein einfaches Modell sind, zeigen sie ein vielfältiges dynamisches Verhalten mit einem Phasenübergang zwischen einer gefrorenen und einer ungeordneten Phase und eine sehr komplexe Dynamik am kritischen Punkt zwischen diesen Phasen.

In dieser Arbeit werden die Dynamik und die Evolution von Booleschen Zufallsnetzwerken untersucht. Die Untersuchung der dynamischen Eigenschaften des Modells beginnt mit der einfachsten Realisierung eines Booleschen Zufallsnetzwerkes, das heißt mit Netzwerken mit nur einem Eingang pro Knoten. Die Topologie dieser Netzwerke wird analysiert, indem Netzwerke mit Hilfe eines Wachstumsprozesses generiert werden. Mit Hilfe wahrscheinlichkeitstheoretischer Argumente und durch Abschätzung unterer Grenzen, wird analytisch bewiesen, dass in dieser Klasse von Netzwerken sowohl die mittlere Anzahl als auch die mittlere Länge der Attraktoren schneller als jedes Potenzgesetz mit der Netzwerkgröße anwächst.

Als nächstes wird die Dynamik von kritischen Netzwerken mit zwei Eingängen pro Knoten untersucht und diese Untersuchungen werden für Netzwerke mit einer größeren Anzahl von Eingängen pro Knoten verallgemeinert. Mit Hilfe von Methoden aus der Theorie stochastischer Prozesse, wird das Skalenverhalten der Anzahl von nicht-gefrorenen und relevanten Knoten analytisch bestimmt. Für alle kritischen Netzwerken mit $K > 1$ werden die gleichen Potenzgesetze gefunden. Die

Ergebnisse, die für die $K = 1$ - Netzwerke erhalten wurden, werden dann benutzt um zu zeigen, dass in allen kritischen Netzwerken die mittlere Anzahl und Länge der Attraktoren schneller als jedes Potenzgesetz mit der Netzwerkgröße divergiert. Für die Modellierung von Genregulationsnetzwerken bedeutet das, dass die Attraktoren zu lang sind und dass es zu viele von ihnen gibt, als dass sie zelluläre Differentiation repräsentieren könnten, auf die das Modell ursprünglich angewendet wurde.

Reale Netzwerke sind nicht zufällig, sondern das Ergebnis evolutionärer Prozesse. Deswegen wir die Evolution von Populationen von Booleschen Netzwerken unter Selektion für Robustheit der Dynamik gegen kleine Störungen untersucht. Die Ergebnisse dieser Untersuchung zeigen, dass die Fitnesslandschaft ein riesiges Plateau maximaler Fitness enthält, das den gesamten Netzwerkraum umspannt. Es kann gezeigt werden, dass die Netzwerke, die in einer solchen Fitnesslandschaft evolviert wurden, robust sind gegen Änderungen in ihrer Struktur, während sie zur gleichen Zeit in der Lage sind ihre Funktion unter kleinen Änderungen der Umweltbedingungen aufrechtzuerhalten.

Contents

1 Introduction **1**
- 1.1 Using networks for modeling complex systems . . . 2
- 1.2 Gene regulation and Boolean networks . . . 3
- 1.3 Overview of the thesis . . . 7

2 Boolean networks **11**
- 2.1 Definition of the model . . . 11
- 2.2 Dynamical regimes . . . 13
- 2.3 The state space of Boolean networks . . . 17
- 2.4 Concept of relevant nodes . . . 20
- 2.5 Variations of the model . . . 22

3 Critical networks with one input per node **25**
- 3.1 Basic properties of the model . . . 26
- 3.2 The mean number of attractors . . . 29
- 3.3 The mean length of attractors . . . 30
- 3.4 Conclusions . . . 34

4 Critical networks with two inputs per node **37**
- 4.1 The class of critical $K = 2$ networks . . . 38
- 4.2 A stochastic process that leads to the frozen core . . . 40
- 4.3 The effect of fluctuations . . . 44
- 4.4 Relevant nodes . . . 50
- 4.5 Conclusions . . . 55

5 General class of critical Kauffman networks **59**
- 5.1 A stochastic process that leads to the frozen core . . . 60
- 5.2 Mean field approximation and the criticality condition . . . 62
- 5.3 The effect of fluctuations . . . 66
- 5.4 Special points and canalizing functions . . . 69
- 5.5 Creating self-freezing loops and their effect . . . 71
- 5.6 Networks without constant functions . . . 73
- 5.7 Generalization to larger K . . . 75

5.8 Relevant nodes and the number and length of attractors 77
5.9 Conclusions 78

6 Evolution of populations of Boolean networks **81**
6.1 Model 83
6.2 Evolution without selection 85
6.3 Evolution with very strong selection 89
6.4 Evolution with finite selection pressure 98
6.5 Conclusions 100

7 Summary and outlook **105**

Bibliography **109**

1 Introduction

The Boolean network model was introduced in 1969 by S. Kauffman [56; 52] as a simple model for gene regulatory networks. A gene regulatory network is the prototype of a complex system. Without incorporating the detailed knowledge of the system, the Boolean network model aims to give only statistical predictions, trying to isolate the mechanism giving raise to the system's behavior. This is a common approach statistical physicists use when dealing with complex systems.

There is no unique definition of what complex systems are. They usually consist of a large number of interacting elements which, when interacting together, have unexpected emergent behavior. The common characteristic of all complex systems is that they display organization without any external organizing principle being applied. The whole is more than just the sum of its parts. This self-organization is often an evolutionary process in which the parts of the system are subjected to evolutionary pressure based on the emergent properties of the whole system. This feed-back loop between system's parts and its emergent behavior is characteristic of many complex systems. The similarities that exist between the evolutionary processes in different complex systems may lead to the number of properties which otherwise very different systems may share.

Complex systems appear in many different areas of science and life. The possibility of exploring such systems with physicists' tools like nonlinear dynamics, statistical physics and networks, challenges physicists to tackle the problems not belonging to areas conventional physics deals with. The methods from statistical physics and nonlinear dynamics have been successfully used in modeling biological, social or economic systems [6].

In modeling complex systems, nonlinear dynamics gives a framework for studying nonlinear interactions which are at the core of the emergence of qualitatively different states of the system, new states that are not mere superpositions of the states of the individual units comprising the system [107]. Statistical physics provides the study of complex systems with techniques particularly suited for investigation of systems with a large number of units, and with two fundamental concepts for the quantitative characterization of complex systems - scaling and universality [102; 101]

1.1 Using networks for modeling complex systems

Recently a wide interdisciplinary scientific community has shown a great interest in the study of complex networks, primarily because a network description of complex systems allows to get relevant information by means of purely statistical coarse-grained analyses, without taking into account the detailed characterization of the system. Moreover, the use of an abstract networked representation makes it possible to compare originally very different systems in the same framework, so that the identification of universal properties becomes much easier.

A network is a system of nodes with connecting links. Since nodes and links can model so many different things, networks seem to appear everywhere [114; 77; 106; 1; 24]. Most of the complex systems can be seen as networked systems. Without enough information about their dynamics and structure, the networked systems were for a long time framed in the random graph paradigm [12]. In the last decade, the network approach to modeling complex systems received a boost from the ever-increasing availability of large data sets of information about real systems and the increasing computer power for storage and manipulation of the data. Thus, a systematic look at these large data sets has become possible. This enabled the search for hidden regularities and patterns, that can be considered as manifestations of underlying laws governing the dynamics and the evolution of these complex systems. And indeed, in spite of the apparent complexity and randomness of the underlying systems, studying the model networks shows that clear patterns and regularities really do exist, and that they can be expressed in mathematical and statistical fashion. Networks turned out to be a new, powerful tool for the description, analysis, and understanding of complex systems.

When modeling complex systems as networks, we can learn about the system by studying the topology of the networks. Detailed experimental data about the interactions existing in a system made the reconstruction of the topology possible. Such graphs are then analyzed, searching for patterns shared by different systems. The topology of many networks changes with time, motivating studies about possible evolutionary scenarios, of how the existing topologies emerged. The characterization of real-world networks is not exhausted by its topological properties and its principles of organization. In real networks, topology and dynamics are intrinsically related. Thus, in addition to studies of networks' topological properties, more effort has recently been put in the study of dynamics and transport processes on networks. Different dynamical processes on networks are studied introducing the elements of the network as dynamical objects on top of the network's topology.

Boolean networks were introduced as discrete dynamical models. Though the model was set up to model genetic networks, Boolean networks are used in modeling other systems too, such as neural networks, social networks, protein interaction

networks, or some aspects of game theory and human language studies [54; 79; 71; 76; 47].

In a more abstract sense, Boolean networks can also be used as a generic model for discrete dynamics on networks. The model is simple and therefore convenient to study. It shows complex dynamical behavior with a phase transition between two dynamical phases. Networks with parameter values on the critical line between the phases show a particularly complex behavior. Most of the studies presented in this thesis will deal with properties of these critical networks.

The simplest and best understood class of Boolean models are *random Boolean networks*. The structure of real networks is different from that of random Boolean networks, with their random wiring and random assignment of update functions. Nevertheless, understanding this simple model is an important step on the way to understanding the more complex real networks.

1.2 Gene regulation and Boolean networks

Living cells are very complex, and detailed knowledge about different mechanisms in the cell such as gene regulation, is limited. Two fundamentally different approaches can be used for modeling chemical activity in living cells. In one, detailed knowledge about a specific function, involving a small number of substances, is used. Using this approach, it is possible to make relatively accurate models, but the investigations are limited to some very specific interactions. Such investigations lead to the predictions and conclusions valid mainly only for the specific function modeled. They usually make only a limited or no contribution to understanding other processes. The opposite approach, which is often used by physicists, is to create a simplified model for the whole system. This approach is unable to capture specific details or to produce realistic quantitative predictions of the system. Instead, it is a way to search for general relations and properties that do not depend on details. Such simple models may also be used to develop concepts and computational techniques which could then be used in investigations of more accurate models. Finally, simplified models serve as valuable test benches and sources of inspiration for new ideas and hypotheses. In modeling gene regulation, Boolean network models are a typical example for using the approach of the second kind.

In a cell, genes regulate each others activity by coding for transcription factors, which may enhance or repress the expression of other genes by binding (possibly in combination) at particular sites. A particular gene regulates, in most of the cases, just a small set of other genes directly, but those genes regulate other genes in turn, so a gene will indirectly influence the activity of many genes downstream. Conversely, a particular gene is indirectly influenced by many genes upstream. A gene may directly

or indirectly contribute to regulating itself. The result is a gene regulatory network, a complex feed-back web of genes turning each other on and off. A simplified model of such a dynamical system includes directed links (transcription factors) and nodes (genes), updating the on-off states in parallel, according to the combinatorial logic of the nodes' inputs. This is Kauffman's random Boolean network model.

The Boolean network model

Kauffman's model assumes that genes are Boolean elements that are either active or inactive, and that the regulatory proteins encoded by them are either fully present or absent at a given point in time. The model has no explicit representation of neither the proteins nor their concentrations. It also assumes that gene activity is completely regulated through transcription, neglecting other important mechanisms in gene regulation. All these simplifications make the model biologically unrealistic, but we can still expect that it shares statistical features of gene regulatory networks which are independent of the system's details.

Kauffman's model was designed to address the diversity of cell types in multicellular organisms. The cells of living organisms differentiate within the developing embryo into the various cell types that form tissues. The process of cellular differentiation is regulated at the molecular level by DNA sequences, encoding genes that produce proteins that regulate other genes. With few exceptions, all eukaryotic cells in an organism carry an identical set of genes, some of which are expressed, others not. Still, cells of distinct types may be very different from each other. A cell type is defined by the particular subset of genes that are expressed. The gene expression pattern of a cell needs to be stable. This is possible if the set of proteins present in the cell regulates the protein production in such a way that the same proteins will continue be produced. This way the cell locks itself to its specific cell type. The same type of locking of the dynamics appears in the Boolean networks. Borrowing the terminology from classical continuous dynamical systems, these steady states of Boolean dynamics are called attractors.

A Boolean network is a discrete dynamical system. The number of possible states of the network is finite, and its dynamics is deterministic. Therefore, attractors are the steady states of the network's dynamics. An attractor is a set of states that, once reached during the network's dynamical evolution, constrains networks dynamics to a perpetual circle of repetitions. The possible dynamical states of networks are organized in different basins of attraction which are collecting all the states evolving to the same attractor. The organization of the network's state space sums up its global dynamics. Kauffman's idea was that the cell types can be defined as the separate attractors or basins of attraction into which networks dynamics settles

from various initial states. Trajectories leading to attractors can then be seen as the pathways of differentiation.

Although Kauffman's model is simple, it shows complex dynamical behavior. In the dynamics of Boolean networks there is a phase transition between the frozen and the chaotic dynamical regime, appearing when the parameters of the network (determining its topology and dynamics) are changing. In the two phases, dynamics of the system is qualitatively different, the number and length of attractors and the overall organization of the network's state space changes abruptly with the change of its parameters leading to the phase transition. Networks with parameter values on the critical line between the phases show a particularly complex behavior.

Kauffman's hypothesis was that real gene regulatory networks should be modeled as such critical random Boolean networks. He based his assumptions on results of computer simulations for the network sizes possible at that time. Kauffman found that the mean number of attractors in critical networks of size N is of the order of $\sqrt{N}$. The biological data available at that time for various species indicated that the number of cell types is proportional to the square root of the number of genes. It seemed that this very simple Boolean network model, with random wiring and random assignment of update functions, displays the same scaling laws as the much more complex reality. Kauffman found also that the mean length of attractors increases as $\sqrt{N}$.

Today we know that the biological data and the computer simulation data were both incorrect. The sequencing of entire genomes in recent years revealed that the number of genes is not proportional to the mass of DNA (as was assumed at that time), but much smaller for higher organisms. In the last decade, random Boolean networks have again been studied numerically, but now with more powerful computers [11; 100; 9; 8]. It was found that for larger N the apparent square-root law does not hold any more, but that the increase with system size is faster. The numerical work was complemented by several analytical papers [90; 27; 29; 58; 73], some of which are presented in this thesis, and today we know that both, attractor number and attractor length, in critical Kauffman networks increase with network size faster than any power law. We also know that, while attractor numbers do not obey power laws, other properties of critical random Boolean networks do obey power laws. These properties, the scaling laws and the way they are obtained will be presented in the thesis.

Some consequences of the new findings on the model's applicability

What we learned about random Boolean networks made it clear that the model has attractors which are too long, and that there are too many of them to represent cellular differentiation. Still, this is in no way the end of the discussion of applicability of Boolean networks in modeling gene regulatory networks. The original model has to be modified and random Boolean networks can not be used as models for gene regulatory networks in the way initially assumed. Nevertheless, Kauffman introduced an interesting hypotheses that living cells may be operating in the critical dynamical regime [53]. The phenomenological arguments he used still sound plausible. Kauffman suggested that gene regulatory networks of living organisms operate at the *edge of chaos*, meaning that the parameters have been adjusted through evolution so that these networks are at or near the critical line. His argument was that only critical networks are at the same time stable and evolvable. Systems in the chaotic phase are very sensitive to perturbations while genetic networks of living organisms have to be stable. At the same time they should allow some degree of sensitivity to external inputs in order to be able to adjust to the environment, which rules out the frozen phase as a physical state which living organisms could be in.

In many other studies, even after the fact that the square-root law is not correct became widely accepted, the discussion about whether real gene regulatory networks operate in the critical regime continued. Kauffman's hypotheses has been even directly studied using biological measurement data [94; 98; 84]. Though it is clear that the original model has to be modified, studies of different variations of the Boolean model show that the existence of different dynamical regimes is the universal property of the model. Therefore, talking about real networks belonging to a certain dynamical regime is still meaningful. However, some of the findings seem contradictory. There are studies that state that real networks should be in the frozen phase and close to the critical line, but in no way chaotic [84; 54]. The studies of networks with more realistic Boolean functions show their stabilizing effect confirming this hypotheses[55]. However, studies of evolution of Boolean networks show that evolved networks can be stable and still have many characteristics of the chaotic networks [108; 74; 96]. Similar findings were obtained in investigations of real system using a different Boolean model. Recently it has been shown that Boolean dynamics can be successfully used for modeling real genetic regulatory networks [64; 2; 72]. In these models the topology of the real networks was used and then a simple Boolean dynamics was applied. The success of these models was quite surprising since Boolean networks were always thought of as a conceptual, statistical models. The networks studied were reduced to only those links and nodes which are important for the function modeled, meaning that they did not represent the gene

regulatory network as a whole, but still, their state space also shows some properties of the state space of chaotic networks.

Random Boolean networks become more realistic if the synchronous updating scheme is abandoned. The large number of attractors in random Boolean networks can be seen as an artifact of the synchronous updating scheme. Klemm and Bornholdt [59] investigated the effect of small disturbances to the synchronous updating, and found that most attractors are not stable. Also, Greil and Drossel [40] found that the number of attractors is a power-law in the system size in fully asynchronously updated networks. The interpretation of the original model is also opened to discussion. If a real system has an attractor that is very hard to find by random sampling, it is not very likely that we will observe it. Hence, there may exist a large number of (possibly pathological) cell types that we normally do not observe. Furthermore, the attractors of the Boolean networks do not have to model the cell types of the living organism. When including a cell size as an external signal, the trajectory of the network in the state space leading to the attractor can be used as a model for the cell cycle as in [64].

The studies of modified and improved models lead to a better understanding of the dynamics of the model, but in the same time raise new questions. The Boolean modeling of gene regulatory networks is thus still an interesting topic, with many possible directions of development.

1.3 Overview of the thesis

Knowing the properties of attractors in the state space of Boolean networks is important not only because of the analogy with cell types, which Stuart Kauffman used when introducing Boolean networks as a model for gene regulatory networks. The attractors are steady states of the network's dynamics, and learning about them is important for any applications of Boolean models. In this thesis, the dynamics of critical random Boolean networks is studied. Investigation of a model's dynamical properties leads to a deeper understanding of the way the networks function, of the way their state space is organized. This enables us to assess how applicable the random networks are for modeling genetic regulation or other systems. When a simple model is well understood, the right ways of improving it are becoming clearly visible. Choosing one of the possibilities to modify the model in order to make it more realistic appears as a natural next step. Real networks are results of evolutionary processes, and thus we choose to evolve the model networks. By evolving random networks, we learn about the evolvability of our model, about the properties of the evolved networks, and we are able to compare these properties with those of

real gene regulatory networks. Results of the evolution of populations of Boolean networks make the studies reported in this thesis complete.

The outline of this thesis is as follows: In the next chapter the Boolean network model is defined in detail. The topology of networks, the rules of the networks' dynamics and the different dynamical regimes a network can be in, are introduced. The state space of networks is defined together with the concept of relevant nodes, which is crucial for the studies of the next three chapters. Different variations of the Boolean model, some of which used in this thesis, are presented. This chapter introduces the concepts which will be the foundation for the analysis presented in the thesis. Together with the Introduction, it provides also the background of the studies presented in the thesis.

The next three chapters investigate the dynamics of different classes of critical random Boolean networks with fixed numbers of inputs per node. In Chapter 3 the simplest case of critical Kauffman networks is studied, the networks with one input per node. The rather simple topology of these networks allows for a fully analytical approach in analysis of their dynamics. The organization of the nodes relevant for dynamics is found by generating the networks through a growth process. By using probabilistic arguments and calculating lower bounds it is shown that the number and length of attractors grow faster than any power law with the network size. The results obtained will prove useful for analysis of other critical random networks with more complex topologies, and will be used in the next two chapters.

In Chapter 4 the class of critical random Boolean networks with two inputs per node is studied. Such networks with a uniform distribution of Boolean functions are the most widely studied example of critical networks. In this thesis, a more general model is studied, in which the functions from various classes can be chosen with different weights. The deterministic description of a stochastic process, introduced to describe the formation of the frozen core (the set of nodes not changing their value in the asymptotic dynamics) in the network, will give the constraint on the choice of these weights, if the network is to be critical. Including noise in the description of the process reveals the properties and the scaling behavior of the nonfrozen nodes in critical networks. Another stochastic process is then used to find the relevant nodes among those which are nonfrozen. The analysis of this process gives the scaling of the number of relevant nodes with the size of the network, of the organization of relevant nodes, and thus finally, permits conclusions about the mean number and length of attractors.

In Chapter 5, the dynamics of critical networks with a larger number of inputs per node is investigated, thus completing our investigations of the dynamics of critical Kauffman networks. The process for determining the frozen core of the network from the previous chapter is now modified in the way that networks with any number of inputs per node can be studied. The parameters describing the choice of functions

in a network are defined through the way the function's output is influenced by the different number of fixed inputs. For all possible choices of parameter values for which the network is critical, the stochastic process is analyzed. Additional methods are used to determine the frozen core of networks with some special parameter choices. The results show that all critical networks with a number of inputs per node larger than one, show the same scaling of the number of nonfrozen and relevant nodes and that the conclusions about the attractors found in the Chapter 3 are valid for all critical Kauffman networks.

In Chapter 6, investigations of the evolution of populations of random Boolean networks under selection for robustness of the dynamics under small perturbations is presented. The networks are mutated by changing the links and the nodes' update rules. The change of the diversity of a population, its structure, the topology of networks and their dynamical properties, such as the fitness and the length of attractors, during the evolution is investigated. The studies presented in this chapter start with the case of evolution without selection pressure where the influence of drift and mutations on the population is determined. Then, the evolution under strong selection pressure is investigated, revealing the properties of the fitness landscape and of the fittest networks in the population. Finally, the effect of finite selection pressure is studied. For each fixed value of the selection pressure parameter, the effect of the change of other parameters of the model, the mutation rate, the size of the network and the size of the population, on the networks' evolution is investigated.

Finally, in Chapter 7 a short summary of the results presented in the thesis is given, together with the main conclusions, and with possible directions for future research.

2 Boolean networks

Let us start by defining the model we are going to study. In this chapter Boolean networks are defined and their properties are introduced in detail. The chapter contains information about the model's topological structure, the way the dynamics is introduced in the model, and about the different measures of its dynamical behavior. Different dynamical regimes in which the networks can function will be introduced. In this chapter we will also see how the state space of the model looks like, together with its main characteristics. Some interpretations of the model's characteristics in terms of gene regulatory networks will be given. A special way of looking at the network's dynamics is introduced, namely the concept of relevant nodes, which will be important for understanding results presented in the next tree chapters of the thesis. Different variations of the original model, some of which we will use in the rest of the thesis, are presented at the end of this chapter. In a nutshell, the chapter contains the main information needed for understanding the way the model is used and studied in the thesis. It will serve as a basis, and at the same time a guide for the rest of the thesis where the results of investigations of the model are presented.

2.1 Definition of the model

One way to think of a Boolean network is as of a directed graph, consisting of vertices and directed edges, with the binary discrete dynamics defined on top of it by attributing to the nodes Boolean values and Boolean functions. The other way could be to think of a set of binary elements with inherent Boolean functions, that are connected with directed links according to the way they are interacting, so that first the dynamics and on top of it the topology is introduced. In any case, the properties of Boolean networks that are important for modeling purposes, are an interplay between these two features, the network's topology and the dynamical rules defining the change of the states of nodes in the network. The two determine together the dynamics of the network as a whole, which should then represent the dynamics of the modeled complex system.

Topology of Boolean networks

Networks in general are defined as a set of nodes connected with links (edges). The topology or architecture of a network defines the way these links are connecting nodes in a network. In Boolean networks the links are directed. In mathematical formalism the topology of Boolean networks is defined as directed graph. Since links are directed, for each of them a source and a target node can be defined. Nodes from which the incoming links, the inputs of a node come are its predecessors or we will also call them input nodes. Similarly, the nodes to which the outgoing links, the outputs of a node point are the node's successors or its output nodes. As we will see, the directionality of the links, the existence of input and output nodes, is important for the definition of networks dynamics. The links can be assigned to nodes in different ways. Since Boolean networks have directed links, the topology depends on the distributions of incoming and outgoing links. Each link is at the same time an incoming and an outgoing link, which means that the number of incoming and outgoing links in the network has to be the same. Although the incoming and the outgoing link distributions can be chosen independently, they must have the same mean value.

In the model that Kauffman originally introduced, called *Kauffman* or $N - K$ *model*, the inputs of each of the N nodes are chosen at random from all nodes in the network, including the node itself. The number of inputs per node is fixed to the same value, K, for each node in the network. From this rule for connecting the nodes, it follows that the outgoing links in the network are Poisson distributed with the mean value K. The topology of networks in the Kauffman model is specified by the number of nodes in the the network N and the number of inputs per node K.

In the next three chapters we will study this model and in Chapter 6 we will use it as the starting point of the evolutionary process. Other possibilities of defining the topology of Boolean networks are going to be discussed later in this chapter, in 2.5.

Dynamics of Boolean networks

Dynamics is introduced into Boolean networks by defining the nodes as Boolean variables. A Boolean variable is a binary variable. It can have only two distinct values which could be, for example, on/off, true/false, or 1/0, as in digital circuits. Apart from the Boolean variable, a Boolean function is assigned to each node in the network. These functions are the update rules which are going to define the dynamics of each node, and consequently of the whole network. The state of a node is the value of the Boolean function of the states of its input nodes in the previous

time step. If the node i has k_i incoming links, the update rule can be presented in symbols as

$$\sigma_i(t) = f_i[\sigma_{j_1(i)}(t-1), \sigma_{j_2(i)}(t-1), ..., \sigma_{j_{k_i}(i)}(t-1)]. \quad (2.1.1)$$

Here σ_i represents the binary value of the node, $\sigma_{j_1(i)}$, $\sigma_{j_2(i)}$, ..., $\sigma_{j_{k_i}(i)}$ are the values of its input nodes, and f_i is a Boolean function associated to it. This function can be any Boolean function of k_i elements.

In the Kauffman model, which we will study, the number of inputs per node is fixed to K and the Boolean functions for all the nodes in the network are chosen at random from the set of 2^{2^K} possible Boolean functions of K elements, using a specified probability distribution of these functions. In our study we will give different classes of functions different weights. Other possibilities for assigning functions to the nodes in the network will be discussed in Section 2.5 of this chapter.

A specific choice of linkages and functions define one *realization* of the network. The realization is not changing during the dynamical evolution of the network. Such models are called quenched. Given the realization, one can define a dynamics by using Equation 2.1.1 to update the nodes in the network. In our model time steps are discrete and in each of them all the nodes are going to be updated at the same time. This is called a synchronous or parallel update. This is going to be the only type of update we will use. Other possible updating schemes will be discussed briefly in Section 2.5.

In Figure 2.1 an illustration of a small Kauffman network with two inputs per node is given together with the update rule assigned to one of its nodes.

Before we continue with introducing the dynamical properties of the systems under study, let us emphasize again the statistical nature of our modeling. The values of N and K, together with the probability distribution for the Boolean functions, specify an ensemble of networks. Except in the case when we study the evolution of populations of Boolean networks (in Chapter 6), all our calculations will assume that the properties obtained are those of a typical ensemble member. Therefore, by defining the object of our study based on only a small number of parameters, we look at the common properties of the whole ensemble of networks, or of its typical member, and not of the characteristics of a specific network. We perform our analytical calculations mainly in the thermodynamic limit (when $N \to \infty$), therefore N is not an important parameter for most of the properties we will study.

2.2 Dynamical regimes

In the limit of infinite network size, all random Boolean models show a phase transition between two phases in which information transfer in the system is qualitatively

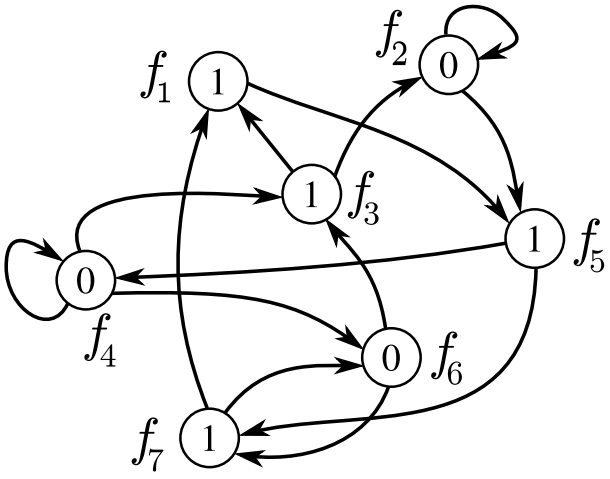

σ_4	σ_6	f_3
0	0	1
0	1	0
1	0	0
1	1	1

Figure 2.1: An illustration of a Boolean network with seven nodes. Each node has two input links, a binary state variable $\sigma_i \in \{0, 1\}$ and a Boolean update rule f_i assigned to it. As an example, the truth table for the function f_3 is given.

different, when the parameters of the networks are changed. In the frozen phase the perturbation of the state of one node propagates on average to less than one node in one time step. When the perturbation of the state of one node propagates on average to more than one node the system is said to be in the chaotic phase. On the boundary between the two phases are critical networks in which the information propagates on average to one node in one time step. The parameter regions in which distinct types of response of the system to perturbations exist can be seen as different dynamical regimes in which the system can function.

One convenient way of assessing whether a network is frozen or chaotic is to follow the time development of two identical systems with the initial states differing only in few nodes. The Hamming distance between the two networks is defined as the number of nodes that are in a different state. The Hamming distance at large times divided by the number of nodes can be seen as the order parameter of the phase transition. In the chaotic phase it becomes finite for large times, and in the frozen phase it approaches zero. In critical networks temporal evolution of Hamming distance is determined mainly by fluctuations.

In order to calculate the point of the phase transition between frozen and chaotic phase Derrida and Pomeau [22] introduced the annealed approximation. In the annealed approximation the inputs and the Boolean function of each node are assigned at every time step anew (according to restrictions given by the model). It is a mean-field theory, which neglects possible correlations between nodes. The assumption of the annealed approximation is that the network is infinitely large. This means

that fluctuations of global quantities are negligible. Similarly to what is done in numerical experiments, Derrida and Pomeau considered the distance between the equal time configurations on two randomly chosen trajectories in the same network (which is the same as the Hamming distance of the two identical network copies that started the time evolution in different states). The annealed approximation for the evolution of this average distance has been shown to be exact in the limit of large systems, up to times of the order of $logN$, when the connection loops can not be neglected anymore [21; 45]. Luque and Sole [68] used the annealed approximation to determine the critical point based on the damage spreading when a single element is modified, and their method reproduced exactly the results obtained by Derrida and Pomeau.

There is another order parameter that can be used to describe the phase transition between the two dynamical regimes. In 1988, Flyvbjerg introduced the concept of a stable core [32; 31], defined as the set of variables that evolve to a constant state not depending on the initial configuration. The fraction of variables belonging to the stable core may be regarded as an order parameter. In the limit of an infinite system it tends to a value less than 1 in the chaotic phase and it tends to 1 in the frozen phase and on the critical line. In the studies presented in Chapters 4 and 5 we will follow the formation of frozen regions and use a similar criterion for determining the critical line. The strength of this method is that it allows analytical considerations of real, quenched networks.

The following way of assigning the update functions to the nodes in the network is commonly used in defining Kauffman networks: for each node i and each of the 2^K possible combinations of values of input nodes, the output value is assigned at random,choosing 0 with probability p and 1 with probability $1-p$. The parameter p is called bias. In this case, there are only two parameters defining the Kauffman model, the number of inputs per node K and the bias p. This way of defining Boolean functions is very convenient when the model is studied in annealed approximation.

Both approaches outlined above, the annealed approximation and the determination of the frozen core, agree on the position of the critical line in the parameter space, which turns out to be given by the equation

$$2p_c(1-p_c) = 1/K\,.$$

We can determine the critical K value for a given bias, or the other way round, find the bias for which the network is going to be critical if the K value is given. In Figure 2.2 the phase diagram for the networks with this rule is shown.

In the case that all Boolean functions of K elements are equally probable (the case of uniformly distributed Boolean functions) which is actually the most simple and the most widely studied Boolean model, the bias p is $1/2$ and the networks are

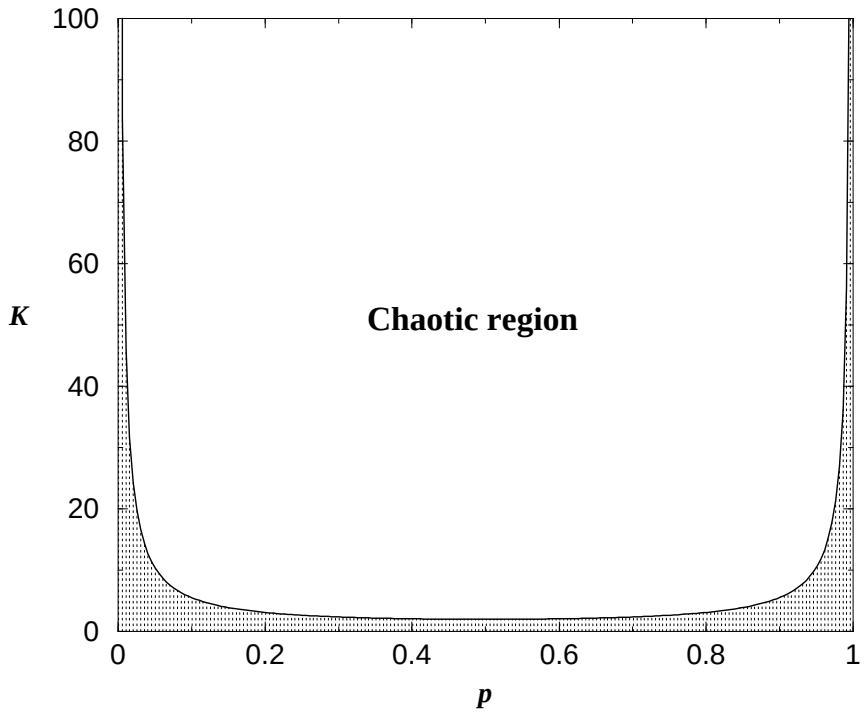

Figure 2.2: Phase diagram for the N-K model. The shaded area corresponds to the frozen phase, whereas the upper region corresponds to the chaotic phase. The curve separating both regions is the critical line $K_c = [2p(1-p)]^{-1}$ [5].

critical when $K = 2$. This result is also obtained in many numerical investigations of the model, including Kauffman's first articles.

Apart from being able to predict the right position of the critical line, the annealed approximation is also useful at predicting the proportion of nodes being in the state 1 in the network. This proportion can change with time, with dynamics depending on the networks parameters. Though in the most systems studied there is one fixed point for the proportion of 1 in the network which is reached after some transient time, there are systems where two fixed points appear [109] or where fixed points are unstable and where the oscillations and chaos occur [39].

However, the annealed approximation is not capable of predicting network's global dynamics, its steady states and the way its state space is organized. These network's properties are important. The knowledge we have about the state space of Boolean networks comes mainly from numerical investigations, which became more reliable only in the last decade when the computer power increased. Recently, some dynamical properties of the networks have been successfully studied analytically as we will see in detail later in the thesis.

2.3 The state space of Boolean networks

The way the state space of quenched Boolean networks is organized gives an insight into the networks' global dynamics. Presenting the network's dynamics in its state space is a convenient way of picturing the dynamics of the network, which makes recognizing the key elements of the dynamics easier. However, it does not help in predicting the behavior of a single network, since we know how the state space looks like only after knowing all the details of the network's dynamics. It is also not explaining the mechanisms behind the network's behavior, what is really important if we want to understand the model completely. Still, finding the state space properties common to different ensembles of networks in the same dynamical regime, helps deepening the understanding of the way the systems function. This picture is also a good background for defining clearly what we are looking for when simulating the network's dynamics. And, as already mentioned in the introduction, the analogies of the model's properties with those of the real genetic networks become much clearer when thinking in terms of the network's state space properties.

In order to see how the state space of a Boolean network is organized, and to define its main properties, let us go back to the definition of the network. A Boolean network consisting of N nodes can be represented as a set of N elements $\{\sigma_1, \sigma_2, \ldots, \sigma_N\}$, each of which is a binary variable $\sigma_i \in \{0, 1\}$, $i = 1, 2, \ldots, N$. The states of nodes and thus the state of the network change with time according to Equation (2.1.1). The set $\{\sigma_1(t), \sigma_2(t), \ldots, \sigma_N(t)\}$ represents the state of the network at time t. We could also think of this set as of a N-dimensional vector. The state space of a network is the collection of such sets of N variables, or vectors of length N, each representing a state of the network. Since every variable σ_i has only two possible values, the number of possible states the whole network can be in is 2^N. Each of the 2^N network states is represented by a point in the state space.

Dynamical evolution of the system, the way the network's state is changing with time, is then described by a trajectory in such a space. When a network's state changes, a link can be drawn in state space, from one state to the following state. The trajectory is a sequence of network's states presented in the state space as the collection of the points and the links connecting them. Since the dynamics is deterministic, each state in the state space has exactly one following state. Each state may at the same time have multiple predecessors, or none. A graphical representation of such an organization of a state space would be a network with nodes representing the states of a Boolean network, and the directed links showing how these states are changing with time. Each node of the network would have exactly one output, while the number of inputs would depend on the characteristics of the Boolean network. In Figure 2.3 a part of such a state space is shown. To differ this network from a graphical representation of a Boolean network, the arrows showing

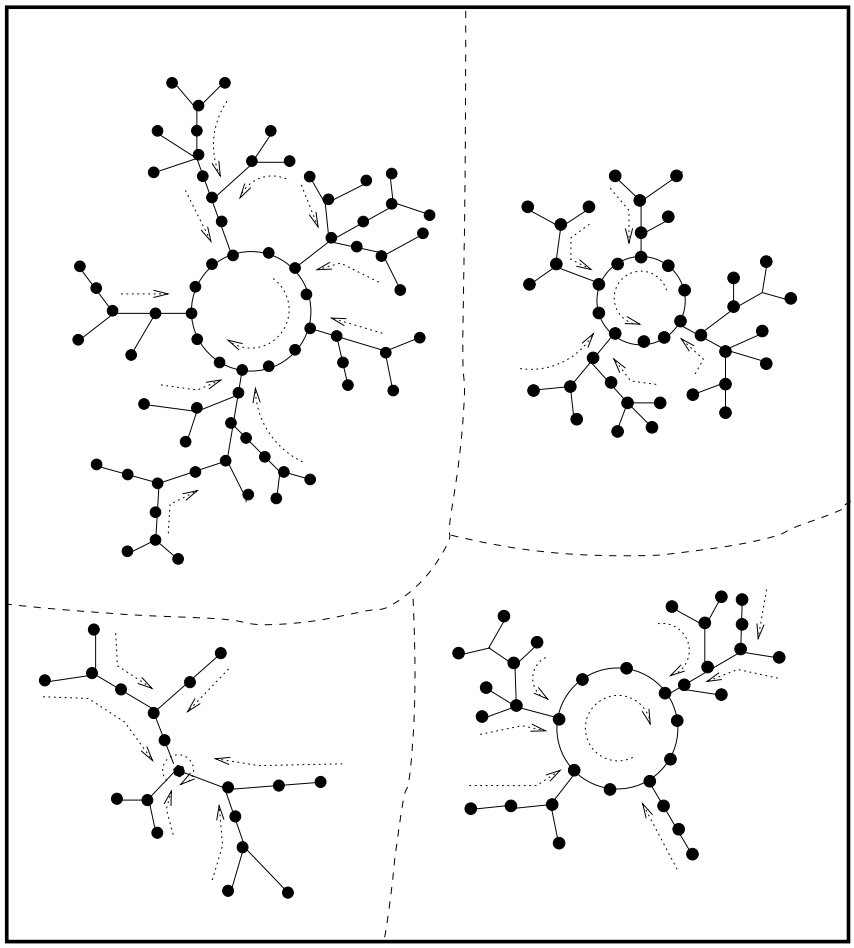

Figure 2.3: Schematic representation of the state space of a Boolean network. Each state is represented as a bold point. The state space is broken down into several attractors, represented as circles. Each initial state eventually will end up in one of these attractors (the arrows show the direction of the flow). The totality of states which evolve towards a given cycle, is the basin of attraction of that attractor. There can be attractors consisting of only one point, corresponding to an attractor of period 1 [5].

the direction of the dynamical evolution of the network are drawn aside the links connecting the states that follow one another.

The realization of the network, the choice of the topology and the functions assigned to its nodes, is defining completely the way the states in the state space are connected. The initial state of the network is then determining the trajectory in the state space the network will go through.

Let us now follow the change of the network's state with time. Since the state space is finite and the dynamics is deterministic, the network will eventually repeat

the state it was already in. From that time on, the dynamics of network is trapped on an *attractor*. In the state space attractors are represented by circles of different lengths. The length of such a circle is the number of states that belong to it, and it is called the size or a period of an attractor. The states leading to an attractor that are not part of it are the *transient states*. All transient states leading to the same attractor, together with the states belonging to that attractor, constitute one *basin of attraction*. In other words, for each attractor there is a basin of attraction, which is the set of initial states which eventually arrive on that attractor. The size, or length, of an attractor, or a transient, or the size of a basin of attraction, is the number of states belonging to it.

The state space of Boolean networks is organized into the set of basins of attraction (Figure 2.3), which sum up network's global dynamics. The number of attractors, their size, the size of the basins of attraction, or the length of transients, are all properties of the network's state space organization which are actually revealing the dynamical behavior of the model. These properties are also measures of convergence indicating the degree of order or chaos in the dynamics of the network. For example, the length of attractors of networks in different phases are quite different. On an attractor the nodes' states can either be fixed to one of the two possible values, or the nodes can change their states. When many nodes change their states, this is a sign of chaotic dynamics. If a large number of nodes are changing their states, a complicated pattern of behavior may arise, and the attractors of network in chaotic phase can be very long. We should note that in a finite system this is no real chaos because every trajectory becomes eventually periodic. If most of the nodes have fixed values on the attractors, the patterns of network's asymptotic activity are simple and the length of attractors remains small even when the size of the network is large. The networks in the frozen phase have mainly short attractors.

The state space properties measured for different network realizations are usually averaged when the characteristics of different dynamical regimes are discussed. If we know how the state space of a network is organized, we know everything about it's dynamics. Therefore, the straightforward way of exploring the properties of network's dynamics is the exhaustive numerical search of the state space. One of the ways to do that, is to initiate the network's dynamics in some chosen state and to follow how is the state of the network changing with time, till one of the states already visited is repeated. This way one of the possible trajectories in the state space has been found. Choosing always a new, not previously visited, state to start from, the same procedure could then be repeated for many many times till all the states in the state space have been visited. Keeping the record of the order in which the states are visited in each of the runs gives finally the complete picture of the state space organization. There are also some other alternative numerical procedures that could be faster than this one [115]. Still, the state space of the networks becomes extremely

large with increasing network size (as we have seen, its size is 2^N). Such explorations of the state space are therefore very demanding in the sense of computer time, and become almost impossible as soon as the size of the networks we want to study gets a bit larger. For Boolean networks with more than a handful of nodes, state space is already too vast to be searched exhaustively. Furthermore, since we want to make some general conclusions about networks of a certain kind, a large number of network realizations would have to be studied in this way. Therefore, for investigating properties of ensembles of Boolean networks, methods other than exhaustive search of the state space have to be employed. Most numerical investigations of Boolean networks have been done using random sampling. But, small attractor basins and those that occur in only a few network realizations are very hard to find by random sampling. When such basins are present in a greater number in the state space of the model, numerical studies are hampered by undersampling. Thus, when trying to understand the properties of the dynamics of Boolean networks, we can not rely on the results obtained from numerical investigations of the model only.

We have already mentioned in the introduction how the results of numerical simulations, in the time the model was introduced led to the wrong assumption that the number and the length of attractors grow as a square root with the size of a critical network. Supported by the analogy with biological data, for more than thirty years this prediction was believed to be correct. Only with increasing computer power in the last decade the new numerical experiments were able to show that this assumption may be wrong. The new numerical findings about the organization of the state space and the numerical studies of other properties of the networks motivated by them, made better understanding of the network's dynamics possible. This led to analytical studies which were able to make some final conclusions about the properties of the model's state space.

So, the new numerical results led to deeper understanding of the way the networks function, which then allowed for the analytical calculations confirming the assumption of numerics. This shows the importance of using different approaches when thinking about the way complex systems function. Some of them though abstract and intuitive and probably pretty distant from the way the real systems function may, in combination with numerical investigations simulating the real dynamics of the system, contribute to the understanding of the system's properties.

2.4 Concept of relevant nodes

The concept of relevant nodes is important for the studies presented in this thesis. This concept can be used when trying to understand the mechanism behind the network's global dynamics. It allows for a deeper understanding of the dynamics of

Boolean networks, and introduces alternative ways of analyzing model's properties. The recognition of the relevant elements as the only elements influencing the asymptotic dynamics was an important step in understanding the attractors of Kauffman networks.

Flyvbjerg and Kjær [33] introduced the concept of relevant nodes in the study of Kauffman's model with connectivity one. They recognized that only those nodes having active predecessors can be asymptotically active and that the nodes that are their own ancestors, the self-influencing nodes, are of the special importance. They called these nodes relevant since they found that they determine completely the asymptotic dynamics of the network. In the case of the networks they studied, relevant nodes were those on the loops with non-constant functions.

The definition of relevant elements that we use here was given by Bastolla and Parisi [9; 8]. They gained insight into the properties of the attractors by using numerical experiments based on the modular structure of the relevant nodes. The relevant nodes naturally form themselves into groups called modules [110; 8; 116] (these groups of nodes are also called relevant components [57]). Different modules do not influence one another. In the asymptotic dynamics, the states of the nodes of a module go through a cycle of states depending only on the module's organization. Each of the modules determines such a cycle of its nodes' states. Since the modules are independent, an attractors in the state space, i.e., the asymptotic dynamics of the whole network, is a combination of cycles of the modules. The dynamics of the whole network can therefore be reduced to the dynamics of such modules. The relevant elements determine through their modular organization completely the number and the length of attractors in the network [33; 9; 8].

Let us now repeat the main conclusions concerning the concept of relevant nodes and define some terms we will use in our studies of the dynamics of Boolean networks. The asymptotic dynamics of networks is defined by the states on the attractors in the state space. When the network has settled on an attractor, we can look again at the dynamics of different nodes on such an attractor. The states of nodes on an attractor are either fixed to one of the Boolean values, or are changing their value driving the network to the next state on the attractor. The nodes which are not changing their values are called *frozen* nodes. They comprise the stable or the *frozen core* of the network. All the other nodes we will call *nonfrozen*. Among them we can distinguish between *relevant* and *irrelevant* nodes. Relevant nodes are those changing their values and influencing at least one other relevant node, possibly itself. All other nonfrozen nodes are then irrelevant nodes. The definition of relevant nodes is already saying that they have to be organized in loop-like structures.

The names of different dynamical types of nodes reveal their role in the dynamics of the network. Relevant nodes are those determining completely, through their modular organization, the number and the length of attractors in the network. These

nodes are influencing each other, and the way they are organized defines all possible combinations of the states the network on an attractor can be in. Irrelevant nodes have dynamics which is in the stationary state only slaved to the dynamics of relevant nodes, since they have such nodes among their predecessors and are influenced by them. At the same time, among their successors there are no relevant nodes, and the chain of nodes influenced by their change is eventually ending either with the nodes without output links or with those with the frozen dynamics. This way their influence is lost and they are irrelevant for the network's asymptotic dynamics. Finally, frozen nodes provide constant input to other nodes and are otherwise irrelevant for the networks dynamics.

2.5 Variations of the model

Common to all Boolean network models is the directness of the links between the nodes in the network, and the binary nature of the node's dynamics, with their states being Boolean functions of the input nodes' states in the previous time step. Different variations of the Boolean model are defined by the choice of the network's topology, of the distribution of Boolean functions in the network, and of the order in which the states of the nodes are updated.

In the original random Boolean network model [56], the network's topology is random (with a fixed number of inputs per node and a Poisson distribution in the number of outputs), the functions are chosen from the uniform distribution of Boolean functions, and the nodes are updated in parallel. Modifications to this model led to creation of different variants of the Boolean network model. The modifications were generally inspired by the biological information which became available in the last years.

The modified models are expected to be biologically more realistic. They can also enable studies of the properties the original model does not have, but which could be relevant for modeling real systems. On a more general level, modified models can help to understand which dynamical properties of the Boolean model are independent of the model's details. But, the modified models are mainly more complicated, and their analysis is therefore more difficult. Only recently computers became powerful enough to make such analysis possible. The experimental data motivating and justifying modifications to the original model became also only newly available. Therefore, we are only at the beginning of the studies of different variants of the Boolean model, where many questions are not yet answered and where many other questions are still to be asked.

Some of the possible variations of the model are given below. We will here not go into the consequences of the model's modifications on the network's dynamical

properties. One of the possible modifications of the model, the generation of networks by evolution, is the subject of this thesis. The influence of the modifications to the model on its dynamical properties will in this case be discuss in detail, in Chapter 6 .

The modifications to the model's topology can be done by changing distribution of the number of input links and/or the number of output links per node, in all networks of the ensemble. The standard modification is the use of Poisson instead of the fixed input distribution [87; 5]. Because of their presence in the nature, the use of the power-law distributions for modifying topology of the networks gained special attention in the last few years [3; 35; 93]. Networks with small-world properties [30] have also been studied, as a modification of the Boolean model on a lattice[103; 104; 23].

Instead of defining a model network as a member of an ensemble of networks, whose topologies have given distributions of links, the model can be defined by assigning a specific topology to the network. New experimental data made it possible to use the topologies of real gene regulatory networks. Such models could successfully predict sequences of activation patterns in real networks [64; 2; 72; 20]. Finally, the topology of the model can also be changed using some evolutionary process. These processes can also change the functions of the network and the structure of the ensemble of networks.

Not much is known about the functions of the genes in real networks. Still, biological data can help to choose more realistic subsets of Boolean functions for modeling gene regulation [43; 54; 83; 99; 50]. The most common modification made to the choice of Boolean functions of the original model is the introduction of canalization, which has been argued to be a prevalent property of the updating functions of real-world genetic networks. A canalizing Boolean function is one in which at least one value of at least one input to the function can force the output to take a certain value. In the modified model the functions assigned to the nodes are randomly chosen from the subset of canalizing functions [55; 75] The networks we will evolve in the Chapter 6 will have canalizing functions assigned to the nodes. Properties of networks with other subsets of functions, closely related to canalizing, have also been investigated: chain functions [37], Post-class defined functions [99], and nested canalizing functions [54].

Another subset of Boolean functions has been studied as biologically relevant: threshold functions [109; 60; 61; 87; 46]. In these functions, the output of a node depends on whether the sum of the inputs is larger than some threshold value. The links in the network are defining coefficients in the sum (chosen mainly to be 1,-1). The treatment of case when the sum has exactly the threshold value defines two possible realizations of the model. In addition, models with variations in the coefficients in the sum and in the distribution of the threshold values have been

studied [86; 95] Threshold functions were used in modeling networks with the real topology [64].

The synchronous updating of nodes is not biologically justified. There is usually no central pacemaker telling all nodes in a network when to perform the next update. Therefore, Boolean networks with several different updating schemes have been studied [38; 44; 59; 69; 40]. By the stochastic asynchronous update, a probability for being updated is assigned to each node in the network. This updating scheme can be used to model noise which is ubiquitous in gene regulatory networks [70]. Boolean networks with stochastic update are for instance investigated in [59; 40].

The noise can also affect the update function. In this case the output of a node can deviate from the value prescribed by the update function with a probability that depends on the strength of the noise. Investigations of networks with such a type of noise can be found in [97; 82; 81].

3 Critical networks with one input per node

Networks with one input per node are the simplest possible random Boolean networks. Many properties of these networks can be derived analytically. Nevertheless, they are nontrivial and share many features with networks with larger values of K. Therefore we start our investigations of dynamics of critical Kauffman networks by having a closer look at $K = 1$ networks.

As already mentioned, this thesis focusses on the dynamics of critical Boolean networks, which lie at the boundary between a frozen phase and a chaotic phase [22; 23]. In the frozen phase, a perturbation at one node propagates during one time step on average to less than one node, and the attractor lengths remain finite in the limit $N \to \infty$. In the chaotic phase, the difference between two almost identical states increases exponentially fast, because a perturbation propagates on average to more than one node during one time step [5]. Critical Kauffman networks with one input per node are special since their dynamics does not show chaotic behavior. By adjusting the weights of the different classes of Boolean functions, a network with $K = 1$ can be brought to the border of the frozen regime where its dynamics becomes critical. In such a critical $K = 1$ network, out of the four possible updating functions only the two non-constant ones occur. This network is critical because a perturbation at one node propagates during one time step on average to one other node.

Based on our knowledge of the topology of these networks and on the simplicity of their Boolean functions, we will use simple probabilistic arguments to derive conclusions about networks' dynamical properties such as lengths and numbers of their attractors. The concept of relevant nodes, which was actually first introduced in the study of these networks [33], is particularly useful when investigating dynamics of networks with $K = 1$. All their relevant nodes are organized in loops and since the topology of these networks consists of loops and trees only, conclusions about the number and the length of attractors can be obtained analytically by using some basic knowledge about the dynamical rules and the topology of these networks.

In this chapter we will show that for $K = 1$ critical networks the mean number of attractors as well as their mean length grows faster than any power law with the network size. These results will be derived by generating the networks through a

In	$\mathcal{F}$		$\mathcal{R}$	
0	1	0	0	1
1	1	0	1	0

Table 3.1: The 4 update functions for nodes with 1 input. The first column lists the 2 possible states of the input, the other columns represent one update function each, falling into two classes.

growth process and by calculating lower bounds. In the next section we will define the main topological and dynamical properties of the model. Then, in Section 3.2, the lower bound for the mean number of attractors, and in Section 3.3 the lower bound for the mean length of attractors in critical networks with $K = 1$ is found, showing that both of these properties grow faster than any power law with the network size. At the end of this chapter, the conclusions address implications of our findings. The results presented in this chapter were obtained in collaboration with Barbara Drossel and Florian Greil and are published in *Physical Review Letters* [29].

3.1 Basic properties of the model

Since each node in a network has exactly one input, but can have any number of outputs from zero to N, any of the N nodes of Kauffman network with connectivity $K = 1$ lies either on a loop or on a tree rooted in a loop. A small network of this type is illustrated in Figure 3.1. A number of topological properties of this class of networks can be exactly calculated. Several such results have been obtained by Flyvbjerg and Kjær [33]. We will use some of them and derive some others needed for our calculations.

Table 3.1 lists the 4 Boolean functions of one argument, which are the possible update functions for $K = 1$ networks. The first two functions are constant, or *frozen*, i.e. the state of the node is independent of its inputs. The other two functions change whenever an input changes, i.e., they are *reversible*. The third function is the "copy" function, the fourth is the "invert" function.

Knowing that the topology of $K = 1$ networks consists only of loops and trees rooted in them and that only two types of functions, frozen (constant) and nonfrozen, exist, allows us to calculate the networks' dynamical properties. After a transient time, the state of the nodes on the trees will be independent of their initial state. If a node on a tree does not have a constant function, its state is determined by the state of its input node at the previous time step. All nodes that are downstream of

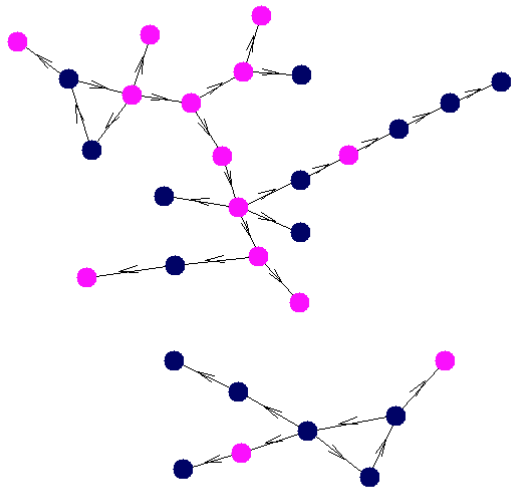

Figure 3.1: Illustration of a network with one input per node. Different colors of the nodes represent two possible states a node can be in. The network has two components, both gathered around loops of length tree. Most of the nodes in the network are on the trees rooted in those loops.

a node with a constant function will become frozen. If there is no constant function in the loop and in the path from the loop to a node, the dynamics of this node is slaved to the dynamics of the loop. Thus, the dynamics on the loops determines the dynamics on the entire network, and the dynamics on the trees is slaved to the dynamics on the loops.

Only loops that contain no constant function can show a nontrivial dynamics. The nodes in such loops are relevant. If all 4 update functions are chosen with a nonzero probability, only short loops have a non-vanishing probability of not containing a constant function [33]. Thus the number of relevant elements remains finite in the limit of infinite network size, and these networks are always in the frozen phase [8].

For this reason, a critical Kauffman network with one input per node has only non-constant Boolean functions assigned to the nodes. In such a network there are no nodes that are frozen on the same value on all attractors. A loop of size 1 can have a state that is constant in time (when having "copy" update function), but it can take two different values. States of nodes on larger loops also have two fixed points. Part of the nodes in a critical $K = 1$ networks are therefore frozen on some attractors or even on all attractors, however, they can be frozen in different states. In

these networks there is no frozen core. The nodes that are on the loops are relevant nodes, and the nodes on the trees are irrelevant for the system's dynamics. All nodes react to a change in their predecessor, thus a perturbation at one node propagates during one time step to one node on average. These networks are therefore critical.

In order to determine the attractors in the state space of a network, it is sufficient to obtain all the cycles of states of all loops. The nodes of each loop can go through cycles of different length. The number and length of these cycles depend on the size of the loop and on the functions that are assigned to the nodes in the loop. Once the cycles on each loop are determined, the attractors of the entire networks can be found from combinatorial arguments.

The following consideration about these cycles will prove useful for the calculations of the next two sections. The number and the lengths of the cycles on a loop does not depend on the exact assignment of the "copy" or "invert" functions to each node, but only on the parity of the number of "invert" functions. If the number of "invert" functions is odd, we call the loop an odd loop. Otherwise it is an even loop. Replacing two "invert" functions with copy functions and replacing the states $\sigma_i(t)$ of the two nodes controlled by these functions and of all nodes in between with $1-\sigma_i(t)$, is a bijective mapping from one loop to another. In particular, the number and length of cycles on the loop is not changed. All odd loops can thus be mapped on loops with only one "invert" function, and all even loops can be mapped on loops with only "copy" functions. [33; 28].

We first consider even loops with only "copy" functions. The cycle lengths of an even loop of length l are 1, l, and divisors of l. These loops have two fixed points (cycles of length one), where all nodes are in the same state. If l is a prime number, all other states belong to cycles of period l. Any initial state occurs again after l time steps. Therefore the number of cycles on an even loop is

$$\frac{2^l-2}{l}+2$$

if l is a prime number. The numerator counts the number of states that are not fixed points. The first term is therefore the number of cycles of length l. Adding the two fixed points gives the total number of cycles. If l is not a prime number, there exist cycles with all periods that are a divisor of l and the number of cycles is different.

Next, let us consider odd loops with one "invert" function. After at most $2l$ time steps, the loop is in its original state. If l is a prime number, there is only one cycle that has a shorter period. It is a cycle with period 2, where at each site 0s and 1s alternate. The total number of cycles on an odd loop with a prime-valued l is therefore

$$\frac{2^l-2}{2l}+1\,.$$

If l is not a prime number, there are also cycles with a period that is twice a divisor of l.

3.2 The mean number of attractors

Let us now show that the mean attractor number increases faster than any power law with N. Let n_l be the number of loops of length l, and $m = \sum_{l=1}^{N} n_l\, l$ the number of nodes in the loops. m is related to the attractors via

$$\sum_i \nu_i A_i \;=\; 2^m\,, \tag{3.2.1}$$

where ν_i is the number of attractors of length A_i. From here we see that finding an upper bound for the attractor length gives us a lower bound for the attractor number.

The attractor length A is the least common multiple of cycle lengths (periods) of the loops,

$$A \le A_{\max} \;=\; \mathrm{LCM}(2l_1, 2l_2, \ldots) \le 2\prod_i l_i\,. \tag{3.2.2}$$

For a fixed m, this product reaches its maximum if all l_i are equal, $l_i = l\,\forall i$. In this case we have $m = n_l\, l$ and $A < 2\, l^{n_l}$. Maximizing this product as a function of the number n_l of loops of length l

$$\frac{\mathrm{d}}{\mathrm{d}n_l}\left(2\, l^{n_l}\right) \;=\; 2\,\frac{\mathrm{d}}{\mathrm{d}n_l}\left(\frac{m}{n_l}\right)^{n_l} = 0$$

we obtain

$$A_{\max} \le 2\prod_i l_i \;\le\; 2\exp\left(\frac{m}{e}\right) = 2\cdot 2^{0.53m}. \tag{3.2.3}$$

A slightly better upper bound of the form $2^{0.5m}$ was derived in [33], using a much more complicated calculation. From Eqs. (3.2.3) and (3.2.1), we obtain a lower bound for the number ν_i of attractors,

$$\sum_i \nu_i \;\ge\; \frac{1}{2}\cdot 2^{0.47m}\,. \tag{3.2.4}$$

Averaging over the different network realizations gives

$$\overline{\sum_i \nu_i} \;\ge\; \frac{1}{2}\cdot\overline{2^{0.47m}} \ge \frac{1}{2}2^{0.47\overline{m}}\,. \tag{3.2.5}$$

An analytical expression for $\overline{m}$ can be derived from the exact results in [33]. One of them is the expectation value for the mean number of the loops of the length l in the large N limit

$$\overline{n_l} \;=\; \frac{1}{l}\exp\left(\frac{-l^2}{2N}\right) . \tag{3.2.6}$$

This result follows also from our Eqs. (3.3.2) and (3.3.1) below. Thus we find for the mean value of the number of nodes that are on loops

$$\overline{m} \;=\; \sum_{l=1}^{N} \overline{n_l}\, l = \sum_{l=1}^{N} \exp\left(\frac{-l^2}{2N}\right) .$$

Approximating this sum with an integral one obtains $\overline{m} \approx \sqrt{\frac{\pi}{2}N}$. Inserting this expression in Equation (3.2.5) gives

$$\overline{\sum_i \nu_i} \;\geq\; \frac{1}{2}\cdot\exp\left(0.4\sqrt{N}\right) . \tag{3.2.7}$$

We see that the mean number of attractors grows at least as fast as $\exp\left(0.4\sqrt{N}\right)$ with the number of nodes. Thus we have proven that in critical Kauffman networks with one input per node mean number of attractors grows faster than any power law with the network size.

3.3 The mean length of attractors

Next, we will show that the mean attractor length diverges faster than any power law. For this purpose, we generate the ensemble of all realizations of networks of size $N+1$ via a growth process from the ensemble of networks of size N. The following rule ensures that each network of the new ensemble is generated exactly once. The nodes are distinguishable and numbered in the sequence in which they were added. To every network of the initial ensemble we insert a new node and add a new link. The new node has either itself as input or is linked to a node from the already existing network. Next, we have to assign to this new node all possible combinations of outgoing links. This is done such that all possible combinations of the predecessor's outgoing links can become the outgoing links of the new node. If the new node is connected to itself any combination of outgoing links of node number 1 that are not on a loop can be moved to it. Different rearrangements of these links are weighed equally and every such network belongs to the new ensemble of the networks with $N+1$ nodes. This procedure guarantees that the number of inputs per node of the already existing network is not changed. If the node being the

one linked to the inserted node was on the loop, there is a probability of $\frac{1}{2}$ that the new node is going to be on the loop (since $\frac{1}{2}$ is the probability that the predecessor's outgoing link that was the part of the loop is shifted to the new node). One can see that the already existing loops become bigger with time, and that new loops with only one node are created.

Size and distribution of loops

We now consider the growth of the networks as a dynamical process, and we focus only on the loops. Since every node has the same distribution of numbers and sizes of trees connected to it, all nodes in all loops become connected to a new node with the same probability in the ensemble. We define the time scale such that the rate of insertion of new nodes at a given position in a given loop is unity,

$$\mathrm{d}t = \frac{1}{2N}\mathrm{d}N \quad \Rightarrow \quad t = \ln\sqrt{N}\,. \tag{3.3.1}$$

Note that N now denotes the mean network size in the growing ensemble. By going from exact insertion numbers to insertion rates, we have made a transition to a "grand canonical" ensemble. Within this ensemble, a loop of size l becomes a loop of size $l+1$ with probability ldt during a time interval dt. We then obtain the following equations for the mean number $\overline{n_l}$ of loops of size l

$$\begin{aligned}
\frac{\mathrm{d}}{\mathrm{d}t}\overline{n_1} &= 1 - \overline{n_1} \\
\frac{\mathrm{d}}{\mathrm{d}t}\overline{n_l} &= (l-1)\overline{n_{l-1}} - l\,\overline{n_l}\;\forall\, l > 1
\end{aligned}$$

With the initial condition $N(0) = 1$, these equations have the solution

$$\begin{aligned}
\overline{n_1}(t) &= 1 \\
\overline{n_2}(t) &= \frac{1}{2} - \frac{1}{2}e^{-2t} \\
\overline{n_3}(t) &= \frac{1}{3} - e^{-2t} + \frac{2}{3}e^{-3t} \\
\overline{n_4}(t) &= \frac{1}{4} - \frac{3}{2}e^{-2t} + 2e^{-3t} - \frac{3}{4}e^{-4t} \\
&\vdots
\end{aligned}$$

For the limiting case of large times, this solution can be approximated by

$$\overline{n_l}(t) = \frac{1}{l} - \frac{l-1}{2}e^{-2t} \tag{3.3.2}$$

which approaches the stationary solution $\overline{n_l} = l^{-1}$ for t $\to \infty$. Introducing the small parameter $\epsilon \ll 1$ as a measure of how far we are from the stationary solution, we find from

$$\overline{n_{l_c}}(t) = \frac{1}{l_c} - \frac{l_c - 1}{2} e^{-2 \ln \sqrt{N}} \quad = \quad (1 - \epsilon) \frac{1}{l_c}$$

that the critical value for the loop size for large ϵN is

$$l_c \quad = \quad \sqrt{2\epsilon N}\,. \tag{3.3.3}$$

In the same manner we may write the master equation for the probability distribution $P(n_1, \ldots, n_l)$ of the loops smaller than l,

$$\frac{\mathrm{d}}{\mathrm{d}t} P(n_1, \ldots, n_l) = -\sum_{i=1}^{l} i\ n_i\ P(n_1, \ldots, n_i, n_{i+1}, \ldots, n_l)$$
$$+ \sum_{i=1}^{l} (i-1)(n_{i-1} + 1)\ P(n_1, \ldots, n_{i-1} + 1, n_{i+1}, \ldots, n_l)$$

The stationary solution for this expression valid for the loops smaller than l_c is

$$P(n_1, \ldots, n_l) \quad = \quad \prod_{i=1}^{l} e^{-1/i} \left(\frac{1}{i}\right)^{n_i} \frac{1}{n_i!}\,. \tag{3.3.4}$$

This solution is time independent and we can conclude that the distribution of the loops smaller than l_c is not changing with time, i.e. with the growth of the system size. Furthermore the probabilities for having n_i loops of size i are independent from each other and Poisson distributed with a mean i^{-1}.

Evaluation of the lower bound for the mean attractor length

Equipped with these results, we can now evaluate the lower bound for the mean attractor length $\overline{A}$. Suppose that the system is enlarged so that its number of nodes is $N' = aN$, with $a > 1$ and N nodes of the previous system. The length of the attractor is the least common multiple of the loop periods, i.e. the cycle lengths of the loops. Since $\overline{A_{l_i \le N'}} \geq \overline{A_{l_i \le l_c(N')}}$, we obtain a lower bound by evaluating only the change of the least common multiple of the periods of loops smaller than l_c, that is the change of $\overline{A_{l_i \le l_c}} \equiv \overline{A_{\sqrt{2\epsilon N'}}}$, with increasing system size. Our above considerations show that the distribution of loops of size smaller than $l_c(N)$ does not change when going to an ensemble of systems of size N'. However, these systems contain additional loops in the interval $[l_c(N), l_c(N')]$. If the period of such an additional loop is a prime number larger than $l_c(N)$, the least common multiple of

all loop periods is multiplied by this period. A loop with a prime number of nodes has only two possible periods: 1 or l if the loop is even, and 2 or $2l$ if the loop is odd. If the additional loop is not on the cycle of length 1 or 2, the least common multiple of the periods of the loops smaller than $l_c(N')$ is at least as large as the product of the new loop size, and the least common multiple of the periods of the loops smaller than $l_c(N)$. The number of primes not exceeding the value of some positive number x is asymptotically expressed as $\pi_x = x/\ln x$ (see, e.g. [42]). The probability that a randomly chosen number in the interval $[l_c(N), l_c(N')]$ is a prime number is

$$P_{\text{prime}} = \frac{\pi_{\sqrt{2\epsilon N'}} - \pi_{\sqrt{2\epsilon N}}}{\sqrt{2\epsilon N'} - \sqrt{2\epsilon N}} \approx \frac{1}{\ln \sqrt{2\epsilon N'}}. \tag{3.3.5}$$

This is identical to the probability that the new loop size is a prime number. Taking all these considerations together, we have

$$\overline{A_{l_i \le N'}} \ge \overline{A_{\sqrt{2\epsilon N'}}} \ge P_{\text{loop}} P_{\text{not1,2}} \frac{1}{\sqrt{a}} \frac{\sqrt{2\epsilon N'}}{\ln(\sqrt{2\epsilon N'})} \overline{A_{\sqrt{2\epsilon N}}}.$$

The probability P_{loop} for having a loop in the interval $[l_c(N), l_c(N')]$ is obtained using (3.3.4). The probability of having no loop of size l, $n_l = 0$, is $e^{-1/l}$. Thus the upper bound for the probability of having no loops with size from the interval $[l_c(N), l_c(N')]$ is

$$\begin{aligned} 1 - P_{\text{loop}} &\le \prod_{i=l}^{a\,l} e^{-\frac{1}{i}} \le \left(\exp\left(-\frac{1}{al}\right)\right)^{al-l+1} \\ &= \exp\left(\frac{1-a}{a} - \frac{1}{al}\right) \overset{0 \le l^{-1} \le 1}{\le} e^{-1} \end{aligned}$$

giving

$$P_{\text{loop}} \ge 1 - e^{-1}. \tag{3.3.6}$$

The probability $P_{\text{not1,2}}$ that the new loop is not on an attractor of length 1 or 2 is obtained as follows: As we have seen in Section 3.1, the number of its cycles is $(2^l - 2)/l + 2$ in the case it is an even loop and $(2^l - 2)/2l + 1$ if it is an odd loop. Among these cycles two are of length 1 for the first type of loop and one is of length 2 for the second type. The probability that the loop of size l is not on a cycle of length 1 or 2 is $1 - 2l/2^l$ for large values of l. The loop we are observing is of size $\sqrt{2\epsilon N}$ and for the probability $P_{\text{not1,2}}$ we obtain

$$P_{\text{not1,2}} = 1 - \frac{2\sqrt{2\epsilon N}}{2^{\sqrt{2\epsilon N}}}. \tag{3.3.7}$$

For a given ϵ this probability is non-vanishing, i.e. $P_{\text{not1,2}} > \eta > 0$, if $N > 2/\epsilon$. Since we are considering the limit of large N, this condition is satisfied. Applying this result to the lower bound for the attractor size we finally have

$$\overline{A_{\sqrt{2\epsilon N'}}} \;\geq\; (1-e^{-1})\eta \frac{1}{\sqrt{a}} \frac{\sqrt{2\epsilon N'}}{\ln\sqrt{2\epsilon N'}} \overline{A_{\sqrt{2\epsilon N}}}\,. \tag{3.3.8}$$

Setting $N = a^{\mu} N_0$ and defining a constant C

$$C \;=\; \left(1-e^{-1}\right) \frac{\eta\sqrt{2\epsilon}}{\ln(\sqrt{2\epsilon a N_0})} \left(\frac{N_0}{a}\right)^{1/4}$$

Equation (3.3.8) can be transformed into

$$\overline{A_{l_i \leq N}} \;\geq\; \frac{C^{\mu} N^{\mu/4}}{\mu!}\,,$$

and finally with $\mu = (\ln(N/N_0)/\ln(a))$ into

$$\overline{A_{l_i \leq N}} \;\geq\; \left(\frac{N}{N_0}\right)^{\frac{4\ln C + \ln N}{4\ln a}} \frac{1}{(\ln(N/N_0)/\ln a)!} \overline{A_{\sqrt{2\epsilon N_0}}}\,. \tag{3.3.9}$$

This increases faster than any power law with N, but slower than a stretched exponential.

3.4 Conclusions

In this chapter we calculated the lower bounds for the mean number and the mean length of attractors in critical networks with connectivity one, and have shown that they both grow faster than any power law with the size of the network. We have also seen how dynamically different nodes in these network are organized. In critical Kauffman networks with one input per node there is no frozen core, so that the number of nonfrozen nodes is identical to the number of nodes in the network. There are of the order of $\sqrt{N}$ nodes on the loops, all of which are relevant, and the number of components of relevant elements is of the order of $\ln N$, since this is the mean number of loops in the network (we have seen in Equation 3.3.4 that the mean number of loops of size l is $1/l$; integrating over all possible loop sizes gives this estimation). In the next two chapters, we will see that these scaling with N of the number of relevant node is different for other critical random Boolean networks, but that the relation between the number of the relevant and nonfrozen nodes is the same, and that the results for the mean number and length of the atractors hold. This means that the attractors are too long and too numerous to represent cellular differentiation, to which the model was originally applied.

In the past, mainly critical $K = 2$ Kauffman networks with a constant probability distribution for the 16 possible updating functions were studied. Based on computer simulations, the mean attractor number of these networks was once believed to scale as $\sqrt{N}$ [56]. With increasing computer power, a faster increase was seen (linear in [11], "faster than linear" in [100], stretched exponential in [9; 8]). Finally, Samuelsson and Troein [90] proved analytically that the mean number of attractors grows indeed faster than any power law with the size of a critical network with two inputs per node. The investigations presented in this chapter show that this is also the property of critical Kauffman network with one input per node, and thus possibly a general property of all critical networks.

It may appear that the value of the studies presented in this chapter lies only in the fact that the findings of [90] were analytically proven to be correct for a rather special class of critical systems. This result is already remarkable, especially in the light of how rare analytically solvable problems in studies of complex systems are. The more intuitive way of treating the system, and the relatively simple mathematical arguments used (when comparing to other publications) have also their own virtue. But, the understanding of the organization of relevant nodes in these networks, and of the implications of their organization on the global dynamics of networks, is the key result. As we will see in the next two chapters, the results for the number of relevant nodes and their organization in $K = 1$ networks will prove crucial when determining the number and length of attractors for critical networks with larger K values, since it turns out that all critical networks have modular organization of relevant nodes similar to that of $K = 1$ critical networks. This becomes intuitively plausible if we think of the reduced network of nonfrozen nodes of critical Kauffman network with any value of K. In critical networks a perturbation of a node propagates to one node in one time step on average, and since nonfrozen nodes propagate these perturbations, this reduced network must have effectively one input per node. Thus, it resembles the critical $K = 1$ network. In the next two chapters we will give analytical arguments for the resemblance between the properties of $K = 1$ critical networks and those of the organization of the nonfrozen nodes in all other critical random Boolean networks.

Concerning the scaling behavior of the mean attractor length, there were no conclusive results in the literature at the time of the studies presented in this chapter. While it appeared that the mean attractor length increases as $\sqrt{N}$ in earlier times [56; 10], Bastolla and Parisi suggest that it might in fact increase faster than any power law [9; 8], and a recent review article treated this as an open question [5]. Just as for the attractor number, computer simulations are hampered by undersampling, which makes it virtually impossible to find attractors that occur only in few realizations or that have a small basin of attraction. The results presented in this chapter were the first analytical proof that the mean length of attractors grows faster

than any power law with the size of a critical network. This result was confirmed afterwards in [88; 27].

4 Critical networks with two inputs per node

Our next step is the study of the dynamics of critical networks with two inputs per node. These networks are the most widely studied example of critical networks. The reason is that networks with two inputs per node are critical when the uniform distribution of Boolean functions is chosen, and this distribution was the one mainly used in constructing the Kauffman model. The justification for using this distribution was in the lack of information about the real systems. When only little is known about the functions real genes might have, a completely random choice of Boolean functions is a valid null hypothesis, which can at the same time easily be implemented in numerical and analytical investigations of the system. In the studies presented in this chapter we will use a more general model in which Boolean functions belonging to different classes can have different weights. The standard unbiased model is then a special case in which all these weights are equal. In order to define the systems we will study, we fix K to 2 and determine for which combinations of weights of the different classes the networks are critical.

In investigating network's dynamics we will use the approach similar to that of the previous chapter. We will study the dynamics and the organization of relevant nodes, and then use the results of such investigations to make conclusions about the dynamics of the whole network. However, this task is much more demanding than in the case of networks with $K = 1$, since the identification of relevant nodes is not as easy.

Nodes of all three types appear in these systems: the relevant nodes, which change their states and influence at least one relevant node, determining completely the number and length of attractors; the irrelevant nodes which change their states but act only as slaves of the relevant nodes, and the nodes frozen on the same value on every attractor, which did not exist in the case $K = 1$. In order to determine which nodes are relevant, we identify the frozen nodes first. For this purpose we will use the approach introduced in [32]. We will define a stochastic process that starts from the nodes with constant update functions and determines iteratively the frozen core. Mean-field calculations for this process will reveal the position of the critical point. We will in addition go beyond mean-field theory which will bring us new insights

into the properties of nonfrozen nodes. Then, we will use another stochastic process to search for the relevant nodes among the nonfrozen nodes.

Socolar and Kauffman [100] found numerically that for critical $K = 2$ networks with uniform distribution of Boolean functions, the mean number of nonfrozen nodes scales as $N^{2/3}$, and the mean number of relevant nodes scales as $N^{1/3}$. The same result is hidden in the analytical work on attractor numbers by Samuelsson and Troein [90], as was shown in [27]. We will here go a step further by deriving these power laws analytically, and for a more general class of networks. We will show the asymptotic probability distribution of nonfrozen and relevant nodes in terms of scaling variables. We will also obtain results for the number of nonfrozen nodes with two nonfrozen inputs, and for the number of relevant nodes with two relevant inputs. This results will lead to new insights into the state space organization.

The outline of this chapter is the following. In the next section we will define the class of networks that we are investigating. In Section 4.2, we will introduce a stochastic process that determines the frozen core of the network starting from the nodes whose outputs are entirely independent of their inputs. Then, in Section 4.3, we are going to analyze the Langevin and Fokker-Planck equations that correspond to this stochastic process and that lead to the scaling behavior of the number of nonfrozen nodes. In order to identify the relevant nodes among the nonfrozen ones, we will introduce in Section 4.4 another stochastic process. This process will also enable us to find their scaling behavior. Finally, we will discuss in the last section the implications of our results. The results presented in this chapter were obtained in collaboration with Viktor Kaufman and Barbara Drossel and are published in *Physical Review E* [58].

4.1 The class of critical $K = 2$ networks

In $K = 2$ networks each node has 2 randomly chosen inputs. An illustration of a network with two inputs per node is shown in Figure 4.1. The 16 possible update functions that can be assigned to nodes with two inputs are shown in table 4.1.

The update functions fall into four classes [5]. In the first class, denoted by $\mathcal{F}$, are the frozen functions, where the output is fixed irrespectively of the input. The class $\mathcal{C}_1$ contains those functions that depend only on one of the two inputs, but not on the other one. The class $\mathcal{C}_2$ contains the remaining canalizing functions, where one state of each input fixes the output. The class $\mathcal{R}$ contains the two reversible update functions, where the output is changed whenever one of the inputs is changed. Critical networks are those where a change in one node propagates to one other node on an average. A change propagates with probability 1/2 to a node that has a canalizing update function $\mathcal{C}_1$ or $\mathcal{C}_2$, with probability zero to a node that has a

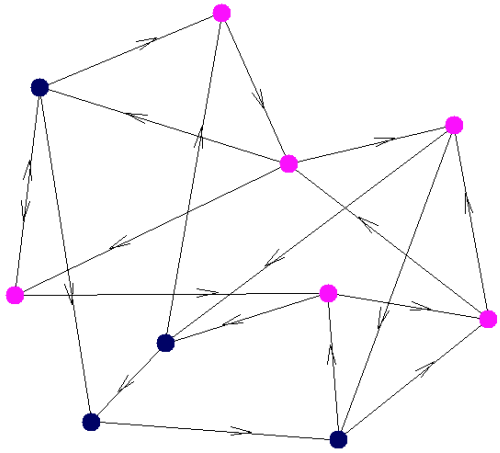

Figure 4.1: Illustration of a network with two inputs per node, different colors of the nodes represent two possible states a node can be in.

frozen update function, and with probability 1 to a node that has a reversible update function. Consequently, if the frozen and reversible update functions are chosen with equal probability, the network is critical. Usually, only those models are considered where all 16 update functions receive equal weight. We here consider the larger set of models where the frozen and reversible update functions are chosen with equal (and nonzero) probability, and where the remaining probability is divided between the $\mathcal{C}_1$ and $\mathcal{C}_2$ functions. Those networks that contain only $\mathcal{C}_1$ functions are different from the remaining ones. Since all nodes respond only to one input, the link to the second input can be cut, and we are left with a critical $K = 1$ network, which was already discussed in [33; 29; 27] and will not be discussed here. All the other models, where the weight of the $\mathcal{C}_1$ functions is smaller than 1, fall into the same class [27]. The treatment presented in the following, is based on the existence of nodes with frozen functions, and it therefore applies to all critical models with a nonzero fraction of frozen functions. Networks with only canalizing functions have to be discussed separately.

Let N_f be the number of nodes with a frozen function, N_r the number of nodes with a reversible function and N_{c_1} and N_{c_2} the number of nodes with a $\mathcal{C}_1$ and a $\mathcal{C}_2$ function. We define the systems we are going to consider through parameters $\alpha = N_{c_1}/N$, $\beta = N_r/N = N_f/N$, $\gamma = N_{c_2}/N$. These parameters give the fraction of each type of nodes in the network. In the next two sections, we determine the properties of the frozen core in the large N limit by starting from the nodes with a frozen function.

In	$\mathcal{F}$		$\mathcal{C}_1$				$\mathcal{C}_2$								$\mathcal{R}$	
00	1	0	0	1	0	1	1	0	0	0	0	1	1	1	1	0
01	1	0	0	1	1	0	0	1	0	0	1	0	1	1	0	1
10	1	0	1	0	0	1	0	0	1	0	1	1	0	1	0	1
11	1	0	1	0	1	0	0	0	0	1	1	1	1	0	1	0

Table 4.1: The 16 update functions for nodes with 2 inputs. The first column lists the 4 possible states of the two inputs, the other columns represent one update function each, falling into four classes.

4.2 A stochastic process that leads to the frozen core

Flyvbjerg [32] was the first one to use a dynamical process that starts from the nodes with constant update functions and determines iteratively the frozen core. Performing a mean-field calculation for this process, he could identify the critical point. We define in the following a process that goes beyond mean-field theory and gives exact results for the frozen core. We consider the ensemble of all networks of size N and with fixed parameters α, β, γ. All nodes with a frozen update function are certainly part of the frozen core. We now construct the frozen core by determining stepwise all those nodes that become frozen due to the influence of a frozen node. In the language of [100], this process determines the "clamped" nodes. Initially, we place the nodes in four containers labelled $\mathcal{F}$, $\mathcal{C}_1$, $\mathcal{C}_2$, and $\mathcal{R}$. These containers contain N_f, N_{c_1}, N_{c_2}, and N_r nodes initially. Since these numbers change during our stochastic process, we denote the initial values as N_f^{ini}, $N_{c_1}^{ini}$, $N_{c_2}^{ini}$, and N_r^{ini}, and the total number of nodes as N^{ini}. We treat the nodes in container $\mathcal{C}_1$ as nodes with only one input and with the update functions "copy" or "invert". The contents of the containers will change with time. The "time" we are defining here is not the real time for the dynamics of the system. Instead, it is the time scale for a stochastic process that we use to determine the frozen core. During one time step, we remove one node from the container $\mathcal{F}$ and determine all those nodes, to which this node is an input. A node in container $\mathcal{C}_1$ chooses this node as an input with probability $1/N$. It then becomes a frozen node. We therefore move each node of container $\mathcal{C}_1$ with probability $1/N$ into the container $\mathcal{F}$. A node in container $\mathcal{C}_2$ chooses the selected frozen node as an input with probability $2/N$. With probability $1/2$, it then becomes frozen,

because the frozen node is with probability 1/2 in the state that fixes the output of a $\mathcal{C}_2$-node. If the $\mathcal{C}_2$-node does not become frozen, it becomes a $\mathcal{C}_1$-node. We therefore move each node of container $\mathcal{C}_2$ during the first time step with probability $1/N$ into the container $\mathcal{F}$, and with probability $1/N$ into the container $\mathcal{C}_1$. Finally, a node in container $\mathcal{R}$ chooses the selected frozen node as an input with probability $2/N$ and becomes a $\mathcal{C}_1$-node. We therefore move each node of container $\mathcal{R}$ during the first time step with probability $2/N$ into the container $\mathcal{C}_1$. In summary, the total number of nodes, N, decreases by one during one time step, since we remove one node from container $\mathcal{F}$, and some nodes move to a different container. The removed nodes are those frozen nodes for which we already have determined whose input they are. Then, we take the next frozen node out of container $\mathcal{F}$ and determine its effect on the other nodes. We repeat this procedure until we cannot continue because either container $\mathcal{F}$ is empty, or because all the other containers are empty. If container $\mathcal{F}$ becomes empty, we are left with the nonfrozen nodes. We shall see below that most of the remaining nodes are in container $\mathcal{C}_1$, with the proportion of nodes left in containers $\mathcal{C}_2$ and $\mathcal{R}$ vanishing in the limit $N^{ini} \to \infty$. Then, the nonfrozen nodes can be connected to a network by choosing the input(s) to every node at random from the other remaining nodes. If all containers apart from container $\mathcal{F}$ are empty at the end, the entire network becomes frozen. This means that the dynamics of the network go to the same fixed point for all initial conditions. Figure 4.2 illustrates the process of determining the frozen core.

Let us first describe this process by deterministic equations that neglect fluctuations around the average change of the number of nodes in the different containers. As long as all containers contain large numbers of nodes, these fluctuations are negligible, and the deterministic description is appropriate. The average change of the node numbers in the containers during one time step is

$$\begin{aligned} \Delta N_r &= -\frac{2N_r}{N} \\ \Delta N_{c_2} &= -\frac{2N_{c_2}}{N} \\ \Delta N_{c_1} &= -\frac{N_{c_1}}{N} + \frac{N_{c_2}}{N} + \frac{2N_r}{N} \\ \Delta N_f &= -1 + \frac{N_{c_1}}{N} + \frac{N_{c_2}}{N} \\ \Delta N &= -1 \end{aligned} \tag{4.2.1}$$

The number of nodes in the containers, N, can be used instead of the time variable, since it decreases by one during each step. The equation for N_r can then be solved by going from a difference equation to a differential equation,

$$\frac{\Delta N_r}{\Delta N} \simeq \frac{dN_r}{dN} = -\frac{2N_r}{N}\,,$$

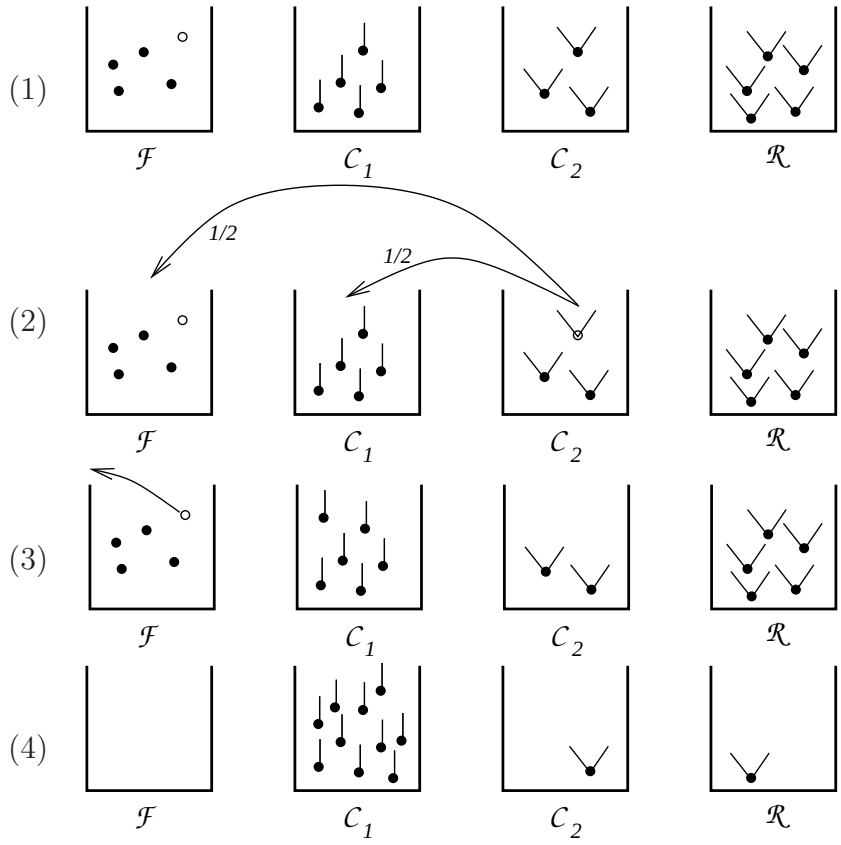

Figure 4.2: Illustration of the freezing process. (1) Initially, a frozen node is chosen (marked in white), (2) then it is determined to which node(s) this is an input and the effect on those nodes is determined. (3) Then, the selected frozen node is removed. (4) The last picture sketches the final state, where all frozen nodes have been removed and most remaining nodes have 1 nonfrozen input [28].

which has the solution

$$N_r = N^2 \frac{N_r^{ini}}{(N^{ini})^2} \,. \tag{4.2.2}$$

Similarly, we find

$$\begin{aligned} N_{c_2} &= N^2 \frac{N_{c_2}^{ini}}{(N^{ini})^2} \\ N_f &= N \frac{N_f^{ini} - N_r^{ini}}{N^{ini}} + N^2 \frac{N_r^{ini}}{(N^{ini})^2} \\ N_{c_1} &= N \frac{N_{c_1}^{ini} + N_{c_2}^{ini} + 2N_r^{ini}}{N^{ini}} - 2N^2 \frac{N_r^{ini} + N_{c_2}^{ini}}{(N^{ini})^2} \,. \end{aligned} \tag{4.2.3}$$

For $N_f^{ini} < N_r^{ini}$, we obtain $N_f = 0$ at a nonzero value of N, and the number of nonfrozen nodes is proportional to N^{ini}. We are in the chaotic phase. For $N_f^{ini} > N_r^{ini}$, the values N_r and N_{c_2} will sink below 1 when N becomes of the order $\sqrt{N^{ini}}$. For smaller N, there are only $\mathcal{F}$ and $\mathcal{C}_1$ nodes left, and the second term contributing to N_f and N_{c_1} in (4.2.3) can be neglected compared to the first one. When N_f falls below 1, there remain $N_{c_1} = \frac{N_{c_1}^{ini} + N_{c_2}^{ini} + 2N_r^{ini}}{N_f^{ini} - N_r^{ini}}$ nodes of type $\mathcal{C}_1$. The network is essentially frozen, with only a finite number of nonfrozen nodes in the limit $N^{ini} \to \infty$. If we now choose the inputs for these nodes, we obtain simple loops with trees rooted in the loops. This property of the frozen phase was also found in [100].

For the critical networks that this chapter focuses on, we have $N_f^{ini} = N_r^{ini} = \beta N^{ini}$, and the stochastic process stops at $N_f = 1 = \beta N^2 / N^{ini}$. This means that

$$N^{end} = \sqrt{\frac{N^{ini}}{\beta}} \,. \tag{4.2.4}$$

The number of nonfrozen nodes would scale with the square root of the network size if the deterministic approximation to the stochastic process was exact. We shall see below that including fluctuations changes the exponent from 1/2 to 2/3. The final number of $\mathcal{C}_2$-nodes for the deterministic process for the critical networks is γ/β, which is independent of network size, and the final number of $\mathcal{R}$-nodes vanishes due to $N_r = N_f$. We shall see below that the fluctuations change these two results to a $(N^{ini})^{1/3}$-dependence.

Introducing $n = N/N^{ini}$ and $n_j = N_j/N^{ini}$ for $j = r, f, c_1, c_2$, Equations (4.2.3) simplify to (using $N_r^{ini} = N_f^{ini}$)

$$\begin{aligned} n_r &= \beta n^2 = n_f \\ n_{c_2} &= \gamma n^2 \\ n_{c_1} &= n - 2\beta n^2 - \gamma n^2 \,. \end{aligned}$$

This means that our stochastic process remains invariant (in the deterministic approximation) when the initial number of nodes in the containers and the time unit

are all multiplied by the same factor. For small n, the majority of nodes are in container $\mathcal{C}_1$, since $n_{c_1} = n - \mathcal{O}(n^2)$. Now, if we choose a sufficiently large N^{ini}, n reaches any given small value while $N_f = N_r = \beta n^2 N^{ini}$ is still large enough for a deterministic description. We can therefore assume that for sufficiently large networks $N_f/N = \beta n$ becomes small before the effect of the noise becomes important. This assumption will simplify our calculations below.

4.3 The effect of fluctuations

The number of nodes in container $\mathcal{C}_1$ that choose a given frozen node as an input is Poisson distributed with a mean N_{c_1}/N and a variance N_{c_1}/N. We now assume that n is small at the moment where noise becomes important, i.e., that the variance of the noise $N_{c_1}/N = n_{c_1}/n = 1 - (2\beta + \gamma)n = 1 - \mathcal{O}(n)$ is unity. The number of nodes in containers $\mathcal{C}_2$ and $\mathcal{R}$ that choose a given frozen node as an input is Poisson distributed with a mean and a variance $2(N_{c_2} + N_r)/N$. The fluctuation around the mean can be neglected as this noise term is very small compared to N_r and N_{c_2}, the final values of which are large for sufficiently large N^{ini}. We therefore obtain the stochastic version of Equations (4.2.1)

$$\begin{aligned} \Delta N_r &= -\frac{2N_r}{N} \\ \Delta N_{c_2} &= -\frac{2N_{c_2}}{N} \\ \Delta N_f &= -\frac{N_r}{N} - \frac{N_f}{N} + \xi \\ \Delta N &= -1 \end{aligned} \tag{4.3.1}$$

The random variable ξ has zero mean and unit variance. As long as the n_j change little during one time step, we can summarize a large number T of time steps into one effective time step, with the noise becoming Gaussian distributed with zero mean and variance T. Exactly the same process would result if we summarized T time steps of a process with Gaussian noise of unit variance. For this reason, we can choose the random variable ξ to be Gaussian distributed with unit variance.

Compared to the deterministic case, the equations for N_r and N_{c_2} are unchanged, and we have again $N_r = N^2 N_r^{ini}/(N^{ini})^2$ and $N_{c_2} = N^2 N_{c_2}^{ini}/(N^{ini})^2$. Inserting the solution for N_r into the equation for N_f, we obtain

$$\frac{dN_f}{dN} = \frac{N_f}{N} + \frac{\beta N}{N^{ini}} + \xi \tag{4.3.2}$$

with the step size $dN = 1$ and $\langle \xi^2 \rangle = 1$. (In the continuum limit $dN \to 0$ the noise correlation becomes $\langle \xi(N)\xi(N') \rangle = \delta(N - N')$). This is a Langevin-equation, and we

will now derive the corresponding Fokker-Planck-equation [85; 111]. Let $P(N_f, N)$ be the probability that there are N_f nodes in container $\mathcal{R}$ at the moment where there are N nodes in total in the containers. This probability depends on the initial node number N_{ini}, and on the parameter β. The sum

$$\sum_{N_f=1}^{\infty} P(N_f, N) \simeq \int_0^{\infty} P(N_f, N) dN_f$$

is the probability that the stochastic process is not yet finished, i.e. the probability that N_f has not yet reached the value 0 at the moment where the total number of nodes in the containers has decreased to the value N. Since systems that have reached $N_f = 0$ are removed from the ensemble, we have to impose the absorbing boundary condition $P(0, N) = 0$. Let $g(\Delta N_f | N_f, N)$ denote the probability that N_f decreases by ΔN_f during the next step, given the values of N_f and N.

We have

$$\begin{aligned}
&P(N_f, N-1) = \\
&\int_0^{\infty} P(N_f + \Delta N_f, N) g(\Delta N_f | N_f + \Delta N_f, N) d(\Delta N_f) \\
&= \int_0^{\infty} \Big[P(N_f, N) g(\Delta N_f | N_f, N) \\
&\quad + \frac{\partial}{\partial N_f} (P(N_f, N) g(\Delta N_f | N_f, N)) \Delta N_f \\
&\quad + \frac{\partial^2}{2\partial^2 N_f^2} (P(N_f, N) g(\Delta N_f | N_f, N)) (\Delta N_f)^2 \\
&\quad + \ldots \Big] d(\Delta N_f) \\
&= P(N_f, N) + \frac{\partial}{\partial N_f} (P(N_f, N) \langle \Delta N_f \rangle) + \\
&\quad \frac{\partial^2}{2\partial N_f^2} (P(N_f, N) \langle (\Delta N_f)^2 \rangle) + \ldots
\end{aligned}$$

The mean change $\langle \Delta N_f \rangle$ during one step is $\langle \Delta N_f \rangle = \frac{N_f}{N} + \frac{\beta N}{N^{ini}}$, and the mean square change is $\langle (\Delta N_f)^2 \rangle \simeq 1$.

This gives the Fokker-Planck equation for our stochastic process

$$-\frac{\partial P}{\partial N} = \frac{\partial}{\partial N_f} \left(\frac{N_f}{N} + \frac{\beta N}{N^{ini}} \right) P + \frac{1}{2} \frac{\partial^2 P}{\partial N_f^2} . \tag{4.3.3}$$

We introduce the variables

$$x = \frac{N_f}{\sqrt{N}} \text{ and } y = \frac{N}{(N^{ini}/\beta)^{2/3}} \tag{4.3.4}$$

and the function $f(x,y) = (N^{ini}/\beta)^{1/3} P(N_f, N)$. We will see below that $f(x,y)$ does not depend explicitely on the parameters N^{ini} and β with this definition. The Fokker-Planck equation then becomes

$$y\frac{\partial f}{\partial y} + f + \left(\frac{x}{2} + y^{3/2}\right)\frac{\partial f}{\partial x} + \frac{1}{2}\frac{\partial^2 f}{\partial x^2} = 0\,. \tag{4.3.5}$$

Let $W(N)$ denote the probability that N nodes are left at the moment where N_f reaches the value zero. It is

$$W(N) \;=\; \int_0^\infty P(N_f, N) dN_f - \int_0^\infty P(N_f, N-1) dN_f\,.$$

Consequently,

$$\begin{aligned} W(N) &= \frac{\partial}{\partial N}\int_0^\infty P(N_f, N) dN_f \\ &= (N^{ini}/\beta)^{-1/3}\frac{\partial}{\partial N}\sqrt{N}\int_0^\infty f(x,y)dx \\ &= (N^{ini}/\beta)^{-2/3}\frac{\partial}{\partial y}\sqrt{y}\int_0^\infty f(x,y)dx \\ &\equiv (N^{ini}/\beta)^{-2/3} G(y) \end{aligned} \tag{4.3.6}$$

with a scaling function $G(y)$. $W(N)$ must be a normalized function, $\int_0^\infty W(N)dN = \int_0^\infty G(y)dy = 1$. This condition is independent of the parameters of the model, and therefore $G(y)$ and $f(x,y)$ are independent of them, too, which justifies our choice of the prefactor in the definition of $f(x,y)$. By integrating Equation (4.3.5) over x from 0 to infinity and by using $f(0,y) = f(\infty, y) = 0$ we obtain

$$\sqrt{y}\frac{\partial}{\partial y}\sqrt{y}\int_0^\infty f dx - \frac{1}{2}\left.\frac{\partial f}{\partial x}\right|_{x=0} = 0\,,$$

which gives us a second relation between $f(x,y)$ and $G(y)$:

$$\sqrt{y}G(y) = \frac{1}{2}\left.\frac{\partial f}{\partial x}\right|_{x=0}\,. \tag{4.3.7}$$

The mean number of nonfrozen nodes is

$$\bar{N} = \int_0^\infty N W(N) dN = (N^{ini}/\beta)^{2/3}\int_0^\infty G(y) y dy\,, \tag{4.3.8}$$

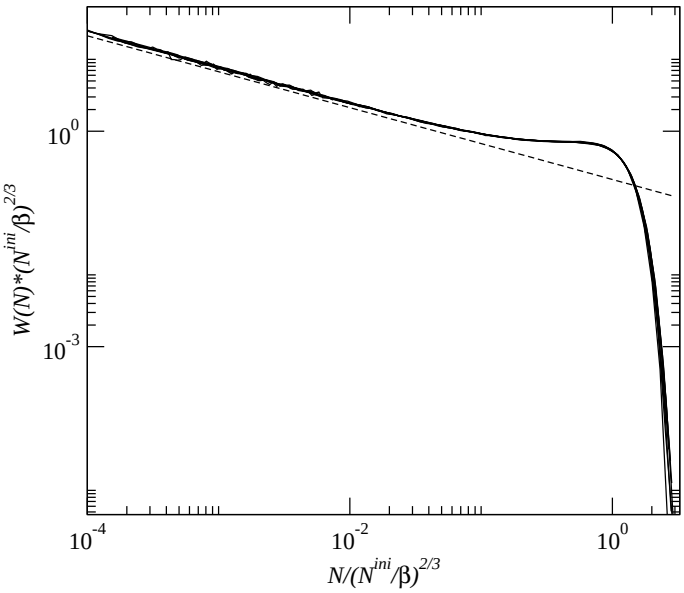

Figure 4.3: The function $W(N)(N^{ini}/\beta)^{2/3}$ vs $N/(N^{ini}/\beta)^{2/3}$ for $\beta = 0.25$ and $N^{ini} = 2^{16}, 2^{17}, 2^{18}, 2^{19}, 2^{20}, 2^{21}$. Furthermore, the graph contains a curve with $\beta = 0.125, N = 2^{16}$ and a curve with $\beta = 0.5, N = 2^{16}$. The curves all collapse, confirming the existence of a scaling function $G(y)$. The dashed line is a power law $\sim 1/\sqrt{N}$.

which is proportional to $(N^{ini}/\beta)^{2/3}$. We did not succeed in extracting an explicit expression for the function $G(y)$. It can be determined by running the stochastic process described by the Equations (4.3.1) on the computer. The result is shown in Figure 4.3, and an almost perfect fit to this result is given by

$$G(y) \simeq 0.25 e^{-y^3/2}(1 - 0.5\sqrt{y} + 3y)/\sqrt{y}\,. \tag{4.3.9}$$

For small y, the data show a power law $G(y) \propto y^{-1/2}$. We can obtain this power law analytically by solving the Fokker-Planck Equation (4.3.5) in the limit of small y. In this limit, the term proportional to $y^{3/2}$ can be dropped, and we have the simpler equation

$$y\frac{\partial f}{\partial y} + f + \frac{x}{2}\frac{\partial f}{\partial x} + \frac{1}{2}\frac{\partial^2 f}{\partial x^2} = 0\,. \tag{4.3.10}$$

The general solution has the form $f(x,y) = \sum_\nu c_\nu y^\nu f_\nu(x)$, with the functions f_ν satisfying

$$2(\nu+1)f_\nu + x f_\nu' + f_\nu'' = 0\,. \tag{4.3.11}$$

The solution is

$$e^{\frac{x^2}{2}} f_\nu(x) = C_1 H_{1+2\nu}\left(\frac{x}{\sqrt{2}}\right) + C_2\, {}_1F_1\left(-\nu - \frac{1}{2}; \frac{1}{2}; \frac{x^2}{2}\right)$$

with two constants C_1 and C_2, and with H denoting the Hermitian functions, and ${}_1F_1$ the appropriate hypergeometric functions. We expect f to be analytical in y for small y, which means that $\nu = 0, 1, 2, \ldots$. For sufficiently small y, only the term $\nu = 0$ contributes, and due to the absorbing boundary condition we have $C_2 = 0$. We obtain therefore for small y

$$f(x, y) = c_0 x e^{-x^2/2}\,. \tag{4.3.12}$$

From our numerical result (4.3.9), together with (4.3.7), we find $c_0 = 0.5$. Inserting Equation (4.3.12) into Equation (4.3.6), we obtain for small N

$$W(N) = \left(\frac{N^{ini}}{\beta}\right)^{-1/3} \frac{c_0}{2\sqrt{N}}\,. \tag{4.3.13}$$

In Equation (4.3.12), the function $f(x, y)$ is independent of y. This means that for sufficiently small N the function $P(N_f, N)$ depends only on the ratio $N_f/\sqrt{N}$. This is also confirmed by our computer simulations (see Figure 4.3).

We can obtain a set of solutions of Equation (4.3.5) with the Ansatz $f(x, y) = \sum_\nu y^\nu \tilde{f}_\nu(z)$ with $z = x - y^{3/2}$. The resulting equation for $\tilde{f}_\nu$, is identical to Equation (4.3.11) for f_ν, which was valid for small y. However, an analytical expression for the function $G(y)$ can only be given if an expansion of the initial condition $P(N_f, N) = \delta(N_f - \beta N^{ini})$ in terms of known solutions can be found.

The probability $W_r(N_r)$ that N_r nodes are left in container $\mathcal{R}$ at the moment where container $\mathcal{F}$ becomes empty, is obtained from the relation

$$N_r = N^2 N_r^{ini}/(N^{ini})^2\,.$$

Defining

$$s = \frac{N_r}{(N^{ini}/\beta)^{1/3}} = y^2$$

and

$$F(s) = \frac{G(\sqrt{s})}{2\sqrt{s}}\,, \tag{4.3.14}$$

and remembering $W(N)dN = W_r(N_r)dN_r$, we find

$$W_r(N_r) = (N^{ini}/\beta)^{-1/3} F(s)\,. \tag{4.3.15}$$

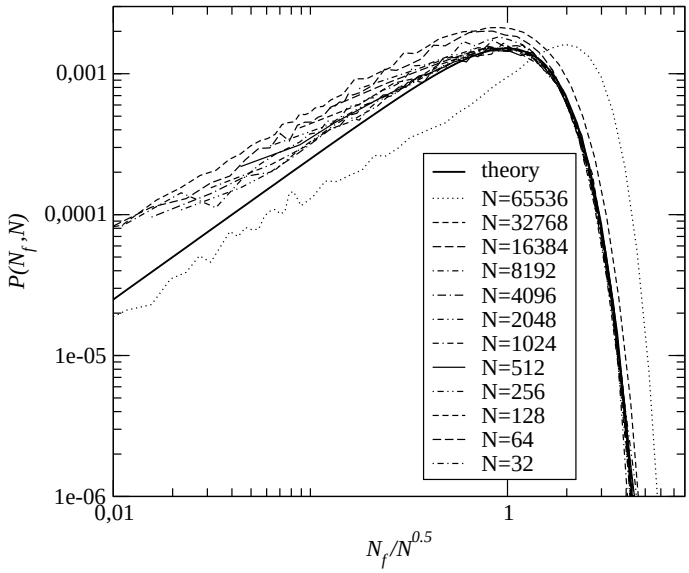

Figure 4.4: $P(N_f, N)$ vs $N_f/\sqrt{N}$ for $N^{ini} = 2^{21}$ and $\beta = 1/4$ for different N. The thick solid line is the theoretical result Equation (4.3.12), which is approached in the limit of small $N/(N^{ini})^{2/3}$.

The mean number of nodes left in in container $\mathcal{R}$ is

$$\begin{aligned} \bar{N}_r &= \int_0^\infty W_r(N_r) N_r dN_r = (N^{ini}/\beta)^{1/3} \int_0^\infty sF(s)ds \\ &= (N^{ini}/\beta)^{1/3} \int_0^\infty y^2 G(y)dy\,. \end{aligned} \tag{4.3.16}$$

The number of nodes left in container $\mathcal{C}_2$ is $N_{c_2} = (\gamma/\beta)N_r$.

We thus have shown that the number of nonfrozen nodes scales with network size N^{ini} as $(N^{ini})^{2/3}$, with most of these nodes receiving only one input from other nonfrozen nodes. The number of nonfrozen nodes receiving two inputs from nonfrozen nodes scales as $(N^{ini})^{1/3}$. We have found scaling functions that describe the probability distribution for these two types of nodes in the limit of large network size. Our next task will be to connect these nonfrozen nodes to a network. This is a reduced network, where all frozen nodes have been cut off.

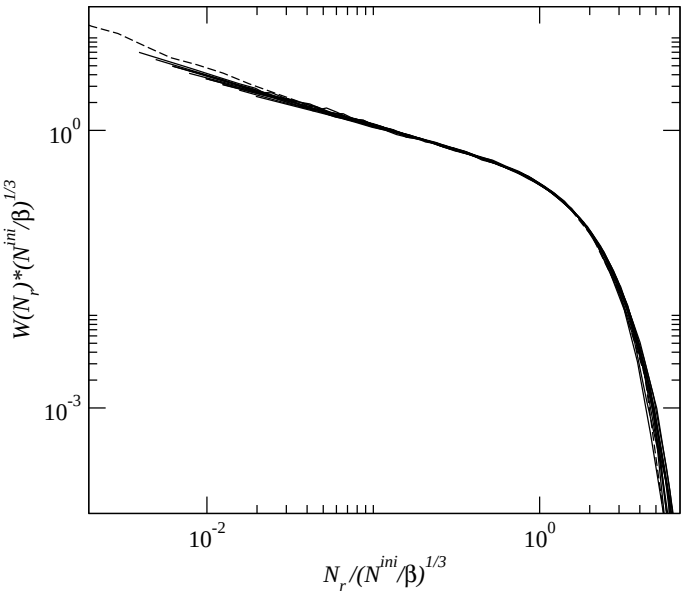

Figure 4.5: The function $W(N_r)(N^{ini}/\beta)^{1/3}$ vs $N_r/(N^{ini}/\beta)^{2/3}$ for $\beta = 0.5$ and $\beta = 0.125$ and for $N^{ini} = 2^{16}, 2^{17}, 2^{18}, 2^{19}, 2^{20}, 2^{21}$. The 12 curves converge with increasing N towards an asymptotic curve, confirming the existence of an asymptotic scaling function $F(s)$. The dashed line shows the function $F(s)$ obtained using the data for $G(y)$ obtained from the same simulation and Equation (4.3.14).

4.4 Relevant nodes

Let us start from the result obtained from the stochastic process of the previous two sections. Each time we run this process we obtain N nonfrozen nodes. Out of these, N_r (N_{c_2}) nodes receive input from two other nonfrozen nodes and have a reversible (canalizing $\mathcal{C}_2$) update function. We define the parameter

$$a = \frac{N_r + N_{c_2}}{\sqrt{N}} = (1 + \gamma/\beta)y^{3/2}\,, \tag{4.4.1}$$

which has a probability distribution $f(a)$ that is determined from the condition $f(a)da = G(y)dy$,

$$f(a) = \frac{2}{3a^{1/3}(1+\gamma/\beta)^{2/3}} G\left(\left(\frac{a}{1+\gamma/\beta}\right)^{2/3}\right)\,. \tag{4.4.2}$$

Just as $G(y)$, the function $f(a)$ is the exact probability distribution only in the thermodynamic limit $N^{ini} \to \infty$. We determine the relevant nodes by a stochastic process that removes iteratively nodes that are not relevant. Each of the N nonfrozen nodes chooses its input(s) at random from the nonfrozen nodes. There are altogether $N(1+a/\sqrt{N})$ inputs to be chosen, and consequently the nonfrozen nodes have together $N(1+a/\sqrt{N})$ outputs. The number of outputs of a node is Poisson distributed with the mean value $(1+a/\sqrt{N})$. The fraction $\exp(-1-a/\sqrt{N})$ of nodes have no output. They are the leaves of the trees of the network of nonfrozen nodes, and we therefore know that they are not relevant. We put them in container number 1. Their number will change during the stochastic process that determines the relevant nodes. The other nodes are placed in container number 2. Their number is N_l ("labelled"), and it will be reduced until only the relevant nodes are left. The total number of outputs of the nodes in container 2 is initially $N(1+a/\sqrt{N})$, while their total number of inputs is $N(1+a/\sqrt{N})(1-\exp(-1-a/\sqrt{N}))$. Now, we remove one node from container 1 and connect its input(s) at random to the outputs of the nodes in container 2. The chosen output(s) are cut off. If a node whose output is cut off has no other output left, we move the node from container 2 to container 1. It cannot be a relevant node since relevant nodes influence other relevant nodes. We iterate this procedure, until there is no node left in container 1. The nodes remaining in container 2 are the relevant nodes. During the entire process, the number of outputs in container 2 is identical to the number of inputs in container 1 and 2. As long as container 1 is not empty, there are more outputs in container 2 than inputs, and only when the process is finished do the two numbers become identical. We can therefore simplify the stochastic process by removing container 1 altogether. We simply have to continue cutting of outputs from nodes in container 2 and removing nodes with no outputs, until the total number of outputs of the nodes in container 2 has become identical to their total number of inputs. The remaining nodes are relevant, and we have then $N_l^{final} \equiv N_{rel}$. These nodes can then be connected to a network by connecting the inputs and outputs pairwise.

In order to derive analytical results, it is useful to run this process backwards. Starting with N nodes with no outputs, adding outputs at random will eventually generate the Poisson distribution of the number of outputs per node that we have started with. The reverse stochastic process is therefore defined by the following rule: Begin with an empty container (former container 2) and N nodes outside the container. Most of these nodes have one input, and the fraction $a/\sqrt{N}$ have two inputs. Add an output to a randomly chosen node. Put this node in the container. Add another output to a randomly chosen node (choosing every node with equal probability, whether the node is inside or outside the container). If a node from outside the container is chosen, put it in the container. Eventually, the total number of outputs in the container will become larger than the total number of inputs in

the container. The container contains the relevant nodes at the moment when the inputs equal the outputs for the last time.

In order to show that the number of relevant nodes scales with $\sqrt{N}$, we define a scaling variable

$$t = \frac{N_l}{\sqrt{N}} .$$

During one step, an output is added to nodes that are already in the container with probability N_l/N. Let N_o count the number of outputs that have been added to nodes in the container, i.e., N_o =(total number of outputs in the container) $-N_l$. Then the average rate of increase of N_o is given for sufficiently large N by

$$\langle \frac{dN_o}{dN_l} \rangle = \frac{N_l}{N} ,$$

or

$$\langle \frac{dN_o}{dt} \rangle = t .$$

Let N_i count the number of nodes in the container with two inputs. Their rate of increase is

$$\langle \frac{dN_i}{dN_l} \rangle = \frac{a}{\sqrt{N}} ,$$

or

$$\langle \frac{dN_i}{dt} \rangle = a .$$

Consequently, the probability distribution for N_o is given by

$$P_o(N_o|t) = \frac{1}{N_o!} e^{-t^2/2} \left(\frac{t^2}{2} \right)^{N_o} , \tag{4.4.3}$$

and the probability distribution for N_i is given by

$$P_i(N_i|t) = \frac{1}{N_i!} e^{-at} \, (at)^{N_i} . \tag{4.4.4}$$

The stochastic process can be viewed as a random walk that steps to the right with a rate t and to the left with a rate a. It is finished when $N_i = N_o$ for the last time, i.e. when the walk leaves the origin for the last time. We determined the probability distribution $\mathcal{C}_a(t)$ for this last exit time from the origin by a computer simulation. It is shown in Figure 4.4 for $a = 1$. For small t, it increases linearly in t, because the probability of making a step to the right is proportional to t for small times.

For $a = 0$, we can obtain an analytical result from the relation

$$\mathcal{C}_0(t) = -\frac{\partial P_o(0,t)}{\partial t} = t e^{-t^2/2} . \tag{4.4.5}$$

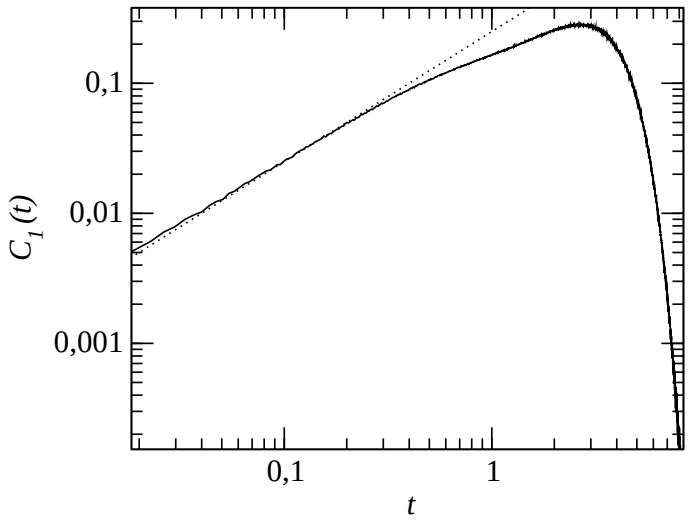

Figure 4.6: The function $\mathcal{C}_1(t)$ as obtained by running the stochastic process described in this section. The dotted line corresponds to the function $0.25t$, which is a good fit to $\mathcal{C}_1(t)$ for small t.

Since we were able to write the stochastic process in terms of t and a alone, the probability distribution for the number of relevant nodes depends only on the combination $N_{rel}/\sqrt{N}$ and on the parameter a,

$$p_a(N_{rel})dN_{rel} = \mathcal{C}_a\left(N_{rel}/\sqrt{N}\right)dN_{rel}/\sqrt{N}\,. \tag{4.4.6}$$

The relation between N and a is obtained using Equation (4.3.4) and (4.4.1):

$$\sqrt{N} = a^{1/3}\left(\frac{N^{ini}}{\beta+\gamma}\right)^{1/3}\,.$$

Taking into account the probability distribution (4.4.2) of the parameter a, we obtain the scaling behavior of the number of relevant nodes,

$$p(N_{rel}) = \int_0^\infty da f(a)\mathcal{C}_a\left(\frac{N_{rel}a^{-1/3}}{(N^{ini}/(\beta+\gamma))^{1/3}}\right)\left(\frac{\beta+\gamma}{aN^{ini}}\right)^{1/3}\,. \tag{4.4.7}$$

The error made by taking the upper limit of the integral to infinity vanishes for $N^{ini}\to\infty$. We introduce the scaling variable

$$z = \frac{N_{rel}}{\left(\frac{N^{ini}}{\beta+\gamma}\right)^{1/3}}\,, \tag{4.4.8}$$

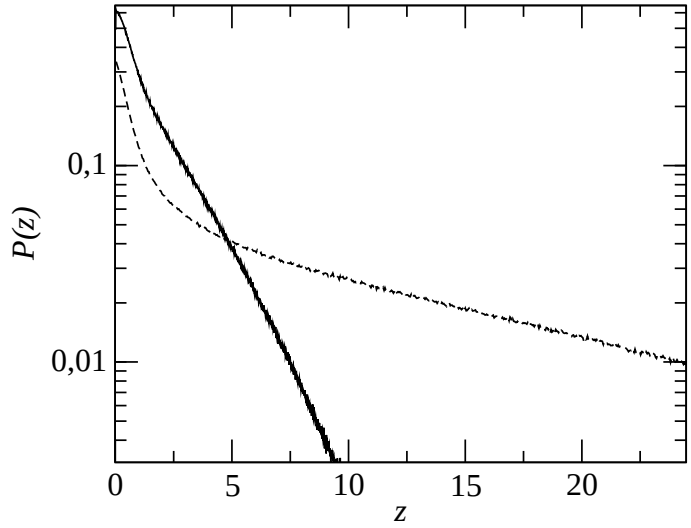

Figure 4.7: The function $P(z)$ for $\gamma/\beta = 0$ (solid line) and $\gamma/\beta = 4$ (dashed line). The results were obtained by running the two coupled stochastic processes for 10^7 samples.

which has then the following probability distribution

$$P(z) = \int_0^\infty da \frac{f(a)}{a^{1/3}} \mathcal{C}_a \left(\frac{z}{a^{1/3}} \right) . \tag{4.4.9}$$

The probability distribution for the number of relevant nodes depends for large N^{ini} only on the scaling variable z. We determined numerically the function $P(z)$ by combining the two stochastic processes described in this chapter. First, we determined a value of a using the process of Section 4.3. Then, we used this value of a to determine the last exit time of the stochastic process of this section, giving a value of z. The shape of the curves $P(z)$ depends on the value of γ/β, and the results are shown in Figure 4.4 for $\gamma/\beta = 0$ and $\gamma/\beta = 4$, which is the original Kauffman model, where each update function has the same weight. It is easy to check analytically that

$$\lim_{z \to 0} P(z) = \sqrt{2\pi}/4(1 + \gamma/\beta)^{1/3} .$$

The mean number of relevant nodes is

$$\bar{N}_{rel} = \int_0^\infty N_{rel} p(N_{rel}) dN_{rel} = \left(\frac{N^{ini}}{\beta + \gamma} \right)^{1/3} \int_0^\infty z P(z) dz , \tag{4.4.10}$$

i.e., it is proportional to $(N^{ini})^{1/3}$. Finally, let us give the probability distribution for the number of relevant nodes with two relevant inputs. Let m denote the number of relevant nodes with two relevant inputs and $\tilde{P}(m;z)dz$ the probability of having the number of relevant nodes in the interval $[N_{rel}(z), N_{rel}(z+dz)]$, with m of them having two relevant inputs. Using Equations (4.4.3) and (4.4.4), we can express $\tilde{P}$ as

$$\begin{aligned}\tilde{P}(m;z) &= \int_0^\infty da \frac{f(a)}{a^{1/3}} \mathcal{C}_a\left(\frac{z}{a^{1/3}}\right) \\ &\quad \times \frac{P_o\left(m|za^{-1/3}\right) P_i\left(m|za^{-1/3}\right)}{\sum_l P_o\left(l|za^{-1/3}\right) P_i\left(l|za^{-1/3}\right)} .\end{aligned} \tag{4.4.11}$$

As P_o and P_i decay exponentially fast with increasing m, the mean number of relevant nodes with two inputs is finite.

4.5 Conclusions

In this chapter we have obtained the asymptotic probability distributions in the limit of large network size for the number of nonfrozen nodes, the number of nonfrozen nodes with two nonfrozen inputs, the number of relevant nodes, and the number of relevant nodes with two relevant inputs. The mean values of these quantities scale with network size N^{ini} as a power law in N^{ini}, with the exponent being 2/3, 1/3, 1/3, and 0 respectively. The implications of the results are manifold.

First, the notion that these networks are "critical" is now corroborated by the existence of power laws and scaling functions. Originally, it was expected that the quantities that display the scaling behavior should be the attractors of the network [56]. In the meantime, it has become clear that mean attractor numbers do not obey power laws [90]. It is the number of nonfrozen and relevant nodes that show scaling behavior.

Next, let us compare the results to those of critical $K = 1$ networks. A $K = 1$ critical network with N nodes corresponds to the nonfrozen part of a critical $K = 2$ network for $a = 0$. In this case, the probability distribution of the number of relevant nodes is given by Equation (4.4.6) with $a = 0$,

$$p_0(N_{rel}) = \frac{1}{\sqrt{N}} \mathcal{C}_0\left(\frac{N_{rel}}{\sqrt{N}}\right) = \frac{N_{rel}}{N} e^{-N_{rel}^2/2N} . \tag{4.5.1}$$

The mean number of relevant nodes is proportional to $\sqrt{N}$. When these relevant nodes are connected to a network by pairwise connecting the inputs and outputs,

one obtains a set of simple loops. From [29], we know that there is a mean number of $\ln \sqrt{N}$ loops and that the number of loops of length l in a critical $K = 1$ network is Poisson distributed with a mean $1/l$ for $l \ll \sqrt{N}$. This can be easily explained by considering the process of connecting inputs and outputs: We begin with a given node and draw the node that provides its input from all possible nodes. Then, we draw the node that provides the input to the newly chosen node, etc., until the first node is chosen and a loop is formed. For small loop size, the probability that the loop is closed after the addition of the lth node is $1/N_{rel}$. Therefore, the probability that a given node is on a loop of size l is $1/N_{rel}$, and the mean number of nodes on loops of size l is 1, and the number of loops of length l is Poisson distributed with a mean $1/l$ for sufficiently small l.

Now, the $K = 2$ critical networks have of the order of $(N^{ini})^{1/3}$ relevant nodes, with only a finite number of them having two relevant inputs. The relevant components are constructed from the relevant nodes by pairwise connecting inputs and outputs. In the asymptotic limit of very large N^{ini} that we are considering, the probability that a randomly chosen relevant node has two inputs or two outputs vanishes. Let us again construct a component by starting with one node and choosing its input node etc., until the component is finished. If the component is small, it consists almost certainly only of nodes with one input and one output and is therefore a simple loop. There is no difference between the statistics of the small relevant components of a $K = 1$ critical network, and the number of loops of length l is Poisson distributed with a mean $1/l$. The total number of relevant nodes in loops of size $l \leq l_c$ with $l_c = \epsilon(N^{ini})^{1/3}$ (with a small ϵ) is l_c, and it is a small proportion of all nodes. If there were no nodes with two inputs or outputs, the number of components larger than l_c would be $(\ln N_{rel} - \ln l_c) = \ln(1/\epsilon)$. The additional links may reduce this number, which is in any case finite. Since these large components contain almost all nodes, they contain almost all relevant nodes with two inputs or outputs.

From these findings, we can obtain results for the attractors of $K = 2$ critical networks. The numbers and lengths of attractors are determined by the relevant components. We now argue that the mean number and length of attractors increases faster than any power law. If we remove the components of size larger than l_c and determine the mean number and length of attractors for this reduced relevant network, we have a lower bound to the correct numbers. Now, the reduced relevant network of a $K = 2$ system is identical to that of a critical $K = 1$ system (where the critical loop size is $l_c = \epsilon\sqrt{N}$). In [29], as presented in the last chapter, it was proven that the mean number and length of attractors for such a reduced $K = 1$ system increases faster than any power law with network size. We therefore conclude that the same is true for critical $K = 2$ networks.

Earlier, Samuelsson and Troein [90] have derived analytically an exact expression for the number of attractors of length L of a critical $K = 2$ network in the limit of large N^{ini}, and they have pointed out that this implies that the mean number of attractors increases faster than any power law with N^{ini}. Using their calculation, it has recently been shown [27] that there is a close relationship between $K = 1$ critical networks and the nonfrozen part of $K = 2$ critical networks, and that the results of [90] can be most naturally interpreted if the relevant components of these two networks look identical for component sizes below the above-given cutoffs. This interpretation is placed on a firm foundation by the findings presented in this chapter.

The dynamical process we used in this chapter for identifying the frozen core of the network, was based on the existence of nodes with constant functions. However, a $K = 2$ network with only canalizing functions assigned to the nodes is also critical. In these networks the frozen core arises through the self-freezing loops. The self-freezing loops and the procedure of their creation were introduced and explained in [80]. There it was found that all results from this chapter are also valid for this class of critical networks with two inputs per node. We will deal with this subject in detail in the next chapter, where for certain choices of functions in critical networks with $K \geq 3$ self-freezing loops play an important role in identifying the frozen core.

5 General class of critical Kauffman networks

When the appropriate distribution of functions assigned to the nodes is chosen, Kauffman networks can be critical for any number of incoming links per node. In this chapter we will once more use the concept of relevant nodes to learn about the dynamics of critical Kuffman networks with larger number of inputs per node. Using analysis similar to that of the previous chapter, we are now going to derive the scaling behavior of the number of nonfrozen and of relevant nodes in critical Kauffman networks with $K \geq 3$. In the last two chapters, we have seen that the scaling behavior of the number of relevant and nonfrozen nodes is different for $K = 1$ and $K = 2$ critical networks. In the first case, these power laws are $N_{nf} \sim N$ and $N_{rel} \sim N^{1/2}$, since there is no frozen core in a $K = 1$ critical network. For critical $K = 2$ networks, the mean number of nonfrozen nodes scales as $N_{nf} \sim N^{2/3}$, and the mean number of relevant nodes scales as $N_{rel} \sim N^{1/3}$. Thus, one could expect that scaling exponents are generally K-dependent. However, we will see that the exponents 2/3 and 1/3 found for networks with $K = 2$ are valid also for networks with larger K and for all possible probability distributions of the Boolean functions, as long as the network is critical. We will also obtain results for the number of nonfrozen nodes with two and more nonfrozen inputs, and for the number of relevant nodes with two and more relevant inputs. This way we will complete our analysis of the scaling behavior of dynamically different types of nodes in critical Kauffman networks. We will also be able to draw conclusions about the mean number and the mean length of attractors in critical Kauffman networks in general.

As in the previous chapter, a stochastic process that yields the frozen core is introduced first. The process is now defined so that it can determine the frozen core of networks with higher K values. The mean-field theory for this process is presented in Section 5.2, and an improved treatment including fluctuations is presented in Section 5.3, yielding the scaling behavior of the number of nonfrozen nodes in critical networks. The next three sections are devoted to special points in parameter space, where the stochastic process does not generate all of the frozen core. In Sections 5.4 and 5.5 those points are considered, where the stochastic process gives a smaller frozen core, and it is shown that "self-freezing" loops generate the rest of the frozen core. In Section 5.6, we consider points in parameter space,

where the stochastic process does not generate any frozen nodes, and where self-freezing loops are responsible for all of the frozen core. Finally, in Sections 5.7 and 5.8 we evaluate the case $K \geq 4$ and the scaling behavior of the relevant nodes and attractor properties. Section 5.9 discusses the implications of our results. The results presented in this chapter were obtained in collaboration with Barbara Drossel, and are published in *Physical Review E* [73].

5.1 A stochastic process that leads to the frozen core

From now on, we set $K = 3$ and derive explicitly the scaling behavior of the non-frozen nodes. The generalization to larger K and the scaling behavior of the relevant nodes will be discussed later. The first step of the calculation, which is performed in this section, consist in defining a stochastic process that determines the frozen core. This process is inspired by the one used for $K = 2$ networks presented in the previous chapter, however it needed to be modified before it could be generalized to larger K. The treatment presented in the following is based on the existence of nodes with constant functions (functions in which the output is fixed irrespectively of the input) and it therefore applies to all critical models that have a nonzero fraction of constant functions. Networks with no constant functions, and in particular networks with only canalizing functions will be discussed separately.

We consider the ensemble of all networks of size N with a fixed number of nodes with constant update functions. All nodes with a constant update function are certainly part of the frozen core. We construct the frozen core by determining stepwise all those nodes that become frozen due to the influence of a frozen node.

In a $K = 3$ network, each node has 3 inputs, and there are consequently $2^{2^3} = 256$ possible Boolean functions. In order to specify a model, one has to specify the probabilities for a node to choose each of these functions. Instead of performing the calculation in terms of all these parameters, it turns out that three parameters are sufficient. For the $K = 2$ networks, we introduced 3 parameters corresponding to the occurrence of three types of Boolean functions. For larger K, there are more types of Boolean functions, and we use therefore a different set of parameters. The first parameter is β, which is the proportion of nonfrozen nodes in the network. $1 - \beta$ is therefore the proportion of nodes with a constant update function. We require $\beta < 1$ for the calculation performed in this and the following section. The case $\beta = 1$ will be discussed further below. The second parameter is ω_2, which is the probability that a randomly chosen node that does not have a constant update function will become a frozen node when one of its 3 inputs is connected to a frozen node. If one input of a node is fixed at some value, the node has effectively two inputs left. We now consider those nodes that have not become frozen by fixing one input, i.e. we

are considering the proportion $1-\omega_2$ of all nonfrozen nodes. The parameter ω_1 is then the probability that such a node becomes frozen when one of the remaining two inputs is connected to a frozen node. This probability can again be expressed in terms of the probabilities of the different possible update functions. Thus all the networks with the same parameters ω_2, ω_1 and β will be treated as of the same type. As we will see below, the properties we are interested in will be the same not only for the functions that belong to the same type of the network (i.e., that have the same parameters but possibly different Boolean functions) but also for the different types as long as their parameters are such that the network satisfies the criticality condition (5.2.3) derived below. This means that we can have critical networks with all possible choices of Boolean functions and that they will all be characterized by the same exponents as a consequence of being critical.

Now, let us define the stochastic process that determines the frozen core. For this purpose, we differentiate 4 types of nodes, the numbers of which will change during the process, and we place these nodes in 4 different "containers". Initially, all nodes with constant functions are placed in a container labelled $\mathcal{F}$, and the remaining nodes in a container labelled $\mathcal{N}_3$. In this container are all those nodes, for which we do not yet know if they are connected to a frozen node. The other two containers, labelled $\mathcal{N}_2$ and $\mathcal{N}_1$, are initially empty. They will contain nodes with one and two frozen inputs that are themselves not (yet) frozen. Since the number of nodes in the different containers is going to change during our stochastic process, we denote the initial values of numbers of nodes in the containers as N_f^{ini}, N_2^{ini}=$N_1^{ini}=0$ and N_3^{ini}, and the total number of nodes as N^{ini} (this is the actual number of nodes in the network). The contents of the containers will change with time. The "time" we are defining here is not the real time for the dynamics of the system. Instead, it is the time scale for a stochastic process that we use to determine the frozen core. During one time step, we choose one node from the container $\mathcal{F}$ and determine the influence of this node on the nodes connected to it. After determining its influence we will remove it from the system, and the number of nodes N in the system is reduced by 1. Now, for each nonfrozen node in container $\mathcal{N}_3$ we ask whether it receives input from the chosen frozen node. If this is the case it freezes with probability ω_2 due to the influence of this node and moves to container $\mathcal{F}$. With probability $1-\omega_2$ it does not become frozen and moves to container $\mathcal{N}_2$. In one time step, we therefore move each node of container $\mathcal{N}_3$ with probability $3\omega_2/N$ to the container $\mathcal{F}$, and with probability $3(1-\omega_2)/N$ to the container $\mathcal{N}_2$. Similarly, a node from the container $\mathcal{N}_2$ receives input from the chosen frozen node with probability $2/N$, and it will then become frozen with probability ω_1 and will be placed in the container $\mathcal{F}$. If it does not freeze, we place it in container $\mathcal{N}_1$, where we find all those nodes that have two inputs from frozen nodes and are not frozen. When nodes from this container choose a frozen node as an input, they automaticly become frozen. During this process, the

probabilities ω_2 and ω_1 will not change since the nodes from containers $\mathcal{N}_3$ and $\mathcal{N}_2$, for which we are in every time step determining whether they are going to freeze, are chosen at random, and moving them from the containers will not change probability distribution of the functions of the nodes left in the containers. In the next time step, we choose another frozen node from container $\mathcal{F}$ and determine its effect on the other nodes. Some nodes move again to a different container, and the chosen frozen node is removed from the system. We repeat this procedure until we can not continue because either container $\mathcal{F}$ is empty, or because all the other containers are empty. If container $\mathcal{F}$ becomes empty, we are left with the nonfrozen nodes. We shall see below that most of the remaining nodes are in container $\mathcal{N}_1$, with the proportion of nodes left in containers $\mathcal{N}_2$ and $\mathcal{N}_3$ vanishing in the limit $N^{ini} \to \infty$. If all containers apart from container $\mathcal{F}$ are empty at the end, the entire network becomes frozen. This means that the dynamics of the network goes to the same fixed point for all initial conditions. Figure 5.1 illustrates the process of determining the frozen core.

5.2 Mean field approximation and the criticality condition

Let us first describe this process by deterministic equations that neglect fluctuations around the average change of the number of nodes in the different containers. As long as all containers contain large numbers of nodes, these fluctuations are negligible, and the deterministic description is appropriate. The average change of the node numbers in the containers during one time step is

$$\begin{aligned} \Delta N_3 &= -\frac{3N_3}{N} \\ \Delta N_2 &= -\frac{2N_2}{N} + (1-\omega_2)\frac{3N_3}{N} \\ \Delta N_1 &= -\frac{N_1}{N} + (1-\omega_1)\frac{2N_2}{N} \\ \Delta N_f &= -1 + \frac{N_1}{N} + \omega_1\frac{2N_2}{N} + \omega_2\frac{3N_3}{N} \\ \Delta N &= -1 \end{aligned} \tag{5.2.1}$$

The total number of nodes in the containers, N, can be used instead of the time variable, since it decreases by one during each step. The equation for N_3 can then be solved by going from a difference equation to a differential equation,

$$\frac{\Delta N_3}{\Delta N} \simeq \frac{dN_3}{dN} = \frac{3N_3}{N},$$

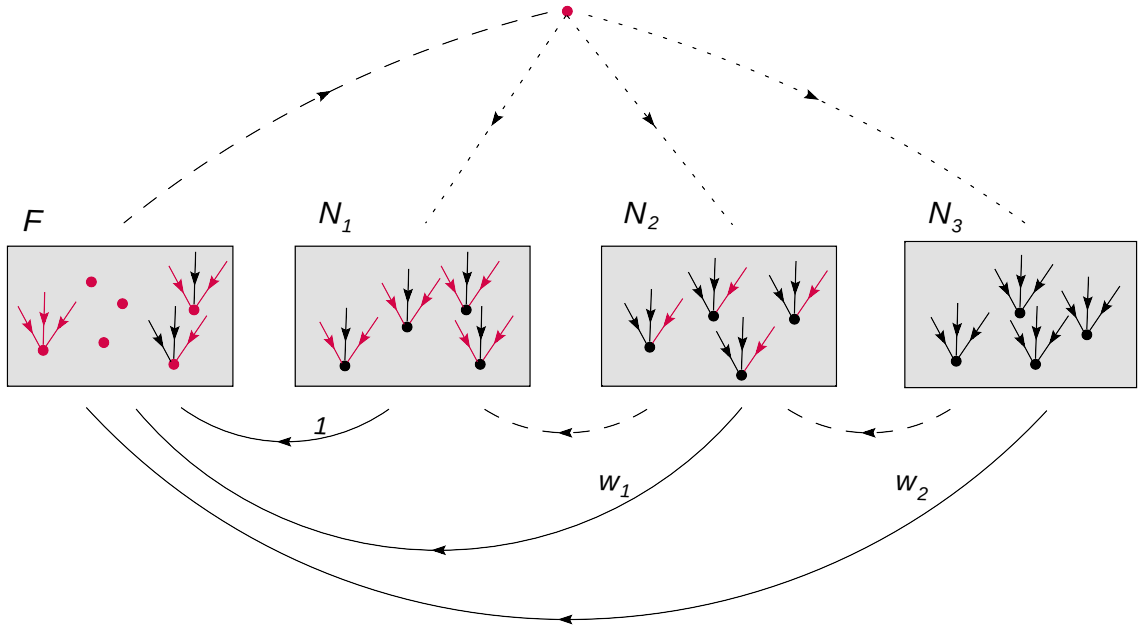

Figure 5.1: Illustration of the freezing process. A frozen node, marked in red, is taken from the container F. First it is determined to which node(s) it is an input, indicated by the arrows in the upper part of the figure. Its effect on these nodes is then determined. Possibilities are pictured with links in the lower part of the figure. Red input links of the nodes are those recognized as coming from the frozen nodes during the process. Red nodes without links are those that initially have frozen functions, which were placed in the container F in the beginning of the process. Other nodes in this container have become frozen during the process, after receiving one, two or all three inputs from the frozen nodes. Nodes in other three containers are those that are not (yet) frozen and that have during the process received two, one or none input from frozen nodes. In the end of each time step of the process, the selected frozen node is removed from the system and a new frozen node is chosen to take its role in the next time step.

which has the solution

$$N_3 = N^3 \frac{N_3^{ini}}{(N^{ini})^3} = \frac{\beta}{(N^{ini})^2} N^3 \,,$$

where $\beta = \frac{N_3^{ini}}{N^{ini}}$. Similarly, we find

$$\begin{aligned} N_2 &= 3(1-\omega_2)\frac{\beta}{N^{ini}}N^2 - 3(1-\omega_2)\frac{\beta}{(N^{ini})^2}N^3 \\ N_1 &= 3(1-\omega_1)(1-\omega_2)\beta N - 6(1-\omega_1)(1-\omega_2)\frac{\beta}{N^{ini}}N^2 \\ &\quad +3(1-\omega_1)(1-\omega_2)\frac{\beta}{(N^{ini})^2}N^3 \\ N_f &= (1-3(1-\omega_1)(1-\omega_2)\beta)N \\ &\quad +3(1-2\omega_1)(1-\omega_2)\frac{\beta}{N^{ini}}N^2 \\ &\quad +(3\omega_1(1-\omega_2)-1)\frac{\beta}{(N^{ini})^2}N^3 \end{aligned} \tag{5.2.2}$$

When $1-3(1-\omega_1)(1-\omega_2)\beta < 0$, the equation $N_f = 0$, which represents the stopping condition for the process, has a solution for an nonzero value N. This solution shows that the number of nonfrozen nodes in each container is proportional to N^{ini}. This means that on an average a nonfrozen node has more than one nonfrozen input. A perturbation at one node propagates during one time step on an average to more than one node and we are obviously in the chaotic phase.

For $1-3(1-\omega_1)(1-\omega_2)\beta \geq 0$ the equation $N_f = 0$ does not have a nonzero solution for $N \in [0, N^{ini}]$. In this case, we will stop the process when N_f drops below 1. We are in the frozen phase, or we have a critical system.

In the case $1-3(1-\omega_1)(1-\omega_2)\beta > 0$, the values N_3 and N_2 will sink below 1 when N becomes of the order $\sqrt{N^{ini}}$, and the higher-order terms contributing to N_f and N_1 can be neglected compared to the first one. For smaller N, only frozen nodes and nodes with one input are left. When N_f falls below 1, there remain only a constant number of the nodes of type $\mathcal{N}_1$,

$$N_1 \simeq \frac{3(1-\omega_1)(1-\omega_2)\beta}{1-3(1-\omega_1)(1-\omega_2)\beta}\,.$$

The network is essentially frozen, with only a finite number of nonfrozen nodes in the limit $N^{ini} \to \infty$. If we now choose the inputs for these nodes, we obtain simple loops with trees rooted in the loops. This property of the frozen phase was also found in [100].

When parameters of the networks are such that

$$1-3(1-\omega_1)(1-\omega_2)\beta = 0 \tag{5.2.3}$$

is fulfilled, we are at the boundary between frozen and chaotic phase in the parameter space. Thus the network is critical. Since the stochastic process stops at $N_f = 1$, we have

$$1 = \frac{(1-2\omega_1)}{(1-\omega_1)}\frac{(N^{end})^2}{N^{ini}} + \left(\frac{\omega_1}{(1-\omega_1)} - \beta\right)\frac{(N^{end})^3}{(N^{ini})^2}\,.$$

In the limit $N^{ini} \to \infty$ the first term is dominant and the number of nonfrozen nodes would scale with the square root of the network size if the deterministic approximation to the stochastic process was exact. We shall see below that including fluctuations changes the exponent from 1/2 to 2/3. The final number of $\mathcal{N}_2$-nodes for the deterministic process for the critical networks is independent of network size, and the final number of $\mathcal{N}_3$-nodes is $\sim (N^{ini})^{-1/2}$ and vanishes for $N^{ini} \to \infty$. We shall see below that the fluctuations change these two results to $N_2 \sim (N^{ini})^{1/3}$ and $N_3 \sim const.$

The deterministic description of our process gives the wrong scaling of the number of nonfrozen nodes in the case of critical networks, but a correct criticality condition (5.2.3). We are interested in the dynamical behavior of the networks in the critical phase and we will from now on study only networks with the parameters such that the criticality condition $1 - 3(1-\omega_1)(1-\omega_2)\beta = 0$ is fulfilled.

Before we proceed by introducing the noise into the deterministic equations, there is one more piece of information we can extract from the deterministic description of the critical process that is going to help us later in determining the noise term. Introducing $n = N/N^{ini}$ and $n_j = N_j/N^{ini}$ for $j = f, 1, 2, 3$, Equations (5.2.2) simplify to (using the criticality condition)

$$\begin{aligned} n_3 &= \beta n^3 \\ n_2 &= \frac{1}{1-\omega_1}(n^2 - n^3) \\ n_1 &= n - 2n^2 + n^3 \\ n_f &= \frac{1-2\omega_1}{1-\omega_1}n^2 + \left(\frac{\omega_1}{1-\omega_1} - \beta\right)n^3\,. \end{aligned} \tag{5.2.4}$$

This means that our stochastic process remains invariant (in the deterministic approximation) when the initial number of nodes in the containers and the time unit are all multiplied by the same factor. For small n, the majority of nodes are in container $\mathcal{N}_1$, since $n_1 = n - \mathcal{O}(n^2)$. Now, if we choose a sufficiently large N^{ini}, n reaches any given small value while $N_f \sim n^2 N^{ini}$ is still large enough for a deterministic description. We can therefore assume that for sufficiently large networks $N_f/N \sim n$ becomes small before the effect of the noise becomes important. This assumption will simplify our calculations below.

5.3 The effect of fluctuations

The number of nodes in container $\mathcal{N}_j$, $j = 1, 2, 3$, that choose a given frozen node as an input is Poisson distributed with a mean jN_j/N and a variance jN_j/N. We now assume that n is small at the moment where the noise becomes important, i.e., that the variance of the three noise terms is $N_1/N = n_1/n = 1-2n+n^2 = 1-\mathcal{O}(n)$ and $2N_2/N = 2n_2/n = \frac{2}{1-\omega_1}(n-n^2) = \mathcal{O}(n)$ and $3N_3/N = 3\beta n^2 = \mathcal{O}(n^2)$. All three noise terms occur in the equation for N_f, and since the first term dominates for small n, we consider only this term in the equation for N_f. In the equations for N_1 and N_2, the noise term is much smaller than the number of nodes in these containers and can therefore be dropped.

The effect of the noise on the final value of N_3 can be obtained by the following consideration: as we will see below, the mean final value of N_3 will be a constant, which is independent of N^{ini}. This means that each node that is initially in the container $\mathcal{N}_3$ has a probability of the order $1/N^{ini}$ of never choosing a frozen input during the stochastic process, and this probability is independent for each node. From this follows that the final number N_3 is Poisson distributed with a variance that is identical to the mean. This variance is finite in the limit $N^{ini} \to \infty$ and it does not affect the final value of N_2 or N_1. Since we have obtained the variance of the final value of N_3 by this simple argument, we will not explicitly consider the noise term in the equation for N_3.

We therefore obtain the stochastic version of Equations (5.2.1), where we need to retain only the noise term in the equation for N_f:

$$\begin{aligned}
\Delta N_3 &= -\frac{3N_3}{N} \\
\Delta N_2 &= -\frac{2N_2}{N} + \frac{1}{\beta(1-\omega_1)}\frac{N_3}{N} \\
\Delta N_f &= -1 + \frac{N_1}{N} + 2\omega_1\frac{N_2}{N} + \left(3 - \frac{1}{\beta(1-\omega_1)}\right)\frac{N_3}{N} - \xi \\
\Delta N &= -1\,.
\end{aligned} \tag{5.3.1}$$

The random variable ξ has zero mean and unit variance. As long as the n_j change little during one time step, we can summarize a large number T of time steps into one effective time step, with the noise becoming Gaussian distributed with zero mean and variance T. Exactly the same process would result if we summarized T time steps of a process with Gaussian noise of unit variance. For this reason, we can choose the random variable ξ to be Gaussian distributed with unit variance.

Compared to the deterministic case, the equations for N_3 and N_2 are unchanged. Inserting the solution for N_3 and N_2 into the equation for N_f, we obtain

$$\frac{dN_f}{dN} = \frac{N_f}{N} + \frac{1-2\omega_1}{1-\omega_1}\frac{N}{N^{ini}} + 2\left(\frac{\omega_1}{1-\omega_1} - \beta\right)\left(\frac{N}{N^{ini}}\right)^2 + \xi \tag{5.3.2}$$

with the step size $dN = 1$ and $\langle \xi^2 \rangle = 1$. (In the continuum limit $dN \to 0$ the noise correlation becomes $\langle \xi(N)\xi(N') \rangle = \delta(N - N')$). This is a Langevin-equation, and the corresponding Fokker-Planck-equation is

$$\begin{aligned} -\frac{\partial P}{\partial N} &= \frac{\partial}{\partial N_f}\left[\frac{N_f}{N} + \frac{1-2\omega_1}{1-\omega_1}\frac{N}{N^{ini}}\right. \\ &+ \left. 2\left(\frac{\omega_1}{1-\omega_1} - \beta\right)\left(\frac{N}{N^{ini}}\right)^2\right] P \\ &+ \frac{1}{2}\frac{\partial^2 P}{\partial N_f^2}\,. \end{aligned} \tag{5.3.3}$$

Since we are investigating networks in the thermodynamic limit, keeping only the leading terms will give a good approximation. Thus, we can neglect the last term in the expression under the partial derivative with respect to N_f once N/N^{ini} has become sufficiently small. We are left with the Fokker-Planck equation of the same type as the one already studied in the previous chapter, but with a different coefficient.

$$-\frac{\partial P}{\partial N} = \frac{\partial}{\partial N_f}\left(\frac{N_f}{N} + \frac{\mu N}{N^{ini}}\right) P + \frac{1}{2}\frac{\partial^2 P}{\partial N_f^2}\,, \tag{5.3.4}$$

where $\mu = (1-2\omega_1)/(1-\omega_1)$.

We introduce the variables

$$x = \frac{N_f}{\sqrt{N}} \text{ and } y = \frac{N}{(N^{ini}/\mu)^{2/3}} \tag{5.3.5}$$

and the function $f(x,y) = (N^{ini}/\mu)^\gamma P(N_f, N)$. The free parameter γ will be fixed below by the condition that the probability distribution of the number of nonfrozen nodes is normalized. The Fokker-Planck equation then becomes

$$y\frac{\partial f}{\partial y} + f + \left(\frac{x}{2} + y^{3/2}\right)\frac{\partial f}{\partial x} + \frac{1}{2}\frac{\partial^2 f}{\partial x^2} = 0\,. \tag{5.3.6}$$

Let $W(N)$ denote the probability that N nodes are left at the moment where N_f reaches the value zero. It is

$$W(N) = \int_0^\infty P(N_f, N)dN_f - \int_0^\infty P(N_f, N-1)dN_f$$

Consequently,

$$\begin{aligned} W(N) &= \frac{\partial}{\partial N}\int_0^\infty P(N_f, N)dN_f \\ &= (N^{ini}/\mu)^{-\gamma-1/3}\frac{\partial}{\partial y}\sqrt{y}\int_0^\infty f(x,y)dx \\ &\equiv (N^{ini}/\mu)^{-\gamma-1/3}G(y) \end{aligned}$$

with a scaling function $G(y)$. $W(N)$ must be a normalized function,

$$\int_0^\infty W(N)dN = (N^{ini}/\mu)^{-\gamma-1/3+2/3}\int_0^\infty G(y)dy = 1\,.$$

This gives $\gamma = 1/3$. This condition is independent of the parameters of the model, and therefore $G(y)$ and $f(x,y)$ are independent of them, too. Now, we have

$$W(N) = (N^{ini}/\mu)^{-2/3}G(y)$$

The mean number of nonfrozen nodes is

$$\bar{N} = \int_0^\infty NW(N)dN = (N^{ini}/\mu)^{2/3}\int_0^\infty G(y)ydy\,,$$

which is proportional to $(N^{ini})^{2/3}$.

The probability $W_2(N_2)$ that N_2 nodes are left in container $\mathcal{N}_2$ at the moment where container $\mathcal{F}$ becomes empty, is obtained from the relation

$$N_2 = \frac{1}{1-\omega_1}\frac{N^2}{N^{ini}} - \frac{1}{1-\omega_1}\frac{N^3}{(N^{ini})^2}\,.$$

Since $W(N)dN = W_2(N_2)dN_2$, we find that the mean number of nodes left in container $\mathcal{N}_2$ is

$$\begin{aligned} \bar{N}_2 &= \int_0^\infty N_2 W_2(N_2)dN_2 = \int_0^\infty N_2 W(N)dN \\ &= \frac{1}{(\mu)^{1/3}(1-2\omega_1)}(N^{ini})^{1/3}\int_0^\infty y^2 G(y)dy \\ &\quad + \frac{1}{\mu}\int_0^\infty y^2 G(y)dy \sim (N^{ini})^{1/3}\,. \end{aligned}$$

In the same manner we find for the number of nodes left in container $\mathcal{N}_3$

$$\begin{aligned}\bar{N_3} &= \int_0^\infty N_3 W_3(N_3) dN_3 = \int_0^\infty N_3 W(N) dN \\ &= \frac{\beta(1-2\omega_1)^2}{(1-\omega_1)^2} \int_0^\infty y^3 G(y) dy \sim const\,.\end{aligned}$$

Thus, we have shown that the number of nonfrozen nodes scales with network size N^{ini} as $(N^{ini})^{2/3}$, with most of these nodes receiving only one input from other nonfrozen nodes. The number of nonfrozen nodes with two nonfrozen inputs scales as $(N^{ini})^{1/3}$ and the number of nodes with three such inputs is independent of the network size.

5.4 Special points and canalizing functions

For $\omega_1 = 1/2$, the second term in the Langevin Equation (5.3.2) is zero. In this case the next order term has to be taken into account since it is the leading one now. We will see that the mechanism of creating the frozen core is different for such systems, but in the end we will find the same scaling behavior of the number of nonfrozen nodes.

Now we have to consider the modified Langevin equation

$$\frac{dN_f}{dN} = \frac{N_f}{N} + 2(1-\beta)\left(\frac{N}{N^{ini}}\right)^2 + \xi \tag{5.4.1}$$

and the corresponding Fokker-Planck equation

$$-\frac{\partial P}{\partial N} = \frac{\partial}{\partial N_f}\left(\frac{N_f}{N} + 2(1-\beta)\left(\frac{N}{N^{ini}}\right)^2\right) P + \frac{1}{2}\frac{\partial^2 P}{\partial N_f^2}\,. \tag{5.4.2}$$

We again introduce new variables

$$x = \frac{N_f}{\sqrt{N}} \text{ and } y = \left(\frac{(N^{ini})^2}{2(1-\beta)}\right)^{-4/5} N^2 \tag{5.4.3}$$

and the function $f(x,y) = \left(\frac{(N^{ini})^2}{2(1-\beta)}\right)^{\gamma} P(N_f, N)$. The Fokker-Planck equation then becomes

$$2y\frac{\partial f}{\partial y} + f + \left(\frac{x}{2} + y^{5/4}\right)\frac{\partial f}{\partial x} + \frac{1}{2}\frac{\partial^2 f}{\partial x^2} = 0\,.$$

For the probability that N nodes are left when N_f reaches zero we obtain

$$W(N) = \left(\frac{(N^{ini})^2}{2(1-\beta)}\right)^{-2/5} \tilde{G}(y)$$

with a new scaling function $\tilde{G}$. We have used the fact that this probability has to be normalized, which gives $\gamma = 1/5$.

Using this result, we find for the mean number of nonfrozen nodes

$$\begin{aligned} \bar{N} &= \int_0^\infty NW(N)dN = \frac{1}{2}\left(\frac{(N^{ini})^2}{2(1-\beta)}\right)^{2/5} \int_0^\infty \tilde{G}(y)dy \\ &\sim (N^{ini})^{4/5}\,. \end{aligned} \tag{5.4.4}$$

For the mean number of nonfrozen nodes left in containers $\mathcal{N}_2$ and $\mathcal{N}_3$ we find

$$\begin{aligned} \bar{N}_2 &= \int_0^\infty N_2 W_2(N_2)dN_2 = \int_0^\infty N_2 W(N)dN \\ &= \frac{(N^{ini})^{3/5}}{(2(1-\beta))^{4/5}} \int_0^\infty y^{1/2}\tilde{G}(y)dy \\ &\quad -\frac{(N^{ini})^{2/5}}{(2(1-\beta))^{6/5}} \int_0^\infty y\tilde{G}(y)dy \\ &\sim (N^{ini})^{3/5} \end{aligned} \tag{5.4.5}$$

and

$$\begin{aligned} \bar{N}_3 &= \int_0^\infty N_3 W_3(N_3)dN_3 = \int_0^\infty N_3 W(N)dN \\ &= \frac{\beta}{2}\frac{(N^{ini})^{2/5}}{(2(1-\beta))^{6/5}} \int_0^\infty y\tilde{G}(y)dy \\ &\sim (N^{ini})^{2/5}\,. \end{aligned} \tag{5.4.6}$$

We see that the number of nodes which become frozen due to the influence of the constant functions is smaller than in the case of other critical networks. When we look at the parameters for these networks more closely, we see that these networks are effectively canalizing with two inputs per node. The probability that a node with two inputs is going to freeze during one time step is $\omega_1 = 1/2$ and this means that the network has Boolean functions such that nodes with two nonfrozen inputs effectively belong to the $\mathcal{C}_1$ or $\mathcal{C}_2$ class of Boolean functions with two variables, i.e., canalizing functions. The class $\mathcal{C}_1$ contains those functions that depend only on one of the two variables, but not on the other one. The class $\mathcal{C}_2$ contains the remaining canalizing functions, where one state of each input fixes the output. It has been

shown in [80] that in $K = 2$ networks with only this type of functions another mechanism of creating the frozen core arises. The only condition for this is that the number of nodes from class $\mathcal{C}_2$ is large enough. We will show that it is exactly what happens in the networks we are analyzing now. The number of nonfrozen nodes with two inputs and canalizing $\mathcal{C}_2$ functions is here large enough to allow for the creation of the self-freezing loops that are going to increase the number of frozen nodes and thus change the scaling of the nonfrozen nodes from $(N^{ini})^{4/5}$ to $(N^{ini})^{2/3}$.

5.5 Creating self-freezing loops and their effect

We are now considering a reduced network consisting of those nodes that are not frozen through the influence of the nodes with constant functions. The size of this network is $N \simeq (N^{ini})^{4/5}$, most of the nodes have one nonfrozen input, $N_2 \simeq (N^{ini})^{3/5}$ have two, and $N_3 \simeq (N^{ini})^{2/5}$ have three nonfrozen inputs. Nodes with two nonfrozen inputs have a probability to freeze $\omega_1 = 1/2$ and as such effectively have canalizing Boolean functions of two arguments, belonging to $\mathcal{C}_1$ or $\mathcal{C}_2$ class. So, the number of nodes with two nonfrozen inputs that belong to the $\mathcal{C}_2$ class has to be $\simeq (N^{ini})^{3/5}$ as it is the fraction of all nonfrozen nodes with two inputs.

Let us now assume that there exist groups of nodes that fix each other's value and do not respond to changes in nodes outside this group. The simplest example of such a group is a loop of $\mathcal{C}_2$ nodes where each node canalyzes (fixes) the state of its successor once it settles on its majority bit (the one occurring 3 times in its update function table). These loops, introduced in [80], are called *self-freezing loops*. They can also contain chains of nodes with one nonfrozen input or with two nonfrozen inputs and a $\mathcal{C}_1$ function between $\mathcal{C}_2$ nodes. If a chain between two $\mathcal{C}_2$ nodes as a whole inverts the state of the first $\mathcal{C}_2$ node, the inverted majority bit of the first $\mathcal{C}_2$ node has to canalyze the second $\mathcal{C}_2$ node. The only effect of nodes with $\mathcal{C}_1$ functions and those with one nonfrozen input in such loops is to delay the signal propagation between two adjacent $\mathcal{C}_2$ nodes. The procedure of finding self-freezing loops is explained in details in [80]. The number of nodes on self-freezing loops is there found by mapping the problem of finding a self-freezing loop in a $\mathcal{C}_2$ network onto the problem of finding the relevant nodes sitting on relevant loops in a critical network that contains no canalizing functions at all, but only reversible (where the output is changed whenever one of the inputs is changed) and constant functions. Using results for these reversible networks obtained in [58] it was found that the number of nodes on self freezing loops scales as $\sim N^{1/3}$ where N is the number of $\mathcal{C}_2$ nodes.

Obviously, nodes depending on or canalyzed by the frozen nodes of the self-freezing loops freeze also, and such nodes may lead to the freezing of further nodes, etc. We

can introduce a dynamical process in order to determine the total number of nodes that become frozen because of the self-freezing loops. This process is almost the same as the one we have used for identifying the influence of the constant functions on the networks dynamics. We again have four containers where the nodes left after determining the influence of the nodes with constant functions are placed. Initially nodes found to be on the self-freezing loops are going to be moved from the container with nodes with two inputs, $\mathcal{N}_2$, to the container $\mathcal{F}$. Thus the initial number of nodes in the containers is going to be $N_f^0 = ((N^{ini})^{3/5})^{1/3} = (N^{ini})^{1/5}$, $N_2^0 = (N^{ini})^{3/5} - N_f^0 \simeq (N^{ini})^{3/5}$ and $N_3^0 = (N^{ini})^{2/5}$, and the total number of nodes is $N^0 = (N^{ini})^{4/5}$. Now we run the same dynamical process as before determining influence of the nodes from the frozen loops on the rest of this reduced network one by one and then removing them from the system. At the end of this process we will again have nodes in the container $\mathcal{N}_2$. They can now make new self-freezing loops made of $\mathcal{C}_2$ nodes with the chains of nodes with one nonfrozen input between them. We can then again move $N_2^{1/3}$ nodes that are on the new self-freezing loops to the container $\mathcal{F}$ and run the same process again. We can even take over the values of N_1, N_2 and N_3 and N at the end of the first process, since ${N_2}^{1/3}$ frozen nodes moved from container $\mathcal{N}_2$ are negligible in comparison to N_2. These processes can be repeated as long as the number of nodes of type $\mathcal{C}_2$ is large enough to allow for the creation of self-freezing loops. The equations for the change of N_3 and N_2 nodes

$$\begin{aligned} \Delta N_3 &= -\frac{3N_3}{N} \\ \Delta N_2 &= -\frac{2N_2}{N} + \frac{2}{\beta}\frac{N_3}{N} \end{aligned} \tag{5.5.1}$$

apply together to all the successive processes of freezing the network through the influence of nodes of the self-freezing loops. Between each two of them the new self-freezing loops have been found and moved from the container with N_2 nodes allowing for the new process to start. The equation for N is $\Delta N = -1$, as before. The solution of these equations is obtained by going to differential equations for dN_2/dN and dN_3/dN. Using the values of N, N_2 and N_3, found in Equations (5.4.4), (5.4.5) and (5.4.6), as initial values of the variables, these differential equations have the solution

$$N_3 = \frac{N_3^0}{(N^0)^3}N^3 \tag{5.5.2}$$

$$N_2 = \frac{N_2^0 + (2/\beta)N_3^0}{(N^0)^2}N^2 - \frac{2N_3^0}{\beta(N^0)^3}N^3\,. \tag{5.5.3}$$

The number of remaining $\mathcal{N}_1$ nodes increases in the second process, the number of $\mathcal{C}_2$ (those in container $\mathcal{N}_2$) nodes decreases, thus leading to an increasing weight of $\mathcal{N}_1$ nodes in the nonfrozen network.

The repeated process of identifying generalized self-freezing loops and the nodes frozen by them breaks down when the remaining nonfrozen nodes cannot be considered as an effective $\mathcal{C}_2$ network any more. This happens when in the process of creating self-freezing loops the probability that a $\mathcal{C}_2$ node is going to be attached to the end of the chain of nodes with one nonfrozen input (thus making closing self-freezing loop possible) becomes of the same order of magnitude as the probability that this chain becomes a loop. Since the mean size of the loops of nodes with one input is found to be of the order of $\sqrt{N}$ [29] the assembly of self-freezing loop becomes improbable when $N_2 \sim \sqrt{N}$.

This condition gives to leading order

$$\frac{(N^0)^2}{N_2^0} \sim N^{3/2} \tag{5.5.4}$$

or $N \sim (N^{ini})^{2/3}$. We again have the same scaling of the number of nonfrozen nodes with the network size. The scaling of the number of nonfrozen nodes with two and three nonfrozen inputs with the network size we find from (5.5.3) and (5.5.2) to be $N_2 \sim (N^{ini})^{1/3}$ and $N_3 \sim const.$ This is the same scaling we have for the case of all other critical networks investigated until now.

When finding the number of nodes on the self-freezing loops and defining our second process we assumed that there the influence of the nodes with three nonfrozen inputs per node is negligible. We can check if our assumption was justified. In the beginning of this process the number of nodes with three inputs was $N_3^0 \simeq (N^{ini})^{2/5}$. The number of nodes that are initially on self-freezing loops is $(N_2^0)^{1/3} = (N^{ini})^{1/5}$. The mean number of nodes with three inputs on the self-freezing loops is then

$$(N_2^0)^{1/3} \frac{N_3^0}{N_2^0} = const\,.$$

In the limit of large network size, only a few (if any) self-freezing loops are destroyed by nodes with three nonfrozen inputs, and this does not change the scaling behavior of the number of nodes on self-freezing loops.

5.6 Networks without constant functions

Case $\omega_1 = 1/2$, $\omega_2 = 1/3$

Until now, we have assumed that the network has nodes with constant functions. In this section, we consider networks without constant functions, i.e., with $\beta = 1$. The criticality condition (5.2.3) then becomes

$$3(1-\omega_1)(1-\omega_2) = 1\,.$$

Although the criticality condition was derived under the assumption that the network has a nonvanishing proportion of frozen nodes (i.e., that $\beta < 1$), it can be extended to $\beta = 1$, since it is valid for any β arbitrarily close to 1. Furthermore, decreasing β slightly for fixed ω_1 and ω_2 moves the system to the frozen phase, indicating that a system satisfying the criticality condition with $\beta = 1$ is at the boundary of the frozen phase. As we will see, the value of the parameters in the critical networks without constant functions we are considering here is allowing the formation of the self-freezing loops and leads to the frozen core of the same size as for all the other critical networks. Canalizing networks and threshold networks are examples of this category of networks, and they are considered important for biological applications.

The procedure of creating self-freezing loops in the case of networks with nodes with two nonfrozen inputs was introduced and explained in details in [80]. It is the same procedure we have used in the previous section. Using a similar line of arguments we can explain the assembly of the self-freezing loops for the networks with three inputs per node determined with parameters being $\omega_1 = 1/2$, $\omega_2 = 1/3$ and $\beta = 1$. In this case there is a mapping of the problem of finding the nodes on the self-freezing loops in this network onto the problem of finding the relevant nodes on relevant loops in critical network with three inputs per node and only reversible and constant functions, i.e., with $\omega_1 = \omega_2 = 0$ and $\beta = 1/3$. Self-freezing loops are found by starting with a node and keeping track of the connection to those inputs that are able to canalize this node if they are canalized themselves. This procedure is iterated for these input nodes etc., until a loop is formed or until it has to stop because no canalizing inputs are found. Similarly, relevant loops in a critical network with $\omega_1 = \omega_2 = 0$ are found by starting with a node and keeping track of the connection to those inputs that do not have a constant function. This procedure is iterated for the nonfrozen inputs etc., until a loop is formed or until it has to stop because no nonfrozen inputs are found. In both cases, a connection to an input is made with probability 1/3, showing that the two processes can be mapped on each other. As we will show in Section 5.8 below, in critical networks with three inputs per node and nonzero fraction of frozen nodes the number of relevant nodes on relevant loops scales as $(N^{ini})^{1/3}$. Therefore, we conclude that in the network with $\omega_1 = \omega_2 = 0$, the number of nodes on self-freezing loops scales also as $(N^{ini})^{1/3}$.

We can now proceed just as in the previous section, but with $\beta = 1$ and $N_j^0 = N_j^{ini}$. We continue making self-freezing loops and determining which nodes are frozen by them, until $N_2 \sim \sqrt{N}$. Inserting this condition in Equation (5.5.3), we find to leading order

$$2\frac{N^{3/2}}{N^{ini}} = 1\,,$$

leading again to $N \sim (N^{ini})^{2/3}$.

General case

Now, let us turn to the case $\beta = 1$ with $\omega_1 < 1/2$. (The situation $\omega_1 > 1/2$ is not possible for nonfrozen Boolean functions with two inputs.) The probability that a node we don't know anything about freezes when connected to a frozen node is now $\omega_2 > 1/3$. Every node has three inputs and this frozen node could be any of them. This means that on an average a node can be frozen by more than one input, and the self-freezing components we look for in the network here consist of at least as many nodes as those in the previous subsection. However, we do not need to know the exact number of frozen nodes in these components. We will build only one self-freezing loop and move its $(N^{ini})^{1/3}$ nodes to the container $\mathcal{F}$. Then we start the calculation of Section 5.1 by setting $\beta = 1 - (N^{ini})^{-2/3}$. Since $\omega_1 < 1/2$, the leading-order terms of the calculation performed in Section 5.1 are retained in this case, and we can take over all the main results of that section. In particular, it follows that a single self-freezing loop is sufficient to generate the entire frozen core, and we do not need to identify other self-freezing loops. As before, the number of nonfrozen nodes scales as $(N^{ini})^{2/3}$.

5.7 Generalization to larger K

The process introduced in Section 5.1 can easily be generalized to networks with $K > 3$. We first consider again the case $\beta < 1$. For network with K inputs we define a set of parameters β and ω_i with $i \in [1, K-1]$. β is again fraction of the nonfrozen nodes and ω_i is the probability that a nonfrozen node that has $K - i$ inputs from frozen nodes freezes when receiving another frozen input in our process. These K parameters are going to define completely the class of networks we observe in the process. Using the deterministic description of the process analogous to the one described in Section 5.2 we find the criticality condition for networks with any K:

$$K(1-\omega_1)(1-\omega_2)\cdots(1-\omega_{K-1}) = 1\,. \tag{5.7.1}$$

Introduction of noise in the process gives the Langevin equation

$$\frac{dN_f}{dN} = \frac{N_f}{N} + \sum_{i=1}^{K-1} f_i(\omega_1, \ldots, \omega_i) \left(\frac{N}{N^{ini}}\right)^i + \xi \tag{5.7.2}$$

where the $f_i(\omega_1, \ldots, \omega_i)$ are functions of the parameters of the system obtained from the stochastic process They satisfy $f_i(\omega_1, \ldots, \omega_i) = 0$ when $\omega_j = 1/(j+1)$ for all $j \in [1, i]$. We see that in this general Langevin equation the leading term in N is the same as in Equation (5.3.2). Therefore we find that in the thermodynamic limit the

number of nonfrozen nodes scales in critical networks as $(N^{ini})^{2/3}$ with the network size.

Just like in the $K = 3$ networks, parameter values can be such that one or more of the leading terms in the Langevin equation vanish. These special points in the parameter space describe networks where the Boolean functions are such that the nodes left nonfrozen after determining the influence of the frozen nodes in our process can additionally generate self-freezing loops. Their influence on the rest of the network has to be determined by generalization of the process introduced in Section 5.5. The number of classes of special points will increase with K, leading to a hierarchy of special points. For each K, there are $K - 3$ classes of points in parameter space that are equivalent to the special points of networks with $K - 1$ inputs per node (that is they have the same leading term in the Langevin equation), and one new class of special points where only the last term in the Langevin equation (5.7.2) is nonzero. Furthermore, there is the case $\beta = 1$. As an illustration, in the case $K = 4$ there are two classes of special points for $\beta < 1$. One of them has $\omega_1 = 1/2$. In this case, the influence of the frozen nodes will lead to $(N^{ini})^{4/5}$ nonfrozen nodes. Boolean functions of the nodes with 2 nonfrozen inputs and the number of them left after the first process are such that self-freezing loops are made and their influence will again give $(N^{ini})^{2/3}$ as the number of nonfrozen nodes in the network. This case can obviously be reduced to the $K = 3$ network. The other class of special points is obtained when the parameters of the network are $\omega_1 = 1/2$ and $\omega_2 = 1/3$. In this case, $(N^{ini})^{6/7}$ nodes will be left nonfrozen after determining the influence of the frozen nodes. One can easily show that the creation of self-freezing loops is possible and that their influence leads to a number of nonfrozen nodes that scales as $(N^{ini})^{2/3}$ with the network size.

For general values of K, the $K - 2$ classes of special points with $\beta < 1$ are given by the condition $\omega_j = 1/(j + 1)$ for all $j \in [1, i]$ where i takes for every class one of the values from the interval $[1, K - 2]$. This means that $f_1 = 0, \ldots, f_i = 0$ in the Langevin equation (5.7.2) and the term $f_{i+1}(\omega_1, \ldots, \omega_{i+1})(N/N^{ini})^{i+1}$ is the leading one. The nodes left nonfrozen after determining the influence of the nodes with constant functions scale with the network size as $(N^{ini})^{(2i+2)/(2i+3)}$. The numbers and Boolean functions of the nodes with $k \in [2, i+1]$ nonfrozen inputs are such that they allow for the creation of the self-freezing loops, and their influence will for each of these special points, i.e., for each $i \in [1, K - 2]$, reduce the number of nonfrozen nodes to $(N^{ini})^{2/3}$.

For networks without constant functions (that is with $\beta = 1$) the frozen core arises only because of the creation of self-freezing loops and their effect on the network. Just like for all other parameter values, there is straightforward generalization of the analysis performed for this type of networks in the case when $K = 3$ in Section 5.6. In the case when $\omega_i = 1/(i + 1)$ for all $i \in [1, K - 1]$ there exists again a mapping

of the self-freezing loops on the relevant loops of a K critical network with only reversible and nonfrozen functions, from which it follows that the number of nodes that are initially on self-freezing loops scales as $(N^{ini})^{1/3}$. The process described in Section 5.5 can then be generalized to these networks. For any other choice of parameters satisfying the criticality condition (5.7.1) for $\beta = 1$, self-freezing loops can also be formed, and after moving only one of them in the container with frozen nodes we will have the same process as for the one of the classes of critical networks with $\beta < 1$ that were already studied. Scaling of the number of nonfrozen nodes in the critical networks without frozen nodes and any fixed number of inputs will be the same as in all other critical networks.

Let us end this section by noting that there is another class of special points when the Boolean functions are chosen such that each of them responds only to one of the K inputs. In this case, the network is effectively a $K = 1$ network, since for each node those $K - 1$ inputs to which the node does not respond, can be cut off. In the calculations of the previous sections we have always assumed that a nonvanishing proportion of functions is not of this type.

5.8 Relevant nodes and the number and length of attractors

Relevant nodes are the nodes whose state is not constant and that control at least one relevant node. These nodes determine completely the number and period of attractors. In the previous sections, we have shown that the number of nonfrozen nodes scales as $(N^{ini})^{2/3}$ for any critical network. We have also seen that among them there are only $(N^{ini})^{1/3}$ nodes having two nonfrozen inputs, and that the number of nonfrozen nodes with more than two nonfrozen inputs vanishes in the thermodynamic limit. The nonfrozen nodes can now be connected to a network. This is a reduced network, where all frozen nodes have been cut off. In the previous chapter, we defined a stochastic process for the formation of this reduced network and the identification of the relevant nodes for critical $K = 2$ networks [58]. The relevant nodes are determined by removing iteratively nodes that are not relevant because they influence only frozen and irrelevant nodes. The number of relevant nodes was found to scale as $(N^{ini})^{1/3}$, and the scaling function characterizing their probability distribution depends on the parameters of the model.

The scaling of the number of nonfrozen nodes as well as the scaling of the number of nonfrozen nodes with two nonfrozen inputs as function of the network size is the same for every critical network, as we have shown in this chapter. Since the fraction of nodes with more than two nonfrozen inputs is vanishing in the thermodynamic limit, the network of nonfrozen nodes, which is the starting point for the process

of determining the relevant nodes, is the same as in the $K = 2$ case. So, we can conclude that the results for the scaling of the number of relevant nodes found in [58] and presented in the Chapter 4 for the $K = 2$ critical networks are valid for any critical network. The number of relevant nodes in critical networks scales as $(N^{ini})^{1/3}$ with the network size. Among them are a constant number of relevant nodes with two relevant inputs and a vanishing number of relevant nodes with more than two relevant inputs in the limit $N^{ini} \to \infty$. If only these nodes and the links between them are considered, they form loops with possibly additional links and chains of relevant nodes within and between loops. It follows that all critical networks with $K > 1$ show the same scaling behavior. The only exception is the case $K = 1$, which is different because there is no frozen core.

As we have seen in the previous section, we can derive properties of attractors from the results for the relevant nodes. In particular, we can take over the result of previous chapter that all relevant components apart from a finite number are simple loops, and that the mean number and length of attractors increases faster than any power law with the network size.

5.9 Conclusions

In this chapter, we have considered the limit of large network size, and we have found the scaling behavior of the number of nonfrozen nodes, of the number of nonfrozen nodes with more than one nonfrozen input, of the number of relevant nodes, and of the number of relevant nodes with more than one relevant input in a general class of critical random Boolean networks with fixed number of inputs per node. The mean values of these quantities scale with network size N^{ini} as a power law in N^{ini}, with the exponents being the same for any critical network. No matter what the distribution of the Boolean functions is and how many inputs per node the critical network has, number of nonfrozen nodes scales with the network size as $(N^{ini})^{2/3}$, the number of nonfrozen nodes with two nonfrozen inputs scales as $(N^{ini})^{1/3}$, the exponent for the number of nonfrozen nodes with three nonfrozen inputs is zero, and it is $-n/3$ for the number of nonfrozen nodes with $n+3$ nonfrozen inputs. The number of relevant nodes scales always as $(N^{ini})^{1/3}$, with a constant number of them having two inputs and a vanishing proportion having more than two.

It follows that all critical random Boolean networks with $K > 1$ belong to the same class of systems. Changing the weights of the different Boolean functions (for instance by choosing threshold networks or canalizing networks) or changing the number of inputs per node (which might make the model more relevant for biological applications) will not change the scaling of the number of nonfrozen and relevant nodes with the size of the network, and it will not change the fact that

the number and length of attractors increases faster than any power law with the network size, as long as the network is critical. Using a different method, Samuelsson and Socolar have recently also found that the number of nonfrozen nodes scales in the same way for all $K > 1$ critical networks [89].

From the calculations performed in this chapter it can be concluded that the results are also valid for networks that have nodes with different values of K. If K_{max} is the largest number of inputs occuring in the network, we can set $K = K_{max}$, and we can view nodes with less inputs as nodes with K_{max} inputs, but with a function that does not depend on all of its inputs. However, there are indications that these results are different in the case when the second moment of the number of inputs is diverging [26; 62] . Our results cannot be generalized to networks with a broad distribution of the number of outputs. The method employed in this chapter is based on a Poissonian distribution of the number of outputs, and is most likely valid also for other distributions as long as the second moment of the number of outputs is finite. This can for instance be concluded from the analogy between the propagation of activity in a Boolean network and percolation on a directed graph, for which many results are known [92].

The finding that the number and length of attractors in critical Boolean networks increases superpolynomially with network size is detrimental to the hypothesis that these networks are models of gene regulation networks, where only a limited number of dynamic pathways should exist. However, by considering asynchronous update instead of parallel update and by requiring that dynamics should be robust with respect to fluctuations in the update sequence, the number of attractors reduces to a power law in system size, which is more realistic than the superpolynomial growth [59; 40]. The method presented in this chapter is independent of the updating scheme, and the scaling of the number of nonfrozen and relevant nodes is therefore same for asynchronous update as for parallel update. The relevant components are consequently also the same. With the insights obtained in the present chapter, we can immediately apply the results for asynchronous update in $K = 2$ critical networks to critical networks with larger values of K, and we can conclude that the number of attractors in critical networks with asynchronous update increases as a power law of the system size.

Finally, let us consider networks where the connections between nodes are not made at random, but that show some degree of clustering. Such networks have a finite proportion of nodes that have correlated inputs and that can therefore become frozen, e.g., because their inputs are always in the same state. In contrast, the randomly wired networks considered here have only a limited and small number of nodes with correlated inputs even in the thermodynamic limit of infinite network size. For small-world networks, which have a high degree of clustering, our method for determining the frozen core is not valid, because it is based on the assumption

that nodes choose their inputs independently from each other. Small-world networks need therefore a separate analytical treatment, which has not been done so far.

With the results of this chapter we will finish the explorations of the dynamics of critical random Boolean networks with fixed number of inputs per node. Our studies of dynamical properties of these networks confirm that the original model has to be modified if we want to use it as a model for gene regulatory networks. Real gene regulatory networks are not random, but the result of long lasting evolutionary processes. In the next chapter, we therefore study evolution of populations of Boolean networks under selection for robustness of their attractors under small perturbations.

6 Evolution of populations of Boolean networks

The results presented in the previous chapters of this thesis have shown that the Boolean network model in the form it was originally introduced can not be used as a model for gene regulatory networks. Since the model possesses various properties which make it worth studying, its modification with the aim to improve it and to make it biologically more realistic is a logical next step in our studies. Out of the many possible ways of doing that, we choose the one inspired by the process that takes place in nature. In this chapter, we study the evolution of Boolean networks. We change the model's structure through specific mutations, and use one of its dynamical properties as a criterion for selecting the networks of the ensemble. The ensembles of networks generated this way are very different from the random ensembles we studied in previous chapters. We can learn a lot about the system by studying the properties shared by the networks in an ensemble and the way this properties depend on the choice of the rules for mutations and selection.

Since mutations change the structure of networks, and since selection is based on their dynamical properties, the evolutionary process combines dynamics *of* network with the dynamics *on* network. Although in evolutionary models this processes take place on different time scales, we can still learn from these models about the interdependence of the two types of dynamics. We will here focus our investigations on the use of the model in biology, where the complex relations between the two types of dynamical changes of networks are important in understanding the origin of systems' properties, but where the investigations of the evolutionary process itself play a central role. However, in many other complex systems modeled by networks, the structures of networks change with time while at the same time different dynamical processes take place on them. These two ways the network is changing are often not independent of each other. The possibility of learning about the interplay between the dynamics of and on networks, makes studies of evolution of networks important direction in the future studies of complex systems using network models.

The Neodarwinian view of biological evolution considers random mutations and natural selection as the main shaping forces of organisms. Mutations act on the genotype, while selection acts on the phenotype. For this reason, the relation between genotype and fitness is very complicated and far from fully understood. Mathe-

matical models of biological evolution [25] often contain a direct mapping of the genotype on the fitness. The "fitness landscape" may be smooth and single-peaked or random and rugged, or the fitness is taken as the additive contribution of the alleles at several loci. However, the "real" fitness landscape might have completely different properties. For this reason, it is important to investigate models that do not make a direct mapping of the genotype to the fitness, but that determine the fitness from some "trait" that is related in a nontrivial way to the genotype.

The most famous example of such models are based on RNA. The genotype is the RNA sequence, while the phenotype is the two-dimensional fold. When fitness is based on some desired fold, it is found that the fitness landscape contains a huge plateau of high fitness that spans the genotype space [34; 91]. The same feature is displayed by the fitness landscape that is based on the three-dimensional fold of proteins, with the genotype being the nucleotide sequence of the corresponding gene [7].

However, most traits of an organism result from the interaction of many genes. For instance, most genes are very similar in different higher organisms, but they differ in the way they are regulated and in the temporal expression pattern during embryonic development. This feature is captured in models for gene regulatory networks, the simplest of which is the random Boolean network model. In this model dynamical behavior of a Boolean network is its phenotype, while the genotype is specified by the logical functions and the connections between the nodes.

Several publications study the evolution of Boolean networks. Mutations are performed by changing the connections or functions. In biological terms, such mutations change the way in which the genes are regulated, as occurs, for example, due to transpositions. In addition, several investigations include recombination of the parental genotypes in the evolutionary simulations [36; 112; 96]. In [4] the effect of gene duplications was additionally studied.

Selection is based on some dynamical property of the networks. In [51; 105; 78] and [63], the fitness is given by the distance of an attractor to a predetermined target pattern. In [14; 15], the selection criterion requires that the daughter network reaches the same attractor as the mother network when both networks are initialized in the same randomly chosen state. In [79; 67; 16; 66], mutations are targeted to those nodes that display a certain type of behavior.

In [108], the fitness criterion is robustness of the dynamics under small perturbations. Robustness is of great importance in biology as a cell has to maintain its biological functions to survive and pass on its genetic material under variations for example of the concentration of proteins in the cell or of the nutrient level. In [108], evolution was simulated by means of a so-called adaptive walk. This is a hill climbing process that leads to a local maximum in the fitness landscape and thus can yield insight in the fitness landscape of a system. The main finding was that

the maximum possible fitness value is always reached after a few mutations during this process, and that there is a huge plateau with this fitness value that spans the network configuration space. This model is therefore an example for the evolution in the presence of a huge neutral space. Such neutral spaces occur not only in the evolution of RNA and proteins, as mentioned above, but appear to be generic feature of biological systems in general [113].

In this chapter the study of the evolution of an entire population of networks under the mutation and selection rules employed in [108] is presented. We will investigate the fitness and the diversity of the population as a function of time, as well as the topological properties of the evolved networks as function of the mutation rate and the selection pressure. One important result is that, while the population quickly reaches the plateau of high fitness, the network topology undergoes a very slow change towards higher connectivity, while at the same time the mean fitness of the population decreases slightly. These long-therm changes are due to the fact that mutations can change the topological features of the networks, which reach their stationary distribution very slowly. Another important finding of the simulations presented in this chapter is that networks evolved with different mutation rates show different mutational robustness. Taken together, the simulations illustrate that even though the population reaches quickly the neutral plateau of high fitness, there occur nevertheless long-term changes in the properties of the population, and populations evolved under different conditions end up in different regions of network space.

The outline of this chapter is as follows: In Section 6.1, the rules of the evolutionary model are presented. In Section 6.2, we investigate the evolutionary process in the absence of selection, where random mutations and genetic drift are the only shaping forces. In Section 6.3, we study the opposite case of very strong selection, where only the networks with the highest fitness value become parents of the networks in the next generation. In Section 6.4, we then study the general case of finite selection pressure. Section 6.5 summarizes and discusses our findings. The results presented in this chapter were obtained in collaboration with Barbara Drossel and are submitted for publication [74].

6.1 Model

A population of P networks with N nodes each is evolved by repeatedly replacing the entire population with a daughter population. Each individual in the daughter population is obtained by choosing an individual from the parent population to be its mother with a probability that depends on the mother's fitness. The daughter is a copy of the mother, but it receives one mutation with a certain probability μ.

The initial population is generated by connecting the nodes of each network at random, with $K_{ini} = 3$ inputs per node, and with the update function of each node chosen at random from the set of canalizing functions used by Moreira and Amaral [75]. Thus, the function at a node is determined by choosing one of the input nodes as the canalizing input. Its canalizing value and the associated output value each are 0 or 1 with probability 1/2. When the input node is not on its canalizing value, the output is a random Boolean function that depends on the remaining variables and is generated by choosing with same probability 0 or 1 as output for every combination of the remaining input variables. The reason for choosing $K_{ini} = 3$ is that this is the critical value for this class of networks. The initial networks are therefore neither completely frozen, nor are they chaotic (in the sense that neighboring initial states diverge exponentially fast).

The fitness of a network is determined by the following rule: First, the network is initialized in a random state and is updated according to Equation (2.1.1) until it reaches an attractor. Then a state σ on the attractor is chosen. We define S as the set of the N states at Hamming distance 1 from σ. For all $\sigma' \in S$ the dynamics is started at σ' and it is decided if the dynamics eventually returns to the attractor (and therefore also to σ). The fitness f of the network is the fraction of elements in S for which this is fulfilled.

The weight with which an individual i is chosen to be the mother of a given individual of the next generation is

$$w_i = \frac{e^{pf_i}}{\sum_{j=1}^{N} e^{pf_j}}\,, \tag{6.1.1}$$

where we call p the selection pressure. In addition to P and N and μ, this is the fourth parameter that was varied in the simulations.

Four different mutations can occur, each with the same probability:

1. A connection is added.
2. A connection is deleted.
3. A connection is redirected.
4. The canalizing part of the function is changed.

When a network is to undergo a mutation, first the type of mutation is chosen. Then, a node is picked at random to receive this mutation. If the mutation cannot be performed at this node (for instance, only the mutation of adding a link can be done at a node with zero inputs) another node is selected at random to receive the mutation. Due to computational restrictions, we imposed the rule that nodes with 10 inputs cannot receive an additional link, and therefore $K_{max} = 10$.

When a connection is added or deleted, the Boolean function of the node has to be changed. This is done by choosing anew the random Boolean function that depends on the non-canalizing variables. If the canalizing input is removed by the mutation, another node takes its role. A connection is redirected by changing at random the origin (source) of one incoming link of the node which is receiving the mutation. Finally, when changing the canalizing function of the node, the value that canalizes it and the associated output value are assigned to the node anew.

6.2 Evolution without selection

In the absence of selection, each network has the same probability $1/P$ to become the mother of a given daughter network. The average number of generations back to the last common ancestor of two networks is therefore P. With probability μ, a daughter network receives a mutation, and therefore two randomly chosen networks of the population differ by $2P\mu$ mutations on average.

With probability 1/2, the mutation consists in the addition or deletion of a link. This means that the total number of links in the network performs a random walk in time, with probability $\mu/2$ for a nonzero step. Even though the number of inputs is initially $K_{ini} = 3$ for each node, it changes during time, and the distribution of the number of inputs becomes eventually stationary. The probability that the number of inputs of a node changes during a given step depends on the number of nodes with 0 and 10 inputs.

These simple considerations are very useful when interpreting the simulation data. Figure 6.1 shows results of simulation run for 100000 generations of a population with $N = P = 50$ and with a mutation rate $\mu = 0.5$. We evaluated the mean fitness of the population, the mean number of inputs per node, the proportion of nodes with 0 inputs, and the topological diversity of the population. The topological diversity of the population is the average number of links of a network that is not shared by a randomly chosen other network, divided by the mean number of links per network.

The data were smoothened by averaging each data point over 1000 generations, otherwise the data are so noisy that variations on larger time scales are hard to see.

From these data, one can draw the following conclusions:

- The mean fitness and the mean number of inputs per node show large fluctuations over time. This is due to the fact that the last common ancestor of the population is not much more than 50 generations back, which means that the networks in the population are strongly correlated.

- The initial fitness of the population is higher than that at later times. This must be due to the changes occurring in network structure, i.e. to the distri-

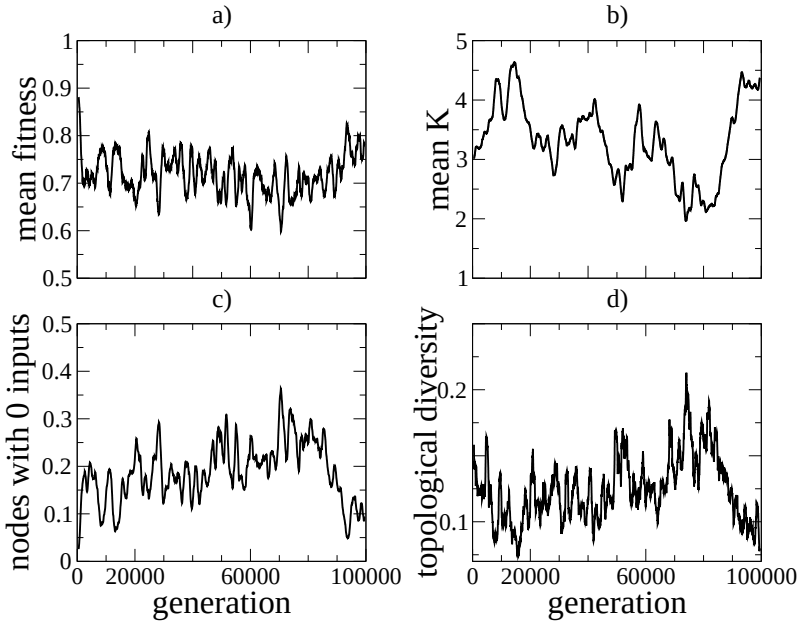

Figure 6.1: Evolution of the a) mean fitness, b) mean number of inputs per node, c) mean number of nodes with zero inputs in a network, d) proportion of different links in two randomly chosen networks, in the population of 50 networks of 50 nodes each, evolved with the mutation rate 0.5 and no selection pressure.

bution of the number of inputs becoming broader. In particular, nodes with zero inputs decrease the fitness (see next point).

- There is an anticorrelation between the fitness and the proportion of nodes with 0 inputs. Clearly, a node with 0 inputs does not return to its initial state after a perturbation. Since it is not affected by the state of any node, it remains in the state in which it was initiated or to which it was set by an external perturbation. If all other nodes did return to the same attractor after a perturbation, the fitness would be identical to the proportion of nodes with at least 1 input.

- There is an anticorrelation between the mean number of inputs and the topological diversity. This is due to the fact that the probability that a given link is mutated becomes smaller when there are more links.

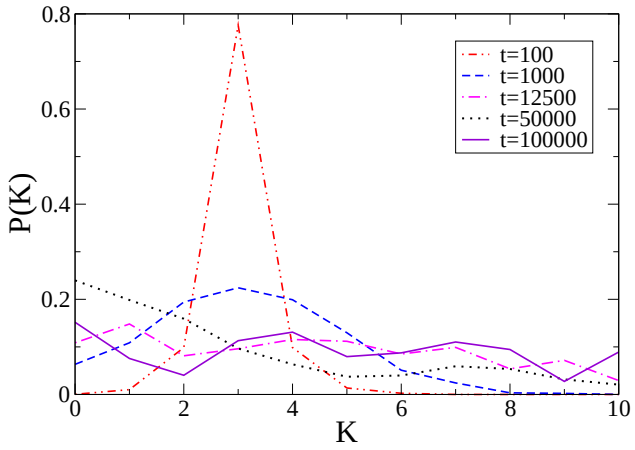

Figure 6.2: Snapshots of the input distribution at different times during the evolution without selection pressure. The input distribution is changing from a delta peak to a broad distribution with an increased number of nodes with zero inputs.

The change in the distribution of the number of inputs is illustrated in Figure 6.2. It is becoming broader, with more nodes with zero inputs, which can temporarily even become the dominant type of nodes in the network. (An example for this is given below in one of the cases illustrated by Figure 6.3.)

Let us now apply analytical considerations in order to estimate the topological diversity of the population. Let T be the average time (in terms of the number of generations) to the last common ancestor of two randomly chosen networks in the population. With no selection pressure, we have $T = P$, but with selection this time becomes shorter. Since their last common ancestor, each network received in each generation a mutation with a probability μ. Therefore the two networks together have received on average $2T\mu$ mutations. If the effect of each of them is different and if there are no back mutations, two randomly chosen networks in the population differ on average by $2T\mu$ links and functions. When evaluating the topological diversity, we consider only links. Since three out of four mutations affect links, we expect that two randomly chosen networks in the population have received together $3T\mu/2$ mutations of links. All these mutations affect different links only if $3T\mu/2$ is small compared to the total number of links of a network, NK. In this case, the topological diversity should be close to $\dfrac{3T\mu}{2NK}$. Otherwise, it is smaller, since two mutations may affect the same link.

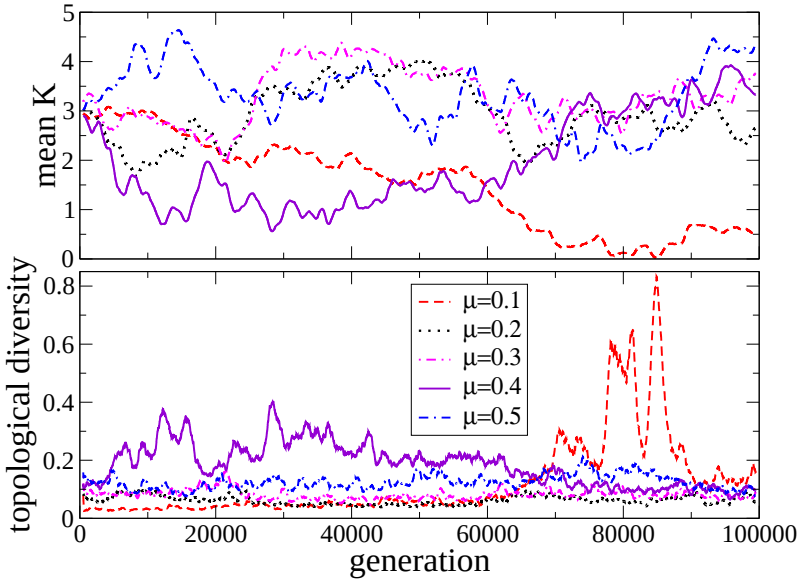

Figure 6.3: Evolution of the mean value of the number of inputs per node (upper figure) and of the topological diversity in the population (lower figure) under no selection pressure and with different mutation rates.

Since K fluctuates strongly with time, the topological diversity fluctuates also and should behave approximately as $1/K$. In Figure 6.1d) we have already seen this anticorrelation. For small K, the number of links that are different in the two networks is much smaller than the number of the link mutations they received, and the topological diversity does not become as large as suggested by our simple estimate. This effect is nicely demonstrated by Figure 6.3, which shows the mean value of K and the topological diversity as function of time for five simulation runs with different mutation rates μ.

Figure 6.4 left shows the number of links by which two networks differ on average, which is the topological diversity multiplied by NK. Our above simple estimate gives link numbers of 7.5, 22.5 and 37.5 for the mutation rates shown in the figure. These numbers are upper bounds, and one can see that for larger mutation rates and for smaller K values the data are farther below these bounds, since multiple mutations of the same link become more frequent.

We investigated also the influence of the size and of the number of networks in the population on the properties of evolved populations by setting N and/or P to

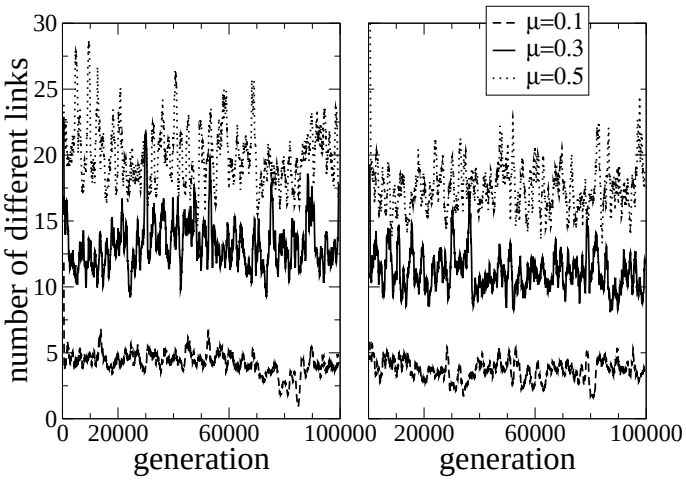

Figure 6.4: Average number of links by which two networks differ, as function of time and for different mutation rates. The selection pressure is zero in the left graph and 100 in the right graph.

30. Most of these properties depend strongly on the mean number of inputs per node, which performs a random walk and shows therefore large fluctuations. For this reason, we could not see a clear trend with N or P in the simulation data, although one can expect that the fitness should not depend on N or P and that the fluctuations should decrease with increasing P. The diversity should change with N and P as P/N, as predicted by analytical estimation earlier in this section.

6.3 Evolution with very strong selection

Next, we consider the opposite case, which is that of very strong selection. In this case, only the networks with the highest fitness value in the population become parents. Now the properties of the fitness landscape play an essential role at determining the evolution of the population. If there were isolated peaks in the fitness landscape, the entire population would perform a hillclimbing process. The fittest individual of the parent population would be the mother of all individuals in the next generation, which would differ from it by at most one mutation. If one of these mutations did lead to a higher fitness, all individuals of the following generation were descendants of the carrier of that mutation. The process would end at a local

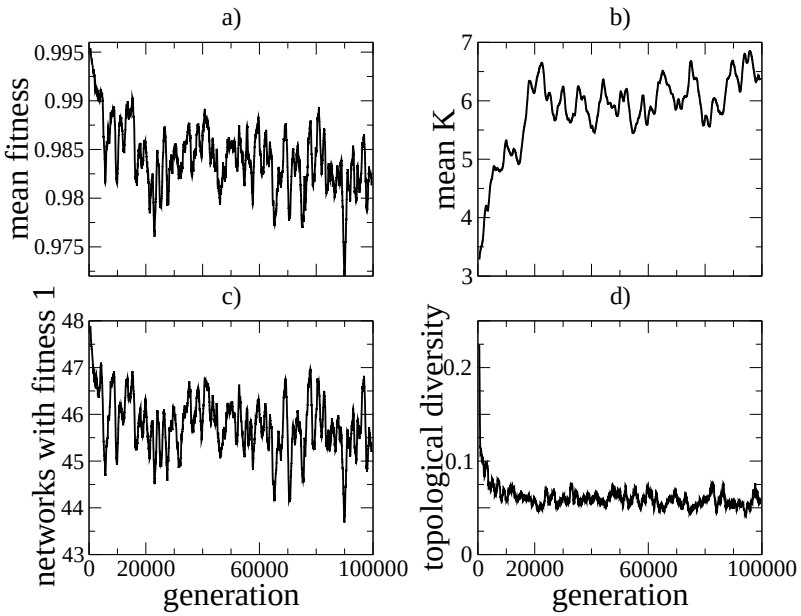

Figure 6.5: Evolution of the a) mean fitness, b) mean number of inputs per node, c) mean number of networks with fitness 1, d) proportion of different links in two randomly chosen networks, in the population of 50 networks of 50 nodes each, evolved with the mutation rate 0.5 and high selection pressure.

peak of the fitness landscape, from where no mutation is possible that increases or retains the fitness value.

However, when the fitness landscape has a plateau with maximum fitness that spans the entire network configuration space, the population can contain several individuals with fitness 1, and mutations can generate other genotypes with fitness 1. In our simulations, already the initial population may contain an individual with fitness 1, so that the mean fitness can be close to 1 already after one generation.

Figure 6.5 shows results of computer simulations for 100000 generations of a population with $N = P = 50$ and with a mutation rate $\mu = 0.5$. The parameters are the same as in Figure 6.1, and each data point represents again an average over 1000 generations. We evaluated the same quantities as in the first simulation, except for the number of nodes with 0 inputs, since these do not occur any more. Instead, we show the number of networks with fitness 1 in the population. The proportion of networks with a fitness smaller than 1 must be identical to μ times the probability that a mutation decreases the fitness of a network with fitness 1.

From these data, one can draw the following conclusions:

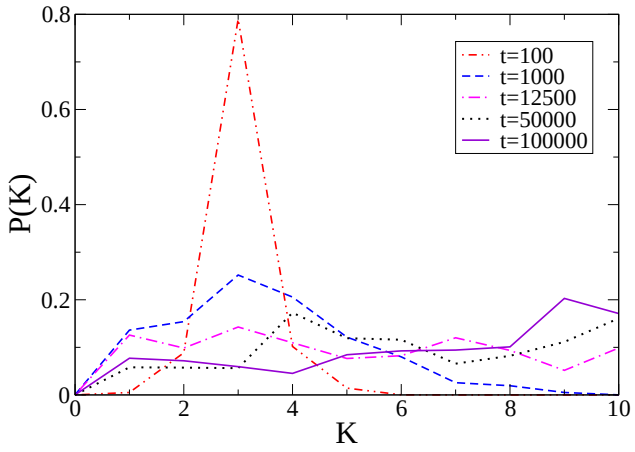

Figure 6.6: Snapshots of the input distribution at different times during the evolution. The input distribution is changing from a delta peak to a broad distribution.

- The fitness of the population decreases slowly with time. Since all networks with a fitness smaller than 1 must be daughters of networks with fitness 1, this means that at later times the average fitness decrease due to a mutation must be larger.

- The mean number of networks with fitness 1 in the population decreases slowly with time. This means that the probability that a mutation decreases the fitness of the network with fitness 1 is larger at later times.

- The mean number of inputs per node increases slowly but steadily. This was already found in the adaptive walk simulations in [108]. This means that mutations that preserve the maximum fitness are more likely to occur when a link is added than when a link is removed.

The change in the distribution of the number of inputs is illustrated in Figure 6.6. As in the situation without selection, it is becoming broader, but now there are more nodes with higher K and less with smaller K. One reason for this is that nodes with zero inputs decrease the fitness, and therefore evolution drives the population into regions in configuration space where such nodes are unlikely to occur.

Let us now estimate the topological diversity using the arguments from the beginning of Section 6.2. The number of networks with fitness 1 in the population is defining the effective population size P', since only these networks can become parents. From Figure 6.5c), we see that this number is around 46 for the parameter

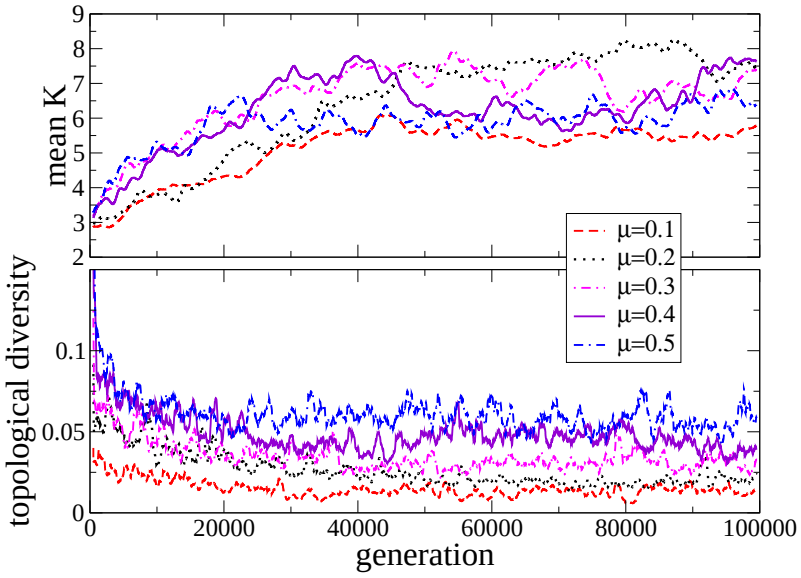

Figure 6.7: Evolution of the mean value of the number of inputs per node (upper figure) and of the topological diversity in the population (lower figure) under strong selection and with different mutation rates.

values used in this simulation. Correspondingly, the data for the number of links that differ between two randomly chosen networks (Figure 6.4 right) are slightly lower compared to the data obtained with zero selection pressure. The estimated upper bound for the topological diversity is now $(3P'\mu)/(2NK)$, with deviations from this bound being again larger for smaller K and larger μ. In Figure 6.7, it can clearly be seen that the topological diversity depends on the mean K value.

We explored in more detail the effect of mutations on networks with fitness 1. The probability that a mutation does not decrease fitness is identical to the proportion of networks with fitness 1, shown in Figure 6.5c). This is because selection pressure is so high that only networks with fitness 1 become parents of the networks in the next generation, each of which then receives a mutation with probability μ. We call a mutation that does not decrease the fitness "neutral".

Figure 6.8 (upper panel) shows the proportion of the four different types of mutations among these neutral mutations, again for $\mu = 0.5$. All four types of mutations were chosen equally often, however, the proportion of neutral mutations is different for the four mutation types. The most frequent neutral mutation is the redirection

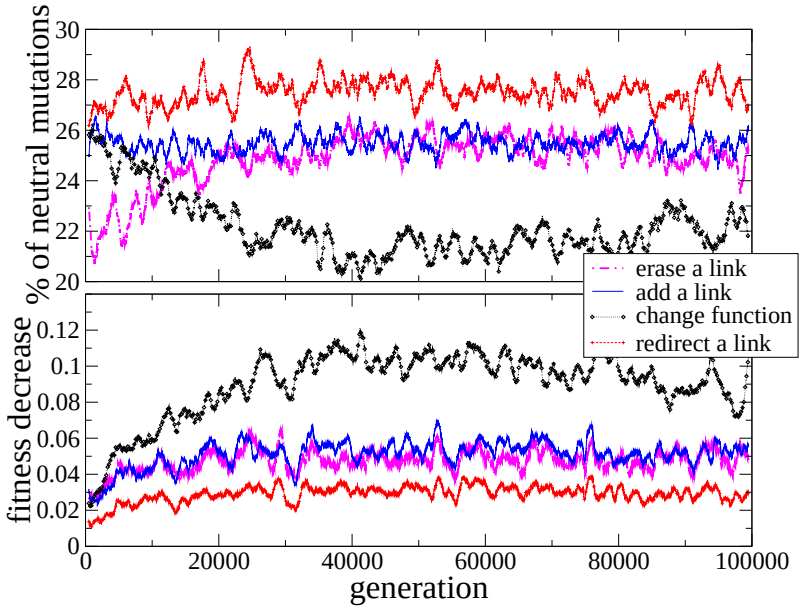

Figure 6.8: Evolution of the proportion of neutral mutations of different types (upper figure) and of the mean fitness decrease per non-neutral mutation (lower figure) under strong selection pressure and with a mutation rate $\mu = 0.5$.

of a link. This means that networks with fitness 1 are most robust (in the sense that their fitness is not decreased) to this type of mutations. The least frequent neutral mutation is initially the deletion of a link; at later times the change of a function is least frequent. The combined contribution of these two types of mutations to the neutral mutations is approximately constant in time. The frequency of mutations that add a link is also approximately constant. This implies that the slow increase of the mean K value is not due to a beneficial effect of mutations that add links, but due to the fact that erasing a link decreases the fitness more often than the addition of a link, in particular in the beginning of the simulation, where also the largest increase of K can be seen. At later times, deletions and additions are equally frequent among the neutral mutations. The increase of K explains why mutations that change the canalizing function become less frequent among neutral mutations. When K is larger, such a change affects more nodes on an average.

In Figure 6.8 (lower panel), we show the amount by which fitness decreases due to a non-neutral mutation. This amount increases with time for all four types of

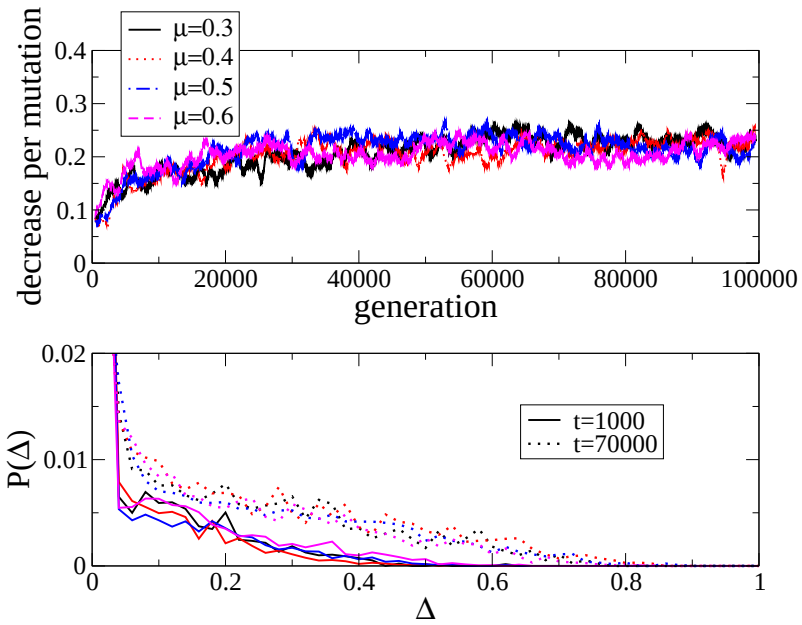

Figure 6.9: Upper graph: Fitness decrease per (non-neutral) mutation as function of time, for four different mutation rates. Lower graph: Probability distribution of the fitness decrease Δ (including zero decrease) due to a mutation, evaluated at two different times during evolution.

mutations. This must be due to the fact that the perturbation of one node affects more nodes when K is larger, and therefore a mutation affects also more nodes. For the same reason, mutations that change the canalizing function lead to a larger fitness decrease than other mutations. The redirection of a link leads to the smallest fitness decrease because it does not involve changes in the update functions.

Next, we investigated the influence of the mutation rate on these results. Figure 6.9 (top) shows the fitness decrease per mutation for different mutation rates. Here, we now do not discriminate between different types of mutations. The mean fitness decrease per non-neutral mutation appears to be independent of the mutation rate with which the networks were evolved.

The lower graph of Figure 6.9 shows the probability distribution of the fitness decrease per mutation at an early and at a late time. Here, neutral mutations, which lead to a fitness decrease of 0, are also included. After approximately 30000 generations, the probability distribution of the fitness decrease reaches a stationary

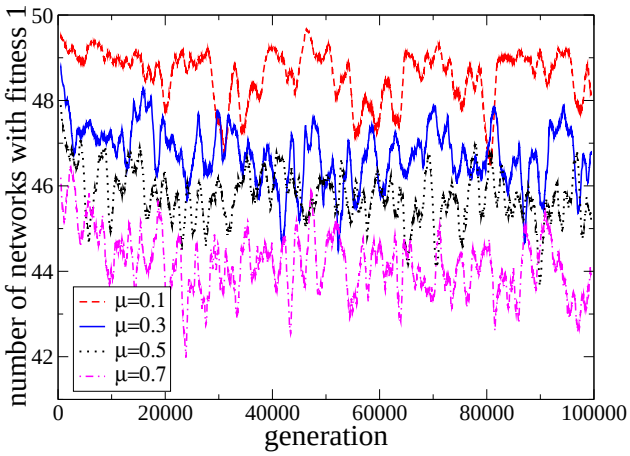

Figure 6.10: Change of the number of networks with fitness 1 in the population during evolution with different mutation rates and high selection pressure

shape. This shape does not depend on the mutation rate with which the networks were evolved. Most of the mutations do not decrease fitness or they decrease it by the smallest possible amount of 0.02 (which means that only after 1 out of the N possible perturbations the network does not return to the same attractor). We do not show completely this part of the curves in order to make the distribution for larger fitness decreases better visible. There are no significant differences between the curves for different μ. We have already discussed above that the mean fitness decrease per non-neutral mutation is larger at later times, when K is larger.

While networks evolved with different mutation rates do not differ in the fitness decrease per (non-neutral) mutation, they do differ in other respects. Figure 6.10 shows the number of networks with fitness 1 in the population as function of time for four different mutation rates. If the probability of a mutation being neutral was the same in all four cases, the distance of the curves from the value 50 should be proportional to μ. Due to the large fluctuations, the data cannot give a clear answer to whether this is the case. We therefore evaluated directly the probability that a mutation decreases fitness, for mutation rates ranging from $\mu = 0.1$ to $\mu = 0.7$. These data show a clear trend, with networks evolved with higher mutation rates being less likely to decrease their fitness under a mutation. They are more robust to mutations. Figure 6.11, upper panel, shows the curves obtained with $\mu = 0.3$ and 0.6. This means that the networks on the plateau of the fitness landscape,

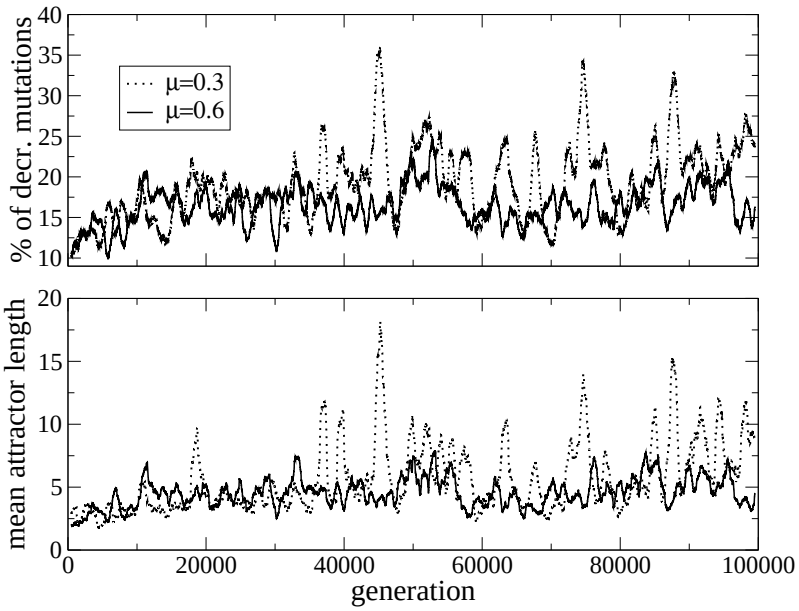

Figure 6.11: Evolution of the percentage of mutations decreasing fitness (upper graph) and of the mean attractor length in the population (lower graph) under strong selection and with two different mutation rates.

reached by evolution under strong selection, have different properties depending on the mutation rate with which they were evolved. This result is not merely due to the fact that populations evolve slower when the mutation rate is smaller. If this were the case, the curves obtained with a smaller mutation rate should resemble those obtained with larger mutation rates at an earlier time.

There is a correlation between the mean attractor length and the frequency of neutral mutations, as revealed by the lower graph of Figure 6.11. This correlation can be seen most clearly by comparing the positions of the peaks. The numerical values of the correlation between the two curves are 0.892 for $\mu = 0.3$ and 0.885 for $\mu = 0.6$. These values are not far from the value 1, which would result if the two curves were proportional to each other. This means that networks with longer attractors are more likely to decrease their fitness under mutations, which is not too surprising. Conversely, networks that are more robust against mutations have smaller attractors.

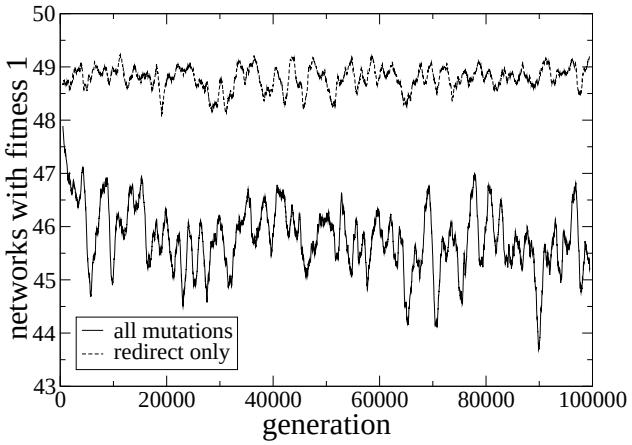

Figure 6.12: Number of networks with fitness 1 as function of time for high selection pressure ($p = 100$) and the mutation rate $\mu = 0.5$. The original model is compared with a model where only the redirection of links is allowed.

In order to investigate how evolution proceeds when there can be no slow change in network structure, we also performed simulations with a different rule, which allows no deletion and addition of links or changes of functions, but only the redirection of the links. In this situation, the number of inputs of every node remains 3, and the distribution of the number of outputs remains Poissonian. The population reaches quickly the stationary fitness value, and the diversity of the population is still large.

In Figure 6.12 the mean number of networks with fitness 1 in a population obtained with this new mutation rule is compared to the results obtained with the original rules, for $P = 50$ and $\mu = 0.5$. The data imply that the mean fitness decrease per mutation is much larger for the original rule. We have seen (Figure 6.8) that when the networks are evolved with all four types of mutations, those mutations redirecting links are decreasing the fitness less than others. Redirections of links could also have smaller effect on the fitness of the networks evolved under the new rule, which would then explain the observed difference.

Figure 6.13 shows the number of mutations by which two randomly chosen networks of a population differ, as function of time, for the two mutation rules. This number is considerably larger when links are only rewired. We attribute this result to the larger effective population size and to the absence of networks with small average K values.

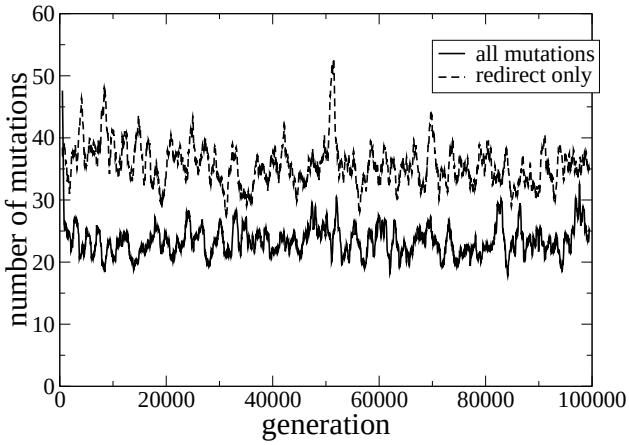

Figure 6.13: Number of mutations by which two randomly chosen networks of a population differ, as function of time, for the two mutation rules. The parameters are again $p = 100$ and $\mu = 0.5$.

Not surprisingly, we do not find any long-term trend in the mean fitness of the population with the modified mutation rule. This confirms our suggestion that the long-term change of the network structure is responsible for the slow and steady decrease of the fitness in the original simulations.

Finally, we investigated the influence of the size and of the number of networks in the population on the properties of evolved populations by setting N and/or P to 30. We found that the mean fitness of the population decreases with decreasing N, since a node is more likely to be affected by a mutation when N is smaller. A decrease of the population size shows even larger effect on the mean fitness, because the influence of genetic drift becomes more important compared to the influence of selection. Earlier in this section we estimated that the topological diversity should change approximately as P/N. In our simulations, we find trends that agree with this assumption. However, due to large fluctuations, we cannot make the statements of this paragraph more quantitative.

6.4 Evolution with finite selection pressure

When selection pressure is finite, the properties of the evolving populations should be between the two extreme cases studied until now. When mutation rates are too

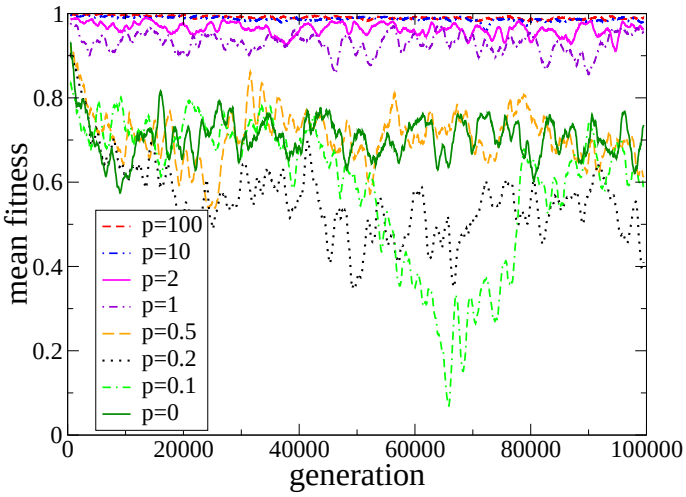

Figure 6.14: Evolution of the mean fitness for different selection pressures and a mutation rate $\mu = 0.2$.

high, selection pressures too low, or population sizes too small, the effect of selection is hardly visible in the population, the evolution of which is then dominated by drift.

Figure 6.14 shows the mean fitness of a population with $N = P = 50$ and a mutation rate $\mu = 0.2$ as a function of time for different values of the selection pressure p. One can clearly see that for $p \leq 0.5$ the evolution of the fitness resembles that of the system with $p = 0$, which means that drift dominates the evolutionary process. The simulation for $p = 0.1$ accidentally goes through a stage where there are very many nodes with 0 inputs (this is correlated with the decrease of the mean K value that can be seen in Figure 6.15), resulting in a very low fitness.

For $p \geq 1$, selection has a clear effect on the fitness. Figure 6.16 shows the number of networks with fitness 1 in the population as a function of time for $p \geq 1$. (For $p \leq 0.5$, there are almost no networks with fitness 1.) When the selection pressure is smaller, this number is also smaller. Just as for the case of very large selection pressure, the populations show a slow and slight decrease of the mean fitness with time. This decrease is again correlated with an increase in the mean connectivity, as shown in Figure 6.15.

The topological diversity is again strongly correlated with the number of inputs per node. In Figure 6.17 we show the number of links by which two randomly

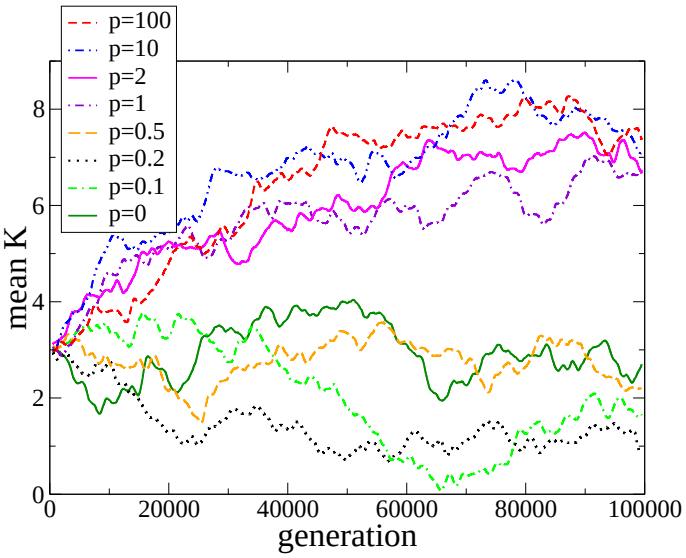

Figure 6.15: Evolution of the mean number of inputs per node under different selection pressures and mutation rate 0.2

chosen networks of the population differ. This number does not depend on K, but on the effective population size. It has approximately the same mean value for all selection pressures, whether they are weak or strong. This is not surprising, as we have already seen that the effective population sizes do not change much when the selection pressure is changed from 0 to a very high value. For weak selection, there are instances where the total number of links becomes very small.

6.5 Conclusions

In this chapter we have investigated the evolution of populations of random Boolean networks under selection for robustness of the dynamics with respect to the perturbation of a node. The fitness landscape of such a model contains a huge plateau of maximum fitness that spans the entire network space.

Even in the absence of selection, we found long-term changes in the network structure. In particular, the distribution of the number of inputs became broad, leading to a decrease in the mean fitness. Furthermore, since links are randomly added or deleted during mutations, the evolutionary process may go through periods where

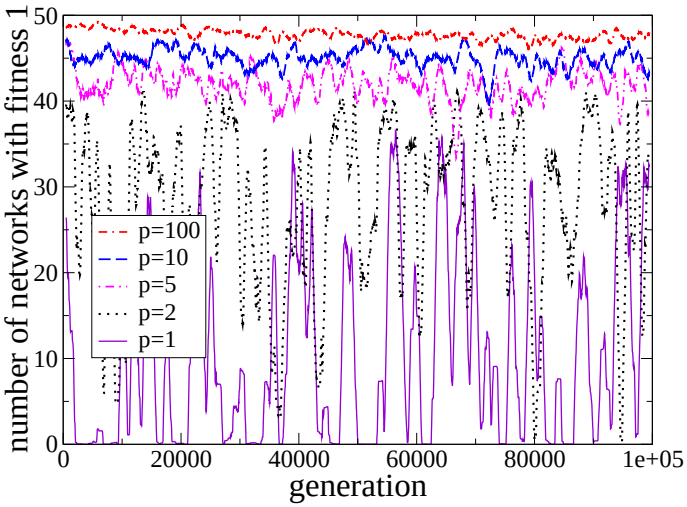

Figure 6.16: Change of the number of networks with fitness 1 during the evolution under different selection pressures and mutation rate 0.2

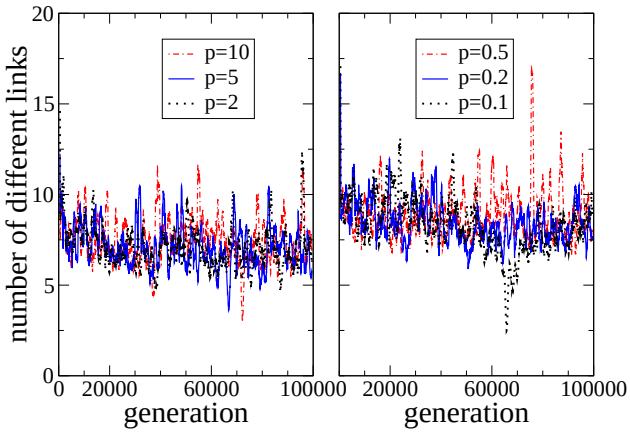

Figure 6.17: Number of links by which two randomly chosen networks differ in the population during evolution with mutation rate 0.2 and under selection pressures $p \geq 1$ (left) and $p \leq 0.5$ (right).

there are very few links in the networks, which implies that fitness is particularly low.

When selection is so strong that only networks with the maximum fitness value 1 can become parents of the next generation, the evolutionary process is accompanied by a slow increase in the mean connectivity and a slow decrease in the mean fitness, lasting for several 10000 generations. In fact, this process was apparently not fully finished at the end of our long-term simulations. We ascribe this long-term trend to the fact that the distribution of the number of inputs becomes broader with time due to mutations that add or delete links, combined with the fact that nodes with 0 inputs decrease the fitness of the network. Therefore mutations that add links are favored with respect to mutations that remove links. Interestingly, the mean fitness of the population decreases nevertheless. This resembles the 'tragedy of commons' [41], where the mean fitness of the population decreases, while each individual strives to obtain maximum fitness. But in contrast to the 'tragedy of the commons', the fitness of an individual in our model does not depend on the other individuals. This effect can in our model be explained by the fact that networks with more links per node are more likely to decrease their fitness when a mutation is performed.

We found furthermore that populations evolved with higher mutation rates show a higher robustness against mutations, i.e., they are less likely to loose fitness under a mutation. This means that even though all the evolved populations move on the plateau of maximum fitness, they end up in different regions of network space. Robustness against mutations evolves because networks with higher mutational robustness have more offspring in the next generation. This trend is countered by the generation of mutationally less robust networks through neutral mutations. When the effect of mutations becomes more important (because mutation rates are higher), the equilibrium point between these two trends moves towards higher mutational robustness. This explains why networks evolved under higher mutation rates are more robust against mutations. We found that higher robustness against mutations is accompanied by a shorter mean attractor length. Furthermore, higher mutational robustness is also correlated with higher dynamical robustness, i.e. with higher mean fitness. The above-mentioned slow decrease (after the initial increase towards the plateau) in the mean fitness of the population is therefore reflected in a similar slight decrease in mutational robustness.

Populations evolved at finite selection pressures behave similarly to those without selection when drift dominates over selection, and they behave similarly to those with high selection pressure when the effect of selection dominates over drift.

Let us now compare the properties of our model with those of real gene regulatory networks. In spite of its simplicity, the network model studied in this chapter

captures several features of real systems and teaches some important lessons: The selection criterion chosen in our study is a criterion of dynamical robustness, which is an important feature of cellular networks. Real gene regulatory networks have to maintain their function under the omnipresent thermal noise and stochastic fluctuations of molecular concentrations. This dynamical robustness should be preserved during evolutionary processes, even when the phenotype of the mutant individual is different from that of the parent. Indeed, experimental studies show robustness of cellular networks under mutations. The gene regulatory network of *Escherichia coli* [48], and the *phage* λ regulatory circuitry, [65], preserved their function under different changes in their structure, implying high robustness under mutations and high dynamical robustness after the mutations. These findings and others reviewed in [113] suggest that the fitness landscape of real cellular networks also contains a huge plateau of high fitness, through which the networks can move without loss of functionality.

Our model shows that evolution within this neutral space can show long-term trends, as manifested by the broadening of the distribution of the number of inputs and by the trend to move farther away from regions in state space where a mutation may radically decrease fitness (as happens in the model when a node loses its last input). Similarly, the long-term trends of evolution of biological systems should be affected by the probability distribution of different types of mutations and by the dangerous regions in state space, even though fitness remains high all the time.

When evolution occurs with higher mutation rates, real networks can continue to function only when their mutational robustness is sufficiently large. Our simulations indicate that during the evolution within the neutral space, an increased mutational robustness evolves naturally when mutation rates are higher. The evolved model networks were less likely to decrease their fitness under a mutation when evolution was preformed with a higher mutation rate. We have presented phenomenological arguments for this effect and similar arguments can be found in the literature [113].

The mutational robustness of our networks is correlated with the dynamical properties of these networks. When mutational robustness is higher, the dynamical robustness (i.e., average fitness) is higher and the attractors are shorter. Other studies of the evolution of Boolean networks show also a connection between dynamical robustness and mutational robustness. In [112; 17; 49; 96], the authors find that robustness to noise (i.e., to small perturbations of the state of the network) and robustness to mutations are highly correlated. In those investigations, mutational robustness and dynamical robustness evolve together and increase with time, while they may also decrease in our simulations. A correlation between dynamical and mutational robustness is biologically meaningful, since the networks must continue to function in the presence of all perturbations whether these perturbations are genetically or environmentally caused [113].

Finally, in order to remain evolvable, networks also have to preserve variability. This is the case in our simulations, since mutations can change the phenotype (i.e., the attractors) even after a long time.

7 Summary and outlook

In this thesis, dynamics and evolution of random Boolean networks has been investigated. In this model the simplest possible dynamics of a node, binary dynamics, is applied to a simple, random topology. These two ingredients define a model which already shows complex dynamical behavior, and can thus be used in modeling dynamics of complex systems. The simplicity of its elements makes the model an important starting point in modeling systems with a dynamics that can be approximated by a binary change of the states, and makes it at the same time a good general model for discrete dynamics on networks.

The particularly complex dynamical behavior of networks at the border between two phases of dynamical behavior was not fully understood for more than 30 years. These critical networks were believed to be a good model for real gene regulatory networks. Analyzing the critical networks using analytical concepts, we have learned about both, the possibilities and the limitations of the model. The studies represented in this thesis contributed to the better understanding of the model's dynamics and have confirmed that the model has to be modified in order to be more realistic. One of the possible modifications, the generation of networks by evolution, is then studied.

Let us now sum up more in detail the most important findings presented in this thesis. In Chapter 3, the simplest case of critical Kauffman networks is studied, the networks with one input per node. The topology of these networks consists of loops and trees only and all relevant nodes of these networks are organized in loops. Therefore, conclusions about the number and the length of attractors can be made using some basic knowledge about the dynamical rules and studying the topology of these networks. We have obtained the topological properties needed by generating the networks through a growth process. Then, using probabilistic arguments and calculating lower bounds we have analytically proven that the number and length of attractors grow faster than any power law with the network size.

The dynamics of the class of critical networks with two inputs per node was studied in Chapter 4. We studied the generalized model of critical networks in which the functions from different classes can be chosen with different weights. This way a network with two inputs per node can be critical for different choices of functions assigned to the nodes. We obtained the constraint on the choice of functions for critical networks from the deterministic description of a stochastic process, which

was introduced to describe the formation of the frozen core in the network. After including noise in the description of the process we were able to find the properties and the scaling behavior of the nonfrozen nodes in critical networks. We have analytically proven that the mean number of nonfrozen nodes scales with the network size N as $N^{2/3}$, with only $N^{1/3}$ nonfrozen nodes having two nonfrozen inputs. We also found the probability distributions for the numbers of these nodes. Using a different stochastic process, we determined the scaling behavior of the number of relevant nodes. Their mean number increases for large N as $N^{1/3}$, and only a finite number of relevant nodes have two relevant inputs. It follows that all relevant components apart from a finite number are simple loops, and that the mean number and length of attractors increases faster than any power law with network size.

In Chapter 5, the dynamics of critical networks with higher values of K was investigated, thus completing our investigations of dynamics of critical Kauffman networks. We have modified the process for determining the frozen core of the network, introduced in the Chapter 4, in the way that networks with any number of inputs per node can be studied. The deterministic description of the process is used again to determine the parameter combinations for which the networks are critical. These parameters reflect the choice of the Boolean functions in the networks. Analyzing this stochastic process for different parameters, we have analytically proven that, in the thermodynamic limit, the mean number of nonfrozen nodes in any critical network with more than one input per node scales with the network size N as $N^{2/3}$, with only $N^{1/3}$ nonfrozen nodes having two nonfrozen inputs and the number of nonfrozen nodes with more than two inputs being finite in the thermodynamic limit. The number of relevant nodes scales as $N^{1/3}$, with a constant number of them having two inputs and a vanishing proportion having more than two. This means that the same conclusions about the mean number and length of attractors, as in the case of $K = 2$ networks, can be made.

To conclude our findings of study of dynamics of random Boolean networks presented in Chapters 3, 4 and 5, it follows that all critical random Boolean networks with fixed number of inputs and $K > 1$ belong to the same universality class. Changing the weights of the different Boolean functions or changing the number of inputs per node will not change the scaling of the number of nonfrozen and relevant nodes with the size of the network, and it will not change the fact that the number and length of attractors increases faster than any power law with the network size, as long as the network is critical. The scaling coefficient is different only in the case of $K = 1$, which is special since these networks have no frozen core. The findings concerning the number and the size of attractors in the critical networks imply that critical Kauffman networks can not be used as a model for gene regulation, since its attractors are too large and there are too many of them to represent the cellular

differentiation. The model has to be modified, if it is to be used for modeling gene regulation. The modification we used is the evolution of Boolean networks.

In Chapter 6 we evolved populations of random Boolean networks under selection for robustness of the dynamics with respect to the perturbation of the state of a node. The networks were mutated by changing the links and the nodes' update rules. We investigated the change of the diversity of a population, its structure, the topology of networks and their dynamical properties, such as the fitness and the length of attractors, during evolution. The parameters determining the evolutionary model were the mutation rate, selection pressure and sizes of networks and populations. First we studied the case of evolution without selection pressure in order to determine the influence of drift and mutations on the change of the structure of evolved populations and on the properties of evolved networks. Then, the evolution under strong selection pressure was studied. This way we explored the properties of the fitness landscape, how population can move on it and the dynamical properties of the fittest networks in the population. We finished by studying the effect of finite selection pressures. For each fixed value of the parameter defining the selection pressure, we have investigated the effect of the change of other parameters, the mutation rate, the size of the network and the size of the population, on network evolution. We have found that the fitness landscape contains a huge plateau of maximum fitness that spans the entire network space. In such a fitness landscape, evolution can show long-term trends. When selection is so strong that it dominates over drift, the evolutionary process is accompanied by a slow increase in the mean connectivity and a slow decrease in the mean fitness. We have also found that the mutational and dynamical robustness of evolved networks are correlated. Furthermore, our simulations have shown that populations evolved with higher mutation rates show a higher robustness under mutations. This means that even though all the evolved populations exist close to the plateau of maximum fitness, they end up in different regions of network space.

Apart from the modification studied in this thesis, there are many other possibilities to modify the random Boolean network model. In Section 2.5 we mentioned some of them. Most of the modifications make Boolean networks better suited for modeling gene regulatory networks, or other systems. Even those modifications that are not successful in bringing model closer to the real system, can be very useful since we can learn about the model in general, improving our understanding of its properties. Let us now mention just a few of the modifications were the results of the studies presented in this thesis could be used.

One of the ways to improve the model is by using some more realistic network structures. In the model's topology input and output distribution could be changed. Real network often have power-law distribution in the number of inputs or the number of outputs [1]. Although Boolean dynamics on such networks has already been

studied [3; 35] dynamical properties of these network are not yet well understood. The stochastic processes and the concept of relevant nodes we used in the studies presented in this thesis could with some modifications be used in scale-free Boolean networks and bring possibly a better understanding of their dynamical properties. A special class of these networks with scale-free input distribution is presently being investigated [26] The method is able to show how scaling exponents for the number of nonfrozen and relevant nodes change with the exponent of the input distribution. It would be interesting to see how different choices of functions influence these results and, how a scale-free output distribution influences the system's dynamical behavior. Scale-free output distributions are thought to be biologically more realistic than the scale-free input-distributions.

The study of the evolution of Boolean networks is an extremely interesting topic, which is in no way exhausted with the studies presented in this thesis. The evolutionary process depends on the choice of the fitness criterion. Imposing the fitness criterion can be seen as asking the question the evolved system should answer. The understanding of networks dynamics gained in the studies presented here can help in asking the right questions.

One natural extension of the studies of evolution presented in this thesis would be to investigate evolution with a fitness criterion that demands that attractors are stable under certain perturbations but are unstable in the case of some others, since real systems have to be stable but also able to respond to external inputs.

Nodes that respond to external inputs can often be found in real networks. Such an external input to a node can be modeled by switching the constant function from 1 to 0 or vice versa. The set of nodes that cannot be controlled in this way is called the computational core [19; 18]. This concept and the way it can be approached is very similar to the one we used in our analysis but has also this new element of external regulation. The understanding of dynamics gained from our studies could help in implementing this model in the evolution of Boolean networks.

Fitness can be defined by the matching of some dynamical property of the network, such as an attractor or a trajectory in state space, with a predefined target. Such investigations have been done already, but recently new Boolean network models for real systems have been developed [13]. The properties of the state space of these real networks would be a good choice of a target.

The success in modeling real biological networks by using Boolean dynamics [64; 2; 20] has intensified the use of Boolean models in modeling other small real networks. This is, in the light of the ever-growing experimental data on the properties of real genetic networks, a promising direction in the use of Boolean network models.

Bibliography

[1] R Albert and A. L. Barabasi. Statistical mechanics of complex networks. *Rev. Mod. Phys.*, 74:47, 2002.

[2] R. Albert and H. G. Othmer. The topology of the regulatory interactions predicts the expression pattern of the segment polarity genes in *Drosophila melanogaster*. *J. Theor. Biol.*, 223(1):1–18, 2003.

[3] M. Aldana. Boolean dynamics of networks with scale-free topology. *Physica D*, 185(1):45–66, 2003.

[4] M. Aldana, E. Balleza, S. Kauffman, and O. Resendiz. Robustness and evolvability in genetic regulatory networks. *J. Theor. Biol.*, 245:433–448, 2007.

[5] Maximo Aldana-Gonzalez, Susan Coppersmith, and Leo P. Kadanoff. Boolean dynamics with random couplings. In Ehud Kaplan, Jerrold E. Mardsen, and Katepalli R. Sreenivasan, editors, *Perspectives and Problems in Nonlinear Science, A celebratory volume in honor of Lawrence Sirovich*, pages 23–89. Springer Applied Mathematical Sciences Series, Springer Verlag, New York, 2003.

[6] L. Amaral and J. Ottino. Complex networks: Augmenting the framework for the study of complex systems. *The European Physical Journal B-Condensed Matter*, 38(2):147–162, 2004.

[7] U. Bastolla, M. Porto, H.E. Roman, and M. Vendruscolo. Statistical properties of neutral evolution. *J. Mol. Evol.*, 57:103–119, 2003.

[8] Ugo Bastolla and Giorgio Parisi. The modular structure of Kauffman networks. *Physica D*, 115(3&4):219, 1998.

[9] Ugo Bastolla and Giorgio Parisi. Relevant elements, magnetization and dynamical properties in Kauffman networks. a numerical study. *Physica D*, 115(3&4):203, 1998.

[10] A. Bhattacharjya and S. Liang. Power-law distributions in some random boolean networks. *Phys. Rev. Lett.*, 77:1644–1647, 1996.

[11] S. Bilke and F. Sjunnesson. Stability of the Kauffman model. *Phys. Rev. E*, 65:016129, 2002.

[12] B. Bollobás. *Random Graphs*. Cambridge University Press, 2001.

[13] S. Bornholdt. Boolean network models of cellular regulation: prospects and limitations. *Journal of The Royal Society Interface*, 5:85–94, 2008.

[14] S. Bornholdt and K. Sneppen. Neutral mutations and punctuated equilibrium in evolving genetic networks. *Phys. Rev. Lett.*, 81:236, 1998.

[15] S. Bornholdt and K. Sneppen. Robustness as an evolutionary principle. *Proc. R. Soc. Lond. B*, 267:2281, 2000.

[16] Stefan Bornholdt and Thimo Rohlf. Topological evolution of dynamical networks: Global criticality from local dynamics. *Phys. Rev. Lett.*, 84(26):6114–6117, 2000.

[17] S Ciliberti, O.C. Martin, and A. Wagner. Robustness can evolve gradually in complex regulatory gene networks with varying topology. *PLoS Comput. Biol.*, 3:164–173, 2007.

[18] L. Correale, M. Leone, A. Pagnani, M. Weigt, and R. Zecchina. Computational core and fixed-point organisation in boolean networks. *J. Stat. Mech.*, 3:P03002, 2006.

[19] L. Correale, M. Leone, A. Pagnani, M. Weigt, and R. Zecchina. Core Percolation and Onset of Complexity in Boolean Networks. *Physical Review Letters*, 96(1):18101, 2006.

[20] M.I. Davidich and S. Bornholdt. Boolean Network Model Predicts Cell Cycle Sequence of Fission Yeast. *PLoS ONE*, 3(2):1–8, 2008.

[21] B. Derrida and G. Weisbuch. Evolution of overlaps between configurations in random boolean networks. *Journal De Physique*, 47:1297–1303, 1986.

[22] Bernard Derrida and Yves Pomeau. Random networks of automata: a simple annealed approximation. *Europhys. Lett*, 1(2):45–49, 1986.

[23] Bernard Derrida and Dietrich Stauffer. Phase transitions in two dimensionalKauffman cellular automata. *Europhys. Lett*, 2(10):739–745, 1986.

[24] SN Dorogovtsev and JFF Mendes. Evolution of networks. *Advances In Physics*, 51(4):1079–1187, 2002.

[25] B. Drossel. Biological evolution and statistical physics. *Adv.Phys.*, 50:209–295, 2001.

[26] B. Drossel and F. Greil. Work in progress, 2008.

[27] Barbara Drossel. Number of attractors in random Boolean networks. *Phys. Rev. E*, 72:016110, 2005.

[28] Barbara Drossel. Random Boolean networks. *Annual Review of Nonlinear Dynamics and Complexity, Vol. 1, Ed. HG Schuster*, 2008.

[29] Barbara Drossel, Tamara Mihaljev, and Florian Greil. Number and length of attractors in a critical Kauffman model with connectivity one. *Phys. Rev. Lett.*, 94:088701, 2005.

[30] C.H.A. Ferraz and H.J. Herrmann. The Kauffman model on small-world topology. *Physica A: Statistical Mechanics and its Applications*, 373:770–776, 2007.

[31] H. Flyvbjerg. Recent results for random networks of automata. *Acta Physica Polonica B*, 20:321–349, 1989.

[32] Henrik Flyvbjerg. An order parameter for networks of automata. *J. Phys. A*, 21:L955, 1988.

[33] Henrik Flyvbjerg and N. J. Kjær. Exact solution of Kauffman's model with connectivity one. *J. Phys. A*, 21:1695, 1988.

[34] W. Fontana, P. F. Stadler, E. G. Bornberg-Bauer, T. Griesmacher, I. L. Hofacker, M. Tacker, P. Tarazona, E. D. Weinberger, and P Schuster. Rna folding and combinatory landscapes. *Phys. Rev. E*, 47:2083, 1993.

[35] J. J. Fox and C. C. Hill. From topology to dynamics in biochemical networks. *Chaos*, 11(4):809–815, 2001.

[36] S. Frank. Population and quantitative genetics of regulatory networks. *J. Theor. Biol.*, 197:281–294, 1999.

[37] I. Gat-Viks and R. Shamir. Chain functions and scoring functions in genetic networks. *Bioinformatics*, 19(Supplement 1):i108–i117, 2003.

[38] C. Gershenson. Updating schemes in random Boolean networks: Do they really matter. In *Artificial Life IX Proceedings of the Ninth International Conference on the Simulation and Synthesis of Living Systems*, pages 238–243, 2004.

[39] F. Greil and B. Drossel. Kauffman networks with threshold functions. *The European Physical Journal B-Condensed Matter and Complex Systems*, 57(1):109–113, 2007.

[40] Florian Greil and Barbara Drossel. The dynamics of critical Kauffman networks under asynchronous stochastic update. *Phys. Rev. Lett.*, 95:048701, 2005.

[41] G. Hardin. The tragedy of the commons. *Science*, 162:1243–1248, 1968.

[42] G. H. Hardy and E. M. Wright. *An introduction to the theory of numbers*. Oxford Press, New York, 1980.

[43] S. E. Harris, B. K. Sawhill, A. Wuensche, and S. A. Kauffman. A model of transcriptional regulatory networks based on biases in the observed regulation rules. *Complexity*, 7(4):23–40, 2002.

[44] I. Harvey and T. Bossomaier. Time out of joint: Attractors in asynchronous random boolean networks. In *Proceedings of the Fourth European Conference on Artificial Life*, pages 67–75, 1997.

[45] H. J. Hilhorst and M. Nijmeijer. On the approach of the stationary state in kauffmans random boolean network. *Journal De Physique*, 48:185–191, 1987.

[46] C. Huepe and M. Aldana-González. Dynamical Phase Transition in a Neural Network Model with Noise: An Exact Solution. *Journal of Statistical Physics*, 108(3):527–540, 2002.

[47] James Hurford. Random boolean nets and features of language. *IEEE Transactions on Evolutionary Computation*, 5(2):111–116, 2001.

[48] M. Isalan, C. Lamerle, K. Michalodimitrakis, C. Horn, P. Beltrao, E. Raineri, M. Garriga-Canut, and L. Serrano. Evolvability and hierarchy in rewired bacterial gene networks. *Nature*, 452:840–845, 2008.

[49] K. Kaneko. Shaping robust system through evolution. *PLoS ONE*, 2:e434, 2007.

[50] S. A. Kauffman. Gene regulation networks: A theory for their global structure and behaviors. *Current topics in developmental biology*, 6(6):145–182, 1971.

[51] S. A. Kauffman and R. G. Smith. Adaptive automata based on darwinian selection. *Physica D*, 22:68, 1986.

[52] Stuart Kauffman. Homeostasis and differentation in random genetic control networks. *Nature*, 224:177–178, 1969.

[53] Stuart Kauffman. *The origins of order*. Oxford University Press, New York, 1993.

[54] Stuart Kauffman, Carsten Peterson, Bjørn Samuelsson, and Carl Troein. Random Boolean network models and the yeast transcriptional network. *Proc. Nat. Acad. Sci.*, 100:14796, 2003.

[55] Stuart Kauffman, Carsten Peterson, Bjørn Samuelsson, and Carl Troein. Genetic networks with canalyzing boolean rules are always stable. *Proc. Nat. Acad. Sci.*, 101:17102, 2004.

[56] Stuart A. Kauffman. Metabolic stability and epigenesis in randomly constructed genetic nets. *J. Theor. Biol.*, 22:437–467, 1969.

[57] V. Kaufman and B. Drossel. Relevant components in critical random boolean networks. *New Journal of Physics*, 8:228, 2006.

[58] Viktor Kaufman, Tamara Mihaljev, and Barbara Drossel. Scaling in critical random Boolean networks. *Phys. Rev. E*, 72:046124, 2005.

[59] Konstantin Klemm and Stefan Bornholdt. Stable and unstable attractors in Boolean networks. *Phys. Rev. E*, 72:055101(R), 2005.

[60] K. E. Kürten. Correspondence between neural threshold networks and Kauffman Boolean cellular automata. *J. Phys. A*, 21:L615–L619, 1988.

[61] K. E. Kürten. Critical phenomena in model neural networks. *Phys. Lett. A*, 129:157–160, 1988.

[62] D.S. Lee and H. Rieger. Broad edge of chaos in strongly heterogeneous Boolean networks. *J. Phys. A: Math. Theor.*, 41:415001, 2008.

[63] N Lemke, J. C. M. Mombach, and B. E. J. Bodmann. A numerical investigation of adaption in populations of random boolean networks. *Physica A*, 301:589–600, 2001.

[64] F. Li, T. Long, Y. Lu, Q. Ouyang, and C. Tang. The yeast cell-cycle network is robustly designed. *Proc. Nat. Acad. Sci.*, 101(14):4781–4786, 2004.

[65] J.W. Little, P. Shepley, and D.W. Wert. Robustness of a gene regulatory circuit. *EMBO J.*, 18:4299–4307, 1999.

[66] M. Liu and K. E. Bassler. Emergent criticality from co-evolution in random boolean networks. *Phys. Rev. E*, 74:041910, 2006.

[67] B. Luque, F. J. Ballesteros, and E. M. Muro. Self-organized critical random boolean networks. *Phys. Rev. E*, 63:051913, 2001.

[68] B. Luque and R. V. Solé. Phase transitions in random networks: simple analytic determination of critical points. *Phys. Rev. E*, 55:257–260, 1997.

[69] M. Matache and J. Heidel. Asynchronous random boolean network model based on elementary cellular automata rule 126. *Phys. Rev. E*, 71:026232, 2005.

[70] H. H. McAdams and A. Arkin. Stochastic mechanisms in gene expression. *Proc. Nat. Acad. Sci.*, 94:814–819, 1997.

[71] Alexander McKenzie. Random boolean networks and evolutionary game theory. *Philosophy of Science Assoc. 18th Biennial Mtg-PSA 2002*, 70:1289–1304, 2002.

[72] L. Mendoza and Alvarez-Buylla E. R. Dynamics of the genetic regulatory network for *Arabidopsis thaliana* flower morphogenesis. *J. Theor. Biol.*, 193(2):307–319, 1998.

[73] T. Mihaljev and B. Drossel. Scaling in a general class of critical random boolean networks. *Phys. Rev. E*, 74:046101, 2006.

[74] T. Mihaljev and B. Drossel. Evolution of a population of random Boolean networks. arXiv:0808.2490, 2008.

[75] A. A. Moreira and L. A. N. Amaral. Canalizing Kauffman networks: nonergodicity and its effect on their critical behavior. *Phys. Rev. Lett.*, 94:218702, 2005.

[76] Ikuo Nakamura. Adaptation and survivors in a random boolean network. *Phys. Rev. E*, 65:046128, 2002.

[77] MEJ Newman. Models of the Small World. *Journal of Statistical Physics*, 101(3):819–841, 2000.

[78] P. Oikonomou and P. Cluzel. Effects of topology on network evolution. *Nature Physics*, 2:532–536, 2006.

[79] M. Paczuski, K. E. Bassler, and Á. Corral. Self-organized networks of competing boolean agents. *Phys. Rev. Lett*, 84:3185, 2000.

[80] Ute Paul, Viktor Kaufman, and Barbara Drossel. Properties of attractors of canalyzing random Boolean networks. *Phys. Rev. E*, 73:026118, 2006.

[81] T.P. Peixoto and B. Drossel. Noise in random Boolean networks. arXiv:0808.3087, 2008.

[82] X. Qu, M. Aldana, and L. P. Kadanoff. Numerical and theoretical studies of noise effects in the kauffman model. *J. Stat. Phys*, 109:967–986, 2002.

[83] L. Raeymaekers. Dynamics of boolean networks controlled by biologically meaningful functions. *J. Theor. Biol.*, 218(3):331–341, 2002.

[84] P. Rämö, J. Kesseli, and O. Yli-Harja. Perturbation avalanches and criticality in gene regulatory networks. *J. Theor. Biol.*, 242:164–170, 2006.

[85] H. Risken. *The Fokker-Planck equation: Methods of Solution and Applications*. Springer-Verlag Berlin and Heidelberg GmbH & Co. K, 1989.

[86] T. Rohlf. The critical line in random threshold networks with inhomogeneous thresholds. arXiv:0707.3621, 2007.

[87] T. Rohlf and S. Bornholdt. Criticality in random threshold networks: annealed approximation and beyond. *Physica A*, 310:245–259, 2002.

[88] B. Samuelsson and C. Troein. Random maps and attractors in random boolean networks. *Phys. Rev. E*, 72:046112, 2005.

[89] Björn Samuelsson and Joshua E. S. Socolar. Exhaustive percolation on random networks. *Phys. Rev. E*, 74:036113, 2006.

[90] Bjørn Samuelsson and Carl Troein. Superpolynomial growth in the number of attractors in Kauffman networks. *Phys. Rev. Lett.*, 90:098701, 2003.

[91] P. Schuster, W. Fontana, P.F. Stadler, and I.L. Hofacker. From sequences to shapes and back: a case study in rna secondary structures. *Proc. Roy. Soc. Lond. B*, 255:279–284, 1994.

[92] N. Schwartz, Reuven Cohen, Daniel ben Avraham, A.-L Barabasi, and Shlomo Havlin. Percolation in directed scale-free networks. *Phys. Rev. E*, 66:015104(R), 2002.

[93] R. Serra, M. Villani, and L. Agostini. On the dynamics of random Boolean networks with scale-free outgoing connections. *Physica A: Statistical Mechanics and its Applications*, 339(3-4):665–673, 2004.

[94] R. Serra, M. Villani, and A. Semeria. Genetic networks models and statistical properties of gene expression data in knock-out experiments. *J. Theor. Biol.*, 227:149–157, 2004.

[95] V. Sevim and P. A. Rikvold. Unbiased random threshold networks are chaotic or critical. arXiv:0708.2244, 2007.

[96] V. Sevim and P.A. Rikvold. Chaotic gene regulatory networks can be robust against mutations and noise. *J. Theor. Biol.*, 253:323–332, 2008.

[97] I. Shmulevich, E. R. Dougherty, and W. Zhang. From boolean to probabilistic boolean networks as models of genetic regulatory networks. *Proceedings of the IEE*, 90:1778, 2002.

[98] I. Shmulevich, S. Kauffman, and M. Aldana. Eukaryotic cells are dynamically ordered or critical but not chaotic. *Proc. Nat. Acad. Sci.*, 102(38):13439–13444, 2005.

[99] I. Shmulevich, H. Lähdesmäki, E. R. Dougherty, J. Astola, and W. Zhang. The role of certain post classes in boolean network models of genetic networks. *Proc. Nat. Acad. Sci.*, 100(19):10734–10739, 2003.

[100] Joshua E. S. Socolar and Stuart A. Kauffman. Scaling in ordered and critical random Boolean networks. *Phys. Rev. Lett.*, 90:068702, 2003.

[101] H. E. Stanley. Scaling, universality, and renormalization: Three pillars of modern critical phenomena. *Rev. Mod. Phys.*, 71(2):S358–S366, Mar 1999.

[102] H.E. Stanley. *Introduction to Phase Transitions and Critical Phenomena, Clarendon.* Oxford, 1971.

[103] D. Stauffer. Random boolean networks - analogy with percolation. *Philosophical Magazine B: Physics of Condensed Matter, Statistical Mechanics, Electronic, Optical and Magnetic Properties*, 56:901–916, 1987.

[104] D. Stauffer. Percolation thresholds in square-lattice kauffman model. *J. Theor. Biol.*, 135:255–261, 1988.

[105] M. D. Stern. Emergence of homeostasis and "noise imprinting" in an evolution model. *Proc. Natl. Acad. Sci. USA*, 96:10746, 1999.

[106] S.H. Strogatz. Exploring complex networks. *Nature*, 410:268, 2001.

[107] S.H. Strogatz and S. Henry. *Nonlinear dynamics and chaos: with applications to physics, biology, chemistry, and engineering.* Westview Press, 2000.

[108] A. Szejka and B. Drossel. Evolution of canalizing boolean networks. *Eur. Phys. J. B*, 56:373–380, 2007.

[109] A. Szejka, T. Mihaljev, and B. Drossel. The phase diagram of random threshold networks. *New Journal of Physics*, 10(6):063009, 2008.

[110] D. Thieffry and D. Romero. The modularity of biological regulator networks. *Biosystems*, 50:49–59, 1999.

[111] NG van Kampen. *Stochastic Processes in Physics and Chemistry*. Amsterdam, New York, 1992.

[112] A. Wagner. Does evolutionary plasticity evolve? *Evolution*, 50:1008–1023, 1996.

[113] A. Wagner. *Robustness and evolvability in living systems*. Princeton University Press, 2005.

[114] D.J. Watts. *Small worlds: the dynamics of networks between order and randomness*. Princeton University Press Princeton, NJ, USA, 1999.

[115] A. Wuensche. Discrete dynamical networks and their attractor basins. *Complexity International*, 6:98–11, 1999.

[116] T. W. Zawidzki. Competing models of stability in complex, evolving systems: Kauffman vs. simon. *Biology and Philosophy*, 13:541–554, 1998.

Acknowledgments

First and foremost, I would like to thank my supervisor, Professor Barbara Drossel. There are so many things I should thank her for, that it is hard to choose just a few to mention. I am very lucky to have had the opportunity to work with her and I am sincerely grateful for all that she has done for me. Her kindness, enthusiasm, competence, support, availability and infinite patience contributed immensely to my research and ensured that I completed my thesis. I have learned so much from working with her. The best advisor and teacher I could have wished for, she is actively involved in the work of all her students, always having their best interest in mind. Her confident, gentle and wise guidance, persistent interest in the progress of my work and her will to discuss different aspects of my studies, made me really enjoy the work on this thesis. Being her PhD student, I did not have only a great supervisor, but also a real friend.

I am very grateful to Professor Markus Porto for being ready to read and referee my thesis in such a short time.

My thanks go to Felix Wissel and Sebastian Schmitt who were there whenever I needed them from the day I came here. I thank Viktor Kaufman for fruitful collaboration. It was a pleasure discussing mathematical problems with Satoshi Uchida. I thank Florian Greil for his help with all the computer stuff that I could not work without, it was really convenient having a friendly system administrator as a room mate.

Special appreciation goes to Florian Teichert whose help in programing meant a lot to me. I am particularly grateful to Agnes Szejka for providing a great background to my studies of evolution. Many interesting discussions we had were not only useful for these studies, but led also to a successful collaboration on another project. I would also like to thank her and Tiago Peixoto for proof-reading this thesis. They both helped a lot being ready to read and discuss late in the evening and on weekends.

I also thank Marianne Heckmann, Christian Guill, Boris Kartascheff, Manuel Bach, Barbara Knell and other present and former members of AG Drossel, for making for a great atmosphere in the group and for their support. The great time we spent together in the breaks made the work more pleasant and productive.

I would like to thank my sister Tanja for being always there for me. *Hvala ljubičice!* I am immensely grateful to my parents Dora and Petar Mihaljev for all the love and support they were giving me through all these years. It is hard to find words

that could express my gratitude properly. *Dragi mama i tata, ovaj rad je, kao i svaki drugi moj uspeh, rezultat vaše ljubavi, podrške i vere u mene. Hvala što mi svojim primerom pokazujete pravi put i što mi svojom ljubavlju dajete siguran oslonac. Teško je naći reči kojima bih mogla da izrazim zahvalnost za žrtvu koju za nas podnosite i za energiju i ljubav koju sve vreme ulažete u Tanju i mene. Vi ste uzor roditelja koji se nadam da ću jednog dana moći da dostignem. Hvala što ste najbolji roditelji na svetu!*

Finally, I am most grateful to my husband Bora. He was always by my side, helping wherever he could in his quiet way, encouraging me and cheering me up with his great humor even when it was really hard. This period of our lives made me once again aware of how lucky I am to have such a wonderful husband. I would have never made it without his love and support.

Lebenslauf

Name	Tamara Mihaljev
Geburtsdatum	11. 06. 1976
Geburtsort	Pula, Kroatien

Juni 1995	Abitur, 13. Belgrader Gymnasium
März 2004	Abschluss als Diplom-Physikerin, Universität Belgrad
seit *August* 2004	Promotionsstudium an der TU Darmstadt
2004-2007	Promotionsstipendium der TU Darmstadt
2007-2008	Wissenschaftliche Mitarbeiterin an der TU Darmstadt

Eidesstattliche Erklärung

Hiermit erkläre ich eidesstattlich, dass ich die vorliegende Dissertation selbständig verfasst, keine anderen als die angegebenen Hilfsmittel verwendet und bisher noch keinen Promotionsversuch unternommen habe.

Darmstadt, im Oktober 2008

(Unterschrift)